Institut de recherche
Robert-Sauvé en santé
et en sécurité du travail

Assessing Embalmer Exposure to Bioaerosols and the Associated Health Risk

Geneviève Marchand
Loïc Wingert
Stéphane Hallé
Maximilien Debia

STUDIES AND
RESEARCH PROJECTS

R-1110-en

CHEMICAL
AND BIOLOGICAL
HAZARD PREVENTION RESEARCH

OUR RESEARCH
is working for you!

The Institut de recherche Robert-Sauvé en santé et en sécurité du travail (IRSST), established in Québec since 1980, is a scientific research organization well-known for the quality of its work and the expertise of its personnel.

Mission

In keeping with the spirit of the Act respecting occupational health and safety (AOHS) and the Act respecting industrial accidents and occupational diseases (AIAOD), the IRSST's mission is:

To contribute to workers' health and safety through research, its laboratories' expertise, and knowledge dissemination and transfer, with a view to promoting prevention and sustainable return to work.

To find out more

Visit our Web site for complete up-to-date information about the IRSST. All our publications can be downloaded at no charge.
www.irsst.qc.ca

To obtain the latest information on the research carried out or funded by the IRSST, subscribe to our publications:

- *Prévention au travail,* the free magazine published jointly by the IRSST and the CNESST (preventionautravail.com)
- InfoIRSST, the Institute's electronic newsletter

Legal Deposit

Bibliothèque et Archives nationales du Québec, 2022
ISBN 978-2-89797-237-0 (PDF)

IRSST – Communications, Strategic Watch and Knowledge Mobilization Division
505 De Maisonneuve Blvd. West
Montréal, Québec
H3A 3C2
Phone: 514 288-1551
publications@irsst.qc.ca
www.irsst.qc.ca

Assessing Embalmer Exposure to Bioaerosols and the Associated Health Risk

Geneviève Marchand[1], Loïc Wingert[1],
Stéphane Hallé[2], Maximilien Debia[3]

[1] IRSST

[2] École de technologie supérieure

[3] Université de Montréal

Collaborators

Yves Cloutier, Nancy Lacombe, Carol-Anne Villeneuve,
Marie Gardette, Yves Beaudet, Jihen Chebil, Julien Trépanier,
Caroline Couture, Luc Bhérer, Jacques Lavoie

STUDIES AND RESEARCH PROJECTS

R-1110-en

This study was funded by the IRSST. The conclusions and recommendations are solely those of the authors.
This publication is a translation of the French original; only the original version (R-1110) is authoritative.

PEER REVIEW
In compliance with IRSST policy, the research results
published in this document have been peer-reviewed.

ACKNOWLEDGMENTS

The research team would like to thank all the people and organizations who helped it in carrying out this study, including the following:

- the Corporation des Thanatologues du Québec, and especially Annie St-Pierre, who made contacts between the research team and the funeral home directors much easier;

- the funeral directors who agreed to let us visit their laboratories so we could do the necessary sampling for the project;

- the embalmers who very kindly allowed our equipment to get in their way for a full workday;

- the members of the monitoring committee for their interest in this research.

SUMMARY

Several of the actions that embalmers take with dead bodies produce bioaerosols that may contain infectious pathogens. General ventilation is often the only method used to control bioaerosols in embalming labs. Nevertheless, there are no specific recommendations for applying it. Moreover, few studies have addressed occupational exposure to bioaerosols in embalming, either quantitatively (level of exposure) or qualitatively (identification and classification of risk groups). The purpose of this study was to assess embalmers' exposure to bioaerosols in order to evaluate the potential risks to their health and examine the effect of certain factors on the behaviour of biological particles in the air.

Three embalming labs were assessed. Bioaerosol sampling was done in the air and on surfaces, using an Andersen 6-stage impactor, CIP-10M and SASS® 3100 air samplers, and Hygiena Q-Swab™ swabs. The different types of sampling were used to count and identify culturable bacteria. Numerical concentrations of fluorescent particles (biological particles) and non-fluorescent particles and granulometric measurements (between 0.5 and 20 µm) were also done in real time near the embalmer, using a laser-induced fluorescence aerosol spectrometer (WIBS-NEO). Calculations of the air changes per hour and fluid dynamics simulations (CFD) were done in each lab. The simulations enabled us to calculate the mean age of the air in various parts of the laboratory and to assess the effect of different ventilation strategies on the concentrations of bioaerosols in the lab.

This study established that workers engaged in embalming were exposed to low levels of bioaerosols, on average, but that certain tasks were likely to generate an increase in bioaerosol concentrations near the worker. Strains of bacteria belonging to non-tuberculous *Mycobacterium* (Risk Group 2) were identified in two of the three labs studied. In addition to *Mycobacterium,* several bacteria from the *Corynebacterium, Dietziaceae, Gordoniaceae. Nocardiaceae* and *Streptomycetaceae* families were also found in the three laboratories. Finally, *Streptococcus pneumoniae,* a human pathogen in Risk Group 2*,* was cultured in samples from Laboratories A and C. The culturing of *Streptococcus pneumoniae* proves that bacteria from the human respiratory tract can be found in culturable state in the air of embalming labs.

Most bioaerosols have diameters of less than 4 µm (so-called respirable fraction), which means that they have a strong possibility of being deposited in the respiratory tract and a strong potential to circulate in the air of embalming rooms. Work tasks that result in a bellows effect and splashing were identified as the most emissive activities.

The ventilation rates calculated were 2.1, 10.3 and 7.9 air changes per hour (ACH), respectively, for Laboratories A, B and C. CFD simulations in the three laboratories showed that particle concentrations were highest at ventilation rates of 1 ACH. An increase from 1 to 4 ACH reduced concentrations by 28% to 67%, depending on the lab being modelled. In Laboratories A and C, a change in the mechanical ventilation by increasing the number of ACH may be a way to control bioaerosol concentrations, even though capture at source is always the preferred option. In Laboratory B, the concentrations in numbers of particles at 10.3 and 12 ACH were comparable. This seems to indicate that an increase beyond 12 ACH will not have a significant impact on concentrations. Other control methods should therefore be considered.

Considering the difficulty of identifying the existence of pathogens in dead bodies and near embalmers, the great diversity of work tasks and the uncertainty associated with the dilution of contaminants by means of general ventilation, the authors of this report recommend that, at minimum, the wearing of air-filtering respiratory protective equipment (RPE) such as a disposable filtering facepiece (N/R/P-95/99/100) or an elastomeric half-mask with P100 filter cartridges, should be considered during embalming tasks.

TABLE OF CONTENTS

LIST OF TABLES

LIST OF FIGURES

1. INTRODUCTION

Embalmers are workers in the funeral industry responsible for embalming, or thanatopraxy. Among other tasks, they must receive the dead body, disinfect it for identification, execute the embalming, engage in restoration of the body, provide aesthetic care and encoffin the body. The objective of embalming is to maintain hygiene by slowing down the process of putrefaction.

In Quebec, in 2018, there were 68,600 deaths, compared with 66,300 in 2017 and 63,600 in 2016, confirming an upward trend in the annual death rate (Azeredo & Payeur, 2019). The aging of the population is partly responsible for this increase. According to data from the Ministère de la Santé et des Services sociaux (MSSS), more than 500 embalmers in slightly under 200 funeral homes applied for a licence to practise in 2019 (unpublished data). Although the annual number of embalmments is not known, in 2011 the “thanatopraxie Montérégie-Montréal” working group estimated that 70% of bodies were embalmed (Lajoie et al., 2011). This would represent more than 48,000 embalmments in Quebec each year, for an annual mean of 90 per worker.

Microorganisms are classified into four risk groups based on their pathogenicity (Public Health Agency of Canada, 2019). There are three infectious risk groups (Risk Groups 2 to 4) and one non-infectious risk group (Risk Group 1). All bodily fluids (blood, internal fluids, secretions, excretions) from dead bodies can be a source or reservoir of microorganisms and must be considered as potentially infectious at all times (Lajoie et al., 2011). In addition, various handling procedures done on the body have been identified as able to produce bioaerosols (Correia et al., 2014). Since infectious agents do not disappear immediately after death, embalming has been identified as presenting a high risk of infection in the funeral industry (Davidson & Benjamin, 2006; Healing et al., 1995; Keane et al., 2013; Lajoie et al., 2011). There are many opportunities for exposure, since embalmers generally work close to the dead body and are regularly exposed to bodily fluids (Keane et al., 2013).

Occupational infections can result in moderate or high risks for workers, especially infections in Risk Group 3, which can cause a disease that is serious or fatal to humans (Burton, 2003). However, few studies have considered occupational exposure to bioaerosols in the field of embalming or addressed the mechanisms whereby infectious diseases are propagated (Su et al., 2019).

2. CURRENT KNOWLEDGE

2.1 Embalming

Embalming consists in preparing, disinfecting and delaying the decomposition (or thanatomorphosis) of a body, in preparation for encoffining and the funeral. It also includes presentation care, which is intended to show the deceased person to their family with the most natural appearance possible. The main working tasks in an embalming laboratory consist in washing and disinfecting the body, and embalming, dressing and encoffining it. In more detail, the steps for preparing a body are as follows:

1. placement of the body on the embalming table
2. cleaning and asepsis of orifices
3. closing of mouth and placement of eye caps
4. preparation of fluids
5. arterial incision and injection (cannula)
6. limb mobilization
7. massage to assist fluid circulation
8. drainage of fluids and gases with a trocar
9. injection of fluid into the body cavity (trocar)
10. sealing of orifices
11. suturing of incisions
12. complete cleaning of body and hair
13. restoration (if necessary)
14. wrapping in a plastic film
15. dressing
16. makeup and hairdressing
17. encoffining

2.2 Microorganisms

Our body contains 100,000 billion bacteria (Rup, 2012). At the time of death, these microorganisms do not all disappear. In fact, after death, the loss of the natural barriers created by tissue membranes and the shutdown of the immune system facilitate the proliferation of certain microorganisms, which find a nutrient-rich environment in a cadaver (Javan et al., 2016; Tuomisto et al., 2013). After death, various changes occur in the body. For example, there is an endogenous invasion of the cerebrospinal fluid by bacteria associated with the colon within 4 to 6 hours following death (Creely, 2004). Propagation into the different parts of the body is due to a microbial invasion of the lymphatic and vascular systems and the mucous membranes of the respiratory system (Paczkowski & Schütz, 2011). Moreover, in the processes of decomposition and

putrefaction, microorganisms, including intestinal bacterial, tend to migrate to the blood and certain internal organs (Morris et al., 2007; Tuomisto et al., 2013). As the body decomposes, several microorganisms proliferate in the blood, liver, spleen, heart and brain. The result is a very varied microbial flora, depending on the organ and the time elapsed since death (Can et al., 2014; Tuomisto et al., 2013). Maximum concentrations of 3.0 to 3.5 x 10^6 microorganisms per millilitre of bodily fluid or per gram of tissue may be reached within 24 to 30 hours following death (Rose & Hockett, 1971). Thus, not only is the thanatomicrobiome very diversified but it also varies considerably over time. This variability depends on many factors, such as the deceased's health condition at the time of death, the organ or tissue sampled, the time since death, the temperature, the pH, and the cause of death (Can et al., 2014; Javan et al., 2016).

Certain microorganisms are known to present a danger to workers in the funeral industry, such as Group A Streptococcus (*Streptococcus pyogenes*), methicillin-resistant *Staphylococcus aureus* (MRSA) and some gastrointestinal pathogens (vancomycin-resistant enterococci (VRE), *Clostridium difficile*) (Davidson & Benjamin, 2006; HSE, 2005; Lajoie et al., 2011). Other pathogens should also be monitored such as *Mycobacterium tuberculosis*, hepatitis B and C viruses, HIV and the prions that cause transmissible spongiform encephalopathies (Creutzfeldt-Jakob Disease). These pathogens are known to represent a health risk to all workers who handle cadavers during the course of their work (Davidson & Benjamin, 2006; Demiryürek et al., 2002; Guez-Chailloux et al., 2005; Gupta et al., 2013; Healing et al., 1995; HSE, 2005; Lajoie et al., 2011; Weed & Baggenstoss, 1951). Emergent viruses such as H1N1 influenza and the coronavirus causing severe acute respiratory syndrome (SARS) have been identified as new potential dangers for embalmers (Lajoie et al., 2011).

As emphasized above, microorganisms do not disappear instantly upon a person's death; many pathogens can retain their infectious power long after death (Burton, 2003; Douceron et al., 1993; Henry et al., 1989; HSE, 2005). For example, *Mycobacterium tuberculosis* remains culturable up to 36 days after death in human remains, whether embalmed or not (Correia et al., 2014); SARS-CoV has been found after death in several of the patients' organs (Farcas et al., 2005; Tang et al., 2007); HIV has been found to be viable up to 16.5 days after death (Creely, 2004; Douceron et al., 1993; Nyberg et al., 1990); and *Streptococcus pyogenes* is frequently found on the bodies of people who have died of invasive diseases (Davidson & Benjamin, 2006). It should also be noted that the brain tissues of persons who have died of Creutzfeldt-Jakob Disease can remain infectious years after their death, even if the tissues were fixed in formaldehyde-based solutions (Demiryürek et al., 2002; Gajdusek et al., 1976; Priola et al., 2013). The possible presence of serological markers of hepatitis B and C viruses in tissue and blood banks should also be noted (Demiryürek et al., 2002). Finally, according to the "thanatopraxie Montérégie-Montréal" working group, the potential for late transmission of an infection from a cadaver to an embalmer is real, since even when a body is embalmed, the tissues cannot be considered to be sterile (Lajoie et al., 2011).

2.3 Risks of exposure to microbial agents

Depending on the exposure pathway and the dose, exposure to an infectious agent can have severe consequences for workers' health. However, the minimum dose is rarely known in relation to risks of infection in the workplace. Nevertheless, the identification of the risk or risks (biological agents present) is still a key step in the process of exposure assessment. Table 1 presents a list of biological agents and their exposure pathways that have been identified as posing a risk for embalmers.

Table 1. List of risky biological agents* and exposure pathways associated with embalmers

Inhalation†	Ingestion (hand-mouth), direct contact with fecal matter or indirect contact with contaminated objects	Mucocutaneous contact with blood or other contaminated biological fluids	Direct or indirect mucocutaneous contact
Mycobacterium tuberculosis	HAV	HIV	*Streptococcus pyogenes* (group A)
SARS-CoV	Nontyphoidal salmonella (e.g., *S. typhimurium* and *S. enteritidis*)	HBV	*Staphylococcus aureus* (MRSA)
Neisseria meningiditis		HCV	
Haemophilus influenzae	*Shigella* spp. (e.g., *S. dysenteriae*)	HTLV 1 and 2	
Corynebacterium diphtheriae	*Salmonella typhi/paratyphi*	Hemorrhagic fever (e.g., Ebola)	
	Helicobacter pylori	Spongiform encephalopathy transmissible by prions (e.g., Creutzfeldt-Jakob Disease)	
	Cryptosporidium		

* HAV, hepatitis A virus; HBV, hepatitis B virus; HCV, hepatitis C virus; HIV, human immunodeficiency virus; HTLV, human T-lymphotropic virus
† Transmission by inhalation: Ebola and prions cannot be ruled out
Sources: Burton (2003); Creely (2004); Davidson and Benjamin (2006); Guez-Chailloux et al. (2005); HSE (2005, 2018)

Working on a dead body potentially exposes workers to pathogens by inhalation (aerosols); inoculation; contact with the mucous membranes of the eyes, nose and mouth; and ingestion (Burton, 2003; Correia et al., 2014; Davidson & Benjamin, 2006; Guez-Chailloux et al., 2005; Keane et al., 2013). Davidson and Benjamin (2006) report several risks of transmission of infectious diseases in funeral industry workers. The analysis of the various actions taken by embalmers made it possible to determine that all activities, except instrument preparation, presented the potential for exposure to biological agents (Guez-Chailloux et al., 2005). After autopsies, embalming is the funeral industry job that exposes workers to biological agents the most (Guez-Chailloux et al., 2005).

It has long been known that workers exposed to cadavers are at risk of contracting occupational lung infections by *Mycobacterium tuberculosis* (inhalation in 90% of cases). Two famous cases are René Laennec (inventor of the stethoscope) and Xavier Bichat (father of histology), both of whom died of tuberculosis after conducting autopsies and examining tissue from tubercular cadavers (Burton, 2003). Gershon et al. (1998) reported a tuberculin reaction rate that was twice as high in funeral industry workers who regularly do embalming as in those who do not (14.9% vs. 7.2%, $p < 0.01$), and this rate is positively associated with the number of embalmments done each week.

Keane et al. (2013) consider that the potential for exposure to bioaerosols exists as soon as a dead body is moved. Movement of the body can produce pressure on the thorax that triggers the expulsion of air and microbial particles contained in the lungs. The great pressure used to disperse embalming fluid through the arteries has also been cited as an activity causing a risk of exposure by inhalation. Pressure-causing actions result in the aerosolization of particles from the cadaver's mouth (Correia et al., 2014). The aspiration of blood and other bodily fluids can also generate bioaerosols (Davidson & Benjamin, 2006).

According to Guez-Chailloux et al. (2005), the risk of contamination is gradual. As long as the embalmer is in contact only with the outside of the body, and there are no lesions, the risk is quite low. However, the risks gradually increase during the steps involving incisions, injections and aspiration (Guez-Chailloux et al., 2005). The risks of hematogenous transmission are mainly attributable to incidents involving needle sticks, cuts or tearing, but exposure of the mucous membranes to bodily fluids due to splashing is also possible. From 11% to 17% of embalmers report exposure due to splashes during embalming (Creely, 2004; Kelly & Reid, 2011).

The risk of infection is lower if all morgue employees consider each cadaver as a potential source of pathogens, whether or not an infection has been documented (Burton, 2003).

2.4 Control methods

The methods for controlling exposure to biological risks follow the same principles as those used for other workplace risks. The hierarchy of controls, or prevention, is the approach that should be favoured in occupational health and safety (Anctil et al., 2017; Barnett & Brickman, 1986; Bourque, 2016; Canadian Centre for Occupational Health and Safety, 2018; Cooper, 1995; Parent & Bouchard, 2017; Plog & Quinlan, 2002). If it is not possible to eliminate the risk, one must follow the hierarchy of controls, bearing in mind that the use of several methods in combination is usually necessary to guarantee workers' health, safety and integrity (Bourque, 2016).

Due to the nature of embalmers' work, it is impossible to eliminate all biological risks. Nevertheless, the *Regulation respecting the application of the Act respecting medical laboratories and organ and tissue conservation* prohibits embalmment of the cadaver of a person who died of smallpox, plague or cholera. In that case, the cadaver "must be incinerated without delay or immediately enclosed in an impervious and hermetically sealed coffin for burial" (Éditeur officiel du Québec, 2019, s. 51). Although embalming of bodies of people who have died of Creutzfeldt-Jakob disease or its variant (CJD or "mad cow disease") is not prohibited in Quebec, it is not recommended (HSE, 2018; Lajoie et al., 2011). In its manual on handling infection risks while handling dead bodies, the UK Health and Safety Executive (HSE) does not recommend embalming the cadavers of people dead of hemorrhagic fever (e.g., Ebola), transmissible

spongiform encephalopathy (e.g., CJD), anthrax, rabies (Lyssavirus) and *Streptococcus pyogenes* (HSE, 2018). It is also possible that, for certain diseases that are rare, emerging or subject to extreme surveillance, public health recommendations may be against embalming. However, to find this out, embalmers must contact the public health authorities in their region (Lajoie et al., 2011).

The control methods used by embalmers include individual and collective measures as well as additional precautions in specific situations (tuberculosis, highly transmissible diseases, rare or emerging diseases) (Lajoie et al., 2011). Collective measures may include implementing preventive policies and procedures, work organization, employee training, general ventilation, linen maintenance and waste management. Individual measures include personal and hand hygiene, wearing personal protective equipment (gloves, protection of mucous membranes in the nose and mouth, eye protection, coveralls), vaccination and the use of the tuberculin skin test (TST). In situations where the cadaver has tuberculosis, chickenpox or measles, specific recommendations are added: (1) administrative (e.g., rapid identification of cadavers with tuberculosis, chickenpox or measles), (2) technical (e.g., improved ventilation in the embalming zone), and (3) personal (e.g., wearing respiratory protective equipment (RPE) and using the TST).

It is important to emphasize that the recommendations regarding control methods frequently vary depending on the group of experts, which leads workers in the field to question them. For example, depending on the organization or expert group, the recommendations regarding wearing RPE vary based on the presence or absence of infectious diseases recorded in the declaration of death, any infectious agents identified, the possible transmission pathway, the tasks to be done, the condition of the cadaver, and the time since death. According to certain experts, RPE is justified only for work on bodies identified as carrying a disease transmissible by means of aerosols, which generally includes tuberculosis, chickenpox and measles (Burton, 2003; Lajoie et al., 2011), but also SARS (HSE, 2018; Michaud, 2003). Note that, according to the Institut national de recherche et de sécurité pour la prévention des accidents du travail et des maladies professionnelles (INRS), wearing RPE is recommended once the body bag has been opened (Guez-Chailloux et al., 2005).

Another important example of confusion among recommendations concerns ventilation. The *Regulation respecting the application of the Act respecting medical laboratories and organ and tissue conservation* specifies that the facility where the embalming will be done must “be equipped with a natural or artificial ventilation system capable of ensuring adequate sanitation” (s. 47), but it does not specify any quantitative requirements. Some experts consider that natural ventilation is not sufficient for embalming and that a capture at source system is necessary to eliminate contaminants before they reach the mortuary worker’s breathing zone (Guez-Chailloux et al., 2005). Lajoie et al. (2011) report that, in a study of embalmers’ exposure to formaldehyde, local ventilation or the use of automatic air washers halved workers’ exposure but did not eliminate it altogether. Various proposals have been formulated regarding the criteria for ventilation in autopsy rooms but few of them concern embalming labs (ASHRAE, 2013a, 2013b; Éditeur officiel du Québec, 2019; Guez-Chailloux et al., 2005). Note that the *Regulation respecting occupational health and safety* and its provisions that aim to protect workers apply to the field of embalming. These sections cover air quality (Division V), individual protective respiratory equipment (Division VI), ventilation and heating (Division XI), special ergonomic measures (Division XX), and means and equipment for individual and group protection (Division XXX).

2.5 Numerical simulations to study ventilation

Several of the tasks carried out by embalmers generate bioaerosols and all present, to varying degrees, a risk of transmission by inhalation of infectious diseases. Some studies have assessed the effect of ventilation on exposure to pathogens by inhalation (Cheong & Lee, 2018; Memarzadeh, 2013; Memarzadeh & Xu, 2012; Yu et al., 2018; Zhou et al., 2018). Following a review of the literature intended to determine the role of ventilation in buildings, Li et al. (2007) concluded that there is a close relation between ventilation, air movements and the risk of aerial transmission of pathogens. The same study stated that there are insufficient data to specify and quantify the minimum requirements regarding ventilation in relation to the risk of transmission. Currently, the optimal ventilation rate that decreases risks of infection to an acceptable level while limiting energy consumption is not known.

The factors responsible for the dispersion of bioaerosols in the air include the supply flow rate, ventilation strategy, spatial arrangement of the premises, and location of the emission source. This finding makes it difficult to set out universal guidelines that are applicable to all exposure scenarios. In this context, computational fluid dynamics (CFD) simulation becomes a valuable technique to understand the movement of air in confined spaces (Beggs et al., 2008). The numerical solution of equations governing the transport and diffusion of an aerosol as a function of air flow conditions makes it possible to obtain quantitative information on the impact of ventilation rate, supply flow strategy and spatial configuration without requiring experimental measurements. However, searches in the Compendex, Inspec, Scopus, PubMed and Google Scholar databases did not identify a single study in which CFD was used to predict the exposure of workers in an embalming lab. To date, studies involving the modelling of bioaerosol dispersion have focused on the hospital and air transport sectors.

Tang et al. (2011) published a review of the literature on the various techniques allowing researchers to study air flow regimes in a hospital context and their impacts on the movement of suspended particles. Such studies have the aim of improving the effectiveness of preventive measures. According to these authors, CFD modelling of a tracer gas is a justified approach to simulate the aerodynamic behaviour of bioaerosols with a diameter of less than 2 µm. Nevertheless, these authors acknowledge that a tracer gas cannot faithfully represent the behaviour of bioaerosols composed of “large” particles, although no maximum diameter is mentioned.

One important factor affecting the control of bioaerosols expelled by a patient while coughing is the flow of air between the source of contamination and the air exhaust. The risk of inhalation is better controlled when the air exhaust is placed close to the patient and the air supply follows a trajectory from clean (uncontaminated) zones to contaminated zones (area immediately around the patient) (Thatiparti et al., 2017). Commercial CFD software was used to model the ventilation in an isolation room and the aerodynamic behaviour of particles emitted by a coughing patient. Another study that had the aim of modelling bioaerosols in a hospital environment was published by Cheong and Lee (2018). The concentration of airborne particles was determined based on three variables: ventilation rate, position of air diffusers, and existence of screens between beds. The most effective method of reducing the concentration of bioaerosols proved to be increasing the ventilation flow. The presence of screens and the relocation of air diffusers contributed very little to reducing the concentration of suspended pathogens in the air.

Stockwell et al. (2019) published a systematic literature review, one of the purposes of which was to determine whether ventilation is an effective means of controlling bioaerosol concentrations in a hospital. Their study concluded that mechanical ventilation is essential to maintain good air quality and control infections in hospitals. In addition, the literature review showed that the lowest bioaerosol concentrations were observed in cases where the ventilation rate was high or when a ventilation strategy involving laminar flow was adopted.

3. RESEARCH OBJECTIVES

The objective of this study is to evaluate embalmers' exposure to bioaerosols in order to assess the potential risks to their health and evaluate the effects of certain factors on the behaviour of biological particles in the air.

The specific objectives are to:

1. determine, in real time, the concentrations of fluorescent particles[1] and non-fluorescent particles[2] in the ambient air of laboratories and their granulometry before, during and after embalmments;

2. characterize (concentration, identification and culturability) the microorganisms present in embalming rooms, using analysis methods involving culturing and molecular biology (comparative biodiversity approach and targeted detection of microbial indicators);

3. apply computational fluid dynamics (CFD) to assess the effect of certain factors – number of air changes per hour (ACH), dimensions of laboratories and ventilation strategy in the aerodynamic behaviour of bioaerosols and their concentrations and dispersion;

4. propose individual and collective corrective and/or preventive measures regarding occupational risk management.

[1] Fluorescent particles correspond to airborne biological particles. The terms *bioaerosols, microbial particles,* and *biological particles* may all be used to refer to them in this report.
[2] Conversely, non-fluorescent particles represent non-biological particles.

4. METHODOLOGY

4.1 Choice and description of laboratories

The three embalming labs were chosen primarily because of their sizes, but also because of the respective funeral director's interest in the project. In this report, the laboratories are identified as "A" for the large one, "B" for the small one, and "C" for the medium-sized one.

Laboratory A has an access door at one end and a second door providing access to a room where families can dress and groom the deceased. This laboratory has eight embalming tables. Access to Laboratory B is directly from the garage, through an accordion door, which separates the lab from the space for cars. This lab has only one table. Laboratory C, which has two tables, has two access doors, located on either side of the tables. All the laboratory tables are made of porcelain, except for one made of stainless steel. In Laboratory B, waste is drained through a basin (flushable), while in the other two labs, waste is evacuated directly into the sewer pipe. Laboratories A and C have an office-type working space inside the labs. For more details on how the laboratories are organized, readers can refer to section 4.6.3 and consult the diagrams of each lab (Figure 2, Figure 3 and Figure 4) and the characteristics of their air outlets.

4.2 Documentation of tasks and keywords

To interpret the variations in concentrations of particles in the air, the embalmers' activities were observed and recorded in a notes file throughout the duration of sampling (at least 5 hours). The various events reported were therefore systematically associated with defined times. Precision to the second favours the documentation of sequences of tasks within a single minute. For this project, note taking was computerized thanks to the development of a software application in Matlab® (Mathworks, Natick, MA, USA) that saves this information directly in a spreadsheet.[3]

To facilitate analysis of the results, keywords were defined, which group characteristic tasks and events of embalming under the same descriptor. The keywords defined for this project were as follows:

A. Trocar: Insertion of the trocar into the abdominal cavity for aspiration of the contents of the various organs (stomach, bladder, intestines, lungs, etc.).

B. Cannula, incision, injection: Incision of the skin or veins and arteries, insertion of cannulas into the veins and arteries to inject preservative fluids (formaldehyde).

C. Suturing using sealing powder: Application of sealing powder to the incisions and suturing them.

D. Orifice occlusion: Insertion of cotton into certain cavities (nose, mouth, etc.) to seal the orifices, absorb bodily fluids and for aesthetic reasons (shape).

[3] The executable of the note-taking tool is available upon request.

E. **Washing, drying:** Washing, rinsing and drying of the body at the different stages of embalming; also includes washing and drying the hair.

F. **Shaving, depilation:** Shaving and depilation of the deceased's face for embalming purposes.

G. **Table cleaning:** Frequent rinsing of the table with a water jet during embalming and washing of the table with a sponge after the embalming.

H. **Plastic wrapping:** Once the embalming is done, the deceased's trunk is placed in a plastic bag (from the ribs to the pelvis) and formaldehyde powder is sprinkled on for preservation. The bag is then sealed with adhesive tape.

I. **Manipulation of the body:** Actions related to moving the body (on the table), manipulation (lifting the limbs) or handling the deceased (placing it on the table or in the coffin).

J. **Massage:** During the injection of preservative fluids into the body's circulatory system, the limbs (especially the extremities) and the face are massaged so that the fluids are properly distributed despite rigor mortis.

K. **Preparation, equipment cleaning:** Often in or near a sink behind the embalming table, preparation of preservative fluids and cleaning of instruments (trocars, cannulas, retractors, scalpels, etc.).

L. **Retractor:** Insertion and back-and-forth movements of a vein retractor to facilitate the removal of blood and clots while preservatives are being injected.

4.3 Air sampling

4.3.1 Positioning of instruments

To obtain the most representative possible data on embalmers' real exposure, all instruments described in this section were placed on a cart positioned very close (5 to 10 cm) to the embalming table. For real-time sampling, to avoid losses due to electrostatic effects, the graphite sampling tube was maintained facing the dead body at the height of the worker's breathing zone, on a trapeze bar (approximately 1.6 m from the floor). The use of a mobile cart made it possible to track embalmers' movements when a task required prolonged standing at one end of the dead body (head, legs).

4.3.2 Sampling of microorganisms

Because of their complementary nature, three sampling devices were used to collect and analyze the bacterial microbiota in the air.

A. Granulometric sampling of the culturable bacterial microbiota in the ambient air

The Andersen 6-stage impactor (Tisch Environmental, OH, USA) was used to collect the culturable bacterial microbiota present in the laboratories' air. This impactor allows one to separate culturable bacterial particles into 6 granulometric classes ranging from an aerodynamic

diameter of 0.6 µm to > 7 µm (stage 1 has a cut-off diameter (d_{50}) of 8 µm). This separation makes it possible to simulate the deposit of aerosols in the human respiratory system, as shown in Table 2 (Andersen, 1958).

Table 2. Granulometric separation by the Andersen impactor and identification of the deposit site in the respiratory system

Stage	Range of granulometric diameters (µm)	Particle deposit site
1	> 7.0	nasal cavity
2	4.7 to 7.0	pharynx
3	3.3 to 4.7	trachea and primary bronchi
4	2.1 to 3.3	bronchi
5	1.1 to 2.1	bronchioli
6	0.6 to 1.1	alveoli

The sampling rate was adjusted to 28 litres/min and monitored continuously during all collections of a duration of 15 minutes each. The sampling was done in sequence in order to properly cover the time needed for embalming. A blank test was done at the beginning of the day before the first actions on the dead body. Tryptic soy agar (TSA) to which 5% defibrinated sheep blood was added (Oxoid Canada, Nepean, ON, Canada) was used to collect the bacteria. At the end of the day, the agar samples were sent to the IRSST's microbiology laboratory and placed in an incubator at 37 °C.

B. Personal sampling

The CIP-10M (Tecora, Villebon-sur-Yvette, France) was used for personal sampling, meaning sampling within the worker's breathing zone. The CIP-10M collects inhalable microbial particles directly in a PCR grade phosphate buffer (PBS). The sampling rate is 10 litres/min for a rotation speed of the cup of approximately 7,000 RPM. The rotation speed was checked at the start and end of sampling with a convertible laser tachometer (Cole-Parmer®, Vernon Hills, IL, USA). The sampling duration ranged from 1.5 to 3.5 hours, depending on the duration of the embalmment. The sterilized rotating cups were initially loaded with 2 ml of PCR grade PBS; thereafter, 1 ml of PBS was added every hour to compensate for the evaporation of the liquid. At the end of the sampling, the contents of the cup were transferred to a sterile, DNA-free 2 ml tube for transfer to the laboratory.

C. Sampling of ambient air

The CIP-10M (Tecora, Villebon-sur-Yvette, France) was also used in a fixed position to sample the ambient air.

The SASS® 3100 (Research International, Inc., Monroe, WA, USA) was used to sample large volumes of ambient air next to the dead body and the embalmer. A filter that is specially designed for collecting bioaerosols was used as sampling medium for this equipment. This filter has a reported collection efficiency of 92% for particles between 0.5 and 5 µm at an airflow rate of 120 litres/min and an efficiency of 50% for 0.5 µm particles at an airflow rate of 300 litres/min.[4] In this study, the airflow rate used was 300 litres/min and sampling durations ranged between 1 and 4 hours. After sampling, the filters were placed in Petri dishes to transfer them to the laboratory without losing any particles.

4.3.3 Real-time measurement of aerosols and bioaerosols

A. Detection of bioaerosols and measurement of numerical concentrations

Numerical concentrations and particle size distributions of the aerosols emitted during embalming were measured in real time with a laser-induced fluorescence aerosol spectrometer (WIBS-NEO,[5] Droplet Measurement Technologies, Longmont, CO, USA). The WIBS-NEO can detect bioaerosols and total aerosols (biological + non-biological particles) in real time. The numerical concentrations and particle sizedistributions of the total aerosols were measured with an optical particle counter with 10 adjustable granulometric classes ranging from 0.5 to 20 µm. This range of diameters corresponds to the particles that are likely to reach the lower respiratory tract. The WIBS-NEO also uses two laser diodes for particle excitation that emit ultraviolet radiation (wavelength of 280 nm and 370 nm), and measures the resulting ultraviolet and visible fluorescence between 310 and 400 nm and between 420 and 650 nm, respectively. This combination makes it possible to measure fluorescence from molecules that are common in living tissues, particularly NADPH, tryptophan and riboflavin. Thus, the WIBS-NEO allows users to differentiate the biological (fluorescent) fraction from the non-biological (non-fluorescent) fraction. The samples, collected every minute, represent averaged concentrations for one minute. This high temporal resolution allows one to associate a specific task or action with a given emission.

B. Measurement and estimation of baseline levels

Baseline levels of fluorescent and non-fluorescent particles were assessed in the three labs with two methods: mean concentration measured with the WIBS-NEO for 15 min before the start of all activities or mean of 10% of the lowest samples for each sampling day. In Laboratory C, the two methods for measuring baseline levels were compared. A relative deviation of only 1.72% between the two methods was obtained for fluorescent particles.

4.4 Sampling of surfaces

Surface samples were taken at the end of the embalming with Hygiena Q-Swab™ swabs (Thermo Fisher Scientific, Waltham, MA, USA) on several horizontal surfaces in order to determine the culturable bacterial microbiota deposited there. A 100 cm^2 template was used and the sampling was done by rotation on the target surface along three axes. After sampling, the swab was placed in the transport tube containing broth to be taken to the laboratory. The swabs were kept at 4 °C

[4] Methodological details from SASS® 3100 Manual Particle Extractor | CBRN International (http://www.cbrnintl.com/SASS_3100_operational_details.html)
[5] https://www.dropletmeasurement.com/product/wideband-integrated-bioaerosol-sensor/

for approximately 12 hours before the bacterial cells were extracted and spread over TSA substrates identical to those used for air sampling with the Andersen impactor.

4.5 Analyses of biological agents

4.5.1 Culturable bacterial microbiota

The bacterial microbiota present on surfaces (smear test) and in the ambient air (Andersen impactor) was analyzed. The agar samples were incubated for 48 hours at 37 °C. Total bacterial counts were then done with a stereomicroscope (Nikon SMZ18, Melville, NY, USA). The counts for air samples were corrected according to the positive-hole method (Andersen, 1958).

To identify bacterial strains, each colony on the original agar medium with a distinct phenotype was isolated to obtain a pure culture. A combination of several identification methods was used to identify each strain as to species. Figure 1 diagrams the analytical process implemented.

The pure cultures were initially characterized by optical microscopy (wet mount, Gram staining) and by oxidase and catalase tests. Then, the fatty acid profile was characterized with gas chromatography (FAME-GC) (IRSST, MA-341 and MA-344 methods). The FAME-GC method produces a fatty acid profile characteristic of each species. To identify a given species, the profile was compared with those in the Sherlock database. Based on the similarity indices (SI) obtained, identifications were brought to the species (SI > 0.6) or genus level (SI > 0.3). When identification was not conclusive, biochemical test panels were used. The panels used for this project were GEN III® (Biolog, Hayward, CA, USA) and two Microscan® panels: Gram Positive ID 3 and Gram Negative ID 2 (Beckman Coulter, Mississauga, ON, Canada). These panels make it possible to do several biochemical tests simultaneously in a 96-well plate. Each plate is inoculated with the bacterial culture to be identified. After incubation, the reaction for each test is read. Identification is based on the reactivity profile and comparison to the reference chart.

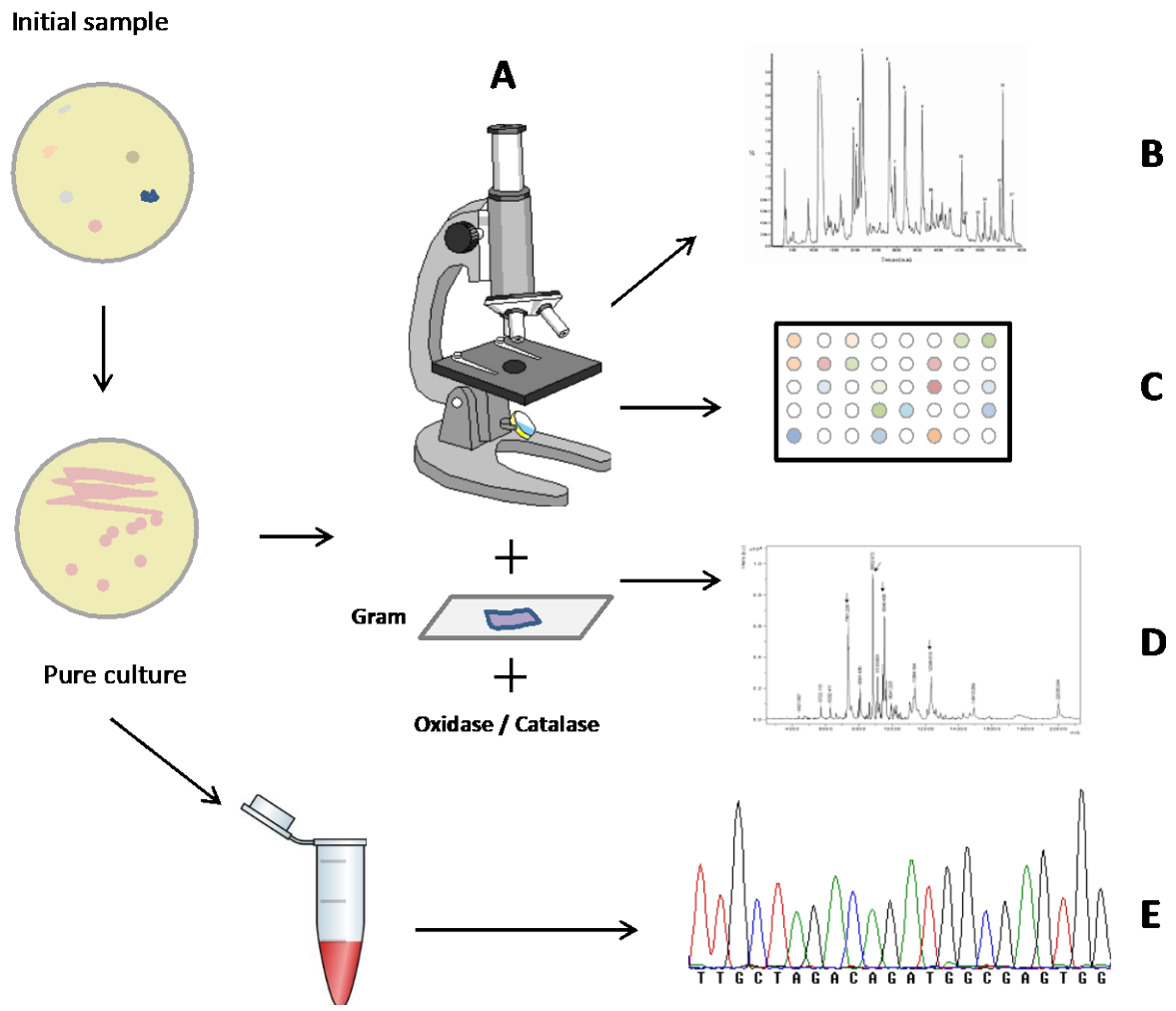

Figure 1. Diagram of analytical techniques used to identify the culturable fraction of sampled bioaerosols.

A – Morphological characterization by means of microscopy, Gram staining, oxidase and catalase tests; B – FAME-GC; C – Microscan® and Biolog®; D – MALDI-TOF; E – Bacterial 16S rRNA sequencing (Sanger).

Two additional methods were used to finalize the identification of certain strains, namely matrix-assisted laser desorption/ionization coupled with time-of-flight mass spectrometry (MALDI-TOF) and Sanger-type sequencing of the bacterial 16S ribosomal RNA gene (16S rRNA).

MALDI-TOF applied to bacterial identification is a technique for characterizing bacterial cell components, which give each species of bacteria a unique signature. A bacterial smear is pulverized and ionized by laser, in a vacuum, using the Vitek-MS (Biomérieux, Marcy-L'Étoile, France). The ionization charges the molecules that are present, which are immediately accelerated and impacted in a mass spectrometer. The device records each molecule impact and compiles them according to their mass-to-charge ratio. The mass spectrum produced in that way is compared to those in a database and associated with a given species.

For the sequencing, a bacterial suspension was first prepared with pure cultures, using PCR grade PBS, and immediately frozen at –80 °C before the analysis. A sample of 200 µl of each bacterial suspension was extracted with the Quick DNA® Fungal/Bacterial Miniprep Kit (Zymo Research, Irvine, CA, USA), following the manufacturer's protocol, to obtain the DNA of the strain to be identified.

16S rRNA is composed of conserved regions, which are useful for fragment amplification, and variable regions, which are useful for discriminating between bacterial species. These variable regions are well defined and are named V1 to V9 (Chakravorty et al., 2007; Van de Peer et al., 1996). The variable gene regions V2 to V9 were amplified with Ai (AGR GTT YGA TYC TGG CTC AGG AYG) and rJ primers (GGT TAC CTT GTT ACG ACT T) (Bekal et al., 2006; Janvier & Grimont, 1995) (Appendix A), in a T100 Thermal Cycler (Bio-Rad, Hercules, CA, USA). The resulting amplicons were cleaned using the ExoSAP-IT Express® kit (Thermo Fisher Scientific, Waltham, MA, USA), which digests short fragments of DNA and excess nucleotides, leaving the amplicons intact. A limited gene area comprising regions V2 to V4 was marked with the BigDye Terminator v3.1 Cycle Sequencing Kit® (Thermo Fisher Scientific – see also Appendix A) and Ai and rE primers (GGA CTA CCA GGG TAT CTA AT) (Harf-Monteil, 2004). The amplicons were analyzed with the SeqStudio® Genetic Analyzer sequencer (Applied Biosystems).

The DNA produced contained approximately 700 pairs of bases. Using the National Center for Biotechnology Information (NCBI) *megablast* algorithm,[6] they were compared with sequences in its 16S ribosomal RNA sequences database. Identifications as to genus were reported for sequences with a similarity of more than 97% and identifications as to species were made for similarities of more than 99%. The "Seqmatch" program[7] from the Ribosomal Database Project (RDP) was used to confirm certain sequences when necessary.

4.5.2 Microbial exposure indicators

A. Development of systems to detect microbial indicators

A polymerase chain reaction (PCR) allows one to detect the DNA of a given microorganism, even at low concentrations. To achieve a good level of performance and minimize the risks of false positive or false negative results, a PCR test must first be optimized in the laboratory. Table 3 summarizes the nine detection systems used and the microorganisms targeted by each.

First, the optimum annealing temperature for the PCR was determined with the temperature gradient (Appendix A), using a C1000 Touch™ thermal cycler, coupled with a CFX96™ optical reaction module (Bio-Rad, Hercules, CA, USA). Then, the specificity of each system was individually tested with a panel containing at least 3 strains of the target microorganism and between 8 and 48 strains of nontarget microorganisms (Appendix A). The concentration of purified DNA for the reference microbial strains was standardized at 0.5 ng/µl. This step allows one to define the sensitivity and specificity of the detection systems.

[6] https://blast.ncbi.nlm.nih.gov/
[7] https://rdp.cme.msu.edu/seqmatch/seqmatch_intro.jsp

Table 3. Detection systems for microbial exposure indicators

Target (gene)	Primer (5' →3')	Probe (5' →3')	PB	Reference
Enterococcus sp. (16S)	**g-Encoc-F**: ATCAGAGGGGGATAACACTT **g-Encoc-R**: ACTCTCATCCTTGTTCTTCTC	**Efae16S390P**: CGTTGCTCGGTCAGACTTTCGTCC	337	Primers, Matsuda (2009); Probe, IRSST
Streptococcus mutans (gtfB)	**SmutGTFB2028F**: AACGGATACAGGGGACCGCAC **SmutGTFB2279R**: CCAGCCGCTTCTTGATCGGAATGAT	**SmutGTFB2151P**: ACGTTTGAAGGCTTCTGATCGC	252	IRSST
Escherichia coli (uspA)	**EcolUSPA222F**: AACACTGAATCTTTACGGCT **EcolUSPA446R**: GAAACTTTCGCATTGTAGGG	**EcolUSPA328P**: TGGAAGGAGTAACACTATGGC	225	IRSST
Staphylococcus aureus (nuc)	**nuc For**: CAAAGCATCCTAAAAAAGGTGTAGAGA **1C-nuc Rev**: CTTCAATTTTCTTTGCATTTTCTACCA	**nuc Probe**: TGGTCCTGAAGCAAGTGCATTTACGAAAA	89	McDonald (2005)
Streptococcus pneumoniae (ply)	**Sp ply F**: TGCAGAGCGTCCTTTGGTCTAT **SpnePLY1046R**: TGCTTCCACTCTGTCTGAGGAGCTAC	**2Sp ply P**: CTCTTACTCGTGGTTTCCAACTTGA	153	Primer F, Corless (2001), Fukasawa (2006); Primer R, IRSST; Probe, Corless (2001)
Mycobacterium tuberculosis (insertion sequence IS6110)	**IS-FIP F2**: CCTACGTGGCCTTTGTCAC **MtubISR**: TCTTTCAGGTCGAGTACGCCTTCT	**MtubP2**: GCCTACGCTCGCAGGAT	145	Primer F, Aryan (2010); Primer R and Probe, IRSST.
Clostridium difficile	**398CLDs**: GAAAGTCCAAGTTTACGCTCAAT **399CLDas**: GCTGCACCTAAACTTACACCA	**551CLD-tq-FAM**: ACAGATGCAGCCAAAGTTGTTGAATT	177	van den Berg (2006)
Hepatitis B virus	**245F**: ACTCGTGGTGGACTTCTCTCAA **432R**: AAGAAGATGAGGCATAGCAGCA	**HBV-P**: TGGATGTGTCTGCGGCGTTTTATCAT	184	Lindh (2006), Sun (2014)
16S rRNA	**E517F**: GCCAGCAGCCGCGGTA **11387r-IRSST**: GGGCGGTGTGTACAAGGC	No probe used	871	Primer F, Soergel (2011); Primer R, Marchesi (1998)

[1] Primer modified from original reference.

[2] Sequence used as probe in this project but as antisense primer in original study.

B. Sample extraction

The samples taken with the SASS® 3100 Dry Air Sampler were extracted with the SASS® 3010 extractor (Research International, Inc., Monroe, WA, USA). The bioaerosol sampling filter was placed in the SASS® 3010 and extracted using 8 ml of extraction buffer (Research International, Inc.), respecting the manufacturer's protocol. The extract was transferred into a sterile 15 ml tube before the DNA was extracted. After each sample, the extractor was rinsed with 8 ml of PREempt® laboratory cleaner (Virox Technologies Inc., Oakville, ON, Canada), the main active ingredient of which is hydrogen peroxide. The device was then rinsed 3 times with PCR grade water to remove any residue of the cleaning solution.

The volumes of the samples obtained with the CIP-10M were topped up to 1.5 ml, with PCR grade PBS before the DNA was extracted.

C. DNA extraction

The samples from the SASS were centrifuged at 10,000 g for 15 minutes to pellet the collected particles. The supernatant was removed, leaving approximately 1 ml, and the pellet was resuspended. Then the samples from the SASS and the CIP-10M, both in 2 ml tubes, were centrifuged at 17,000 g for 5 minutes. The supernatant was eliminated, leaving approximately 200 µl resuspended again. The DNA was extracted with the Quick DNA® Fungal/Bacterial Miniprep Kit (Zymo Research, Irvine, CA, USA), following the manufacturer's protocol.

D. Detection of microbial exposure indicators

The digital droplet PCR (ddPCR) method, which allows absolute quantification, was used for all the detection systems except 16S rRNA, for which quantitative PCR (qPCR) was used. The ddPCR and qPCR tests to detect microbial indicators (conditions presented in Appendix A) were done on the DNA extracted from the samples with the CIP-10M and SASS. ddPCR analyses start

by using the Droplet Generator QX200™ (Bio-Rad Laboratories Inc., Hercules, CA, USA) to produce approximately 20,000 microdroplets, within which the DNA extract is distributed. Then DNA is amplified in each of the droplets with the C1000 Touch™ thermal cycler (Bio-Rad Laboratories Inc.), and finally the terminal fluorescence obtained in each droplet is read with the Droplet Reader QX200 (Bio-Rad Laboratories Inc.). The 16S rRNA was analyzed by means of qPCR with the C1000 Touch™ thermal cycler coupled with the CFX96™ optical module (Bio-Rad Laboratories Inc.).

An internal amplification control was added to each reaction (Prime PCR Assay/Template Tbp, Mmu, qMmuCIP0042759, Bio-Rad Laboratories Inc.). This control makes it possible to individually validate the quality of each ddPCR reaction to detect possible interference, such as the presence of polymerase inhibitors, which would prevent amplification.

The 16S rRNA in all samples was analyzed. However, no sample produced concentrations of 16S rRNA higher than the negative control concentration, which made it impossible to generate results for this analysis. The samples from Laboratories A and C were analyzed for each of the eight microbial indicator detection systems. Once again, since the detected levels were barely higher than the device's detection limit, no result will reported for the ddPCR. The samples from Laboratory B were not analyzed by the detection systems since there was no reason to believe that the quantity of DNA would be any higher in this lab, allowing for processing of the results.

4.5.3 Microbial biodiversity

Because of the overly low quantity of DNA, biodiversity analyses by next-generation sequencing (NGS) were only done on the samples from Laboratory C. The amplicons were prepared by Génome Québec's innovation centre using 515F and 806R primers targeting a fragment of approximately 300 pairs of bases from region V4 of prokaryotic 16S rRNA (Table 4). The sequencing was done on the MiSeq platform (Illumina®, San Diego, CA, USA) using an amplification approach that produced twice 250 pairs of bases.

Table 4. Sequences of primers used for NGS

Primers	515F	GTGCCAGCMGCCGCGGTAA	References
	806R	GGACTACHVGGGTWTCTAAT	References

The sequences obtained were processed by the Canadian Centre for Computational Genomics (C^3G) using a programming script adapted to the project and the DADA2 bioinformatics tool (Callahan et al., 2016). After contiguous regions were assembled, the sequences obtained had fragment lengths between 257 and 264 pairs of bases. The sequences were grouped as amplicon sequence variants (ASV, or operating taxonomic units: OTU) before we started taxonomic identification using the SILVA reference database (Pruesse et al., 2012). The data produced by C^3G's bioinformatic analysis were processed with the MicrobiomeAnalyst tool (Dhariwal et al., 2017). Because of the very low number of ASVs obtained, the prevalence criteria were set at 10% and two counts; thus, two identical sequences had to be present in 10% of the samples to be retained in the analyses.

4.6 Aeraulic conditions and aerosol dispersion

The particle size distribution measurements and numerical concentrations, for which the methods were described above, constitute both independent results and also input parameters for the CFD simulations. These simulations were intended to describe air movements and the influence of ventilation on aerosol dispersion in the labs, with a high level of detail. In addition to the characteristics of the aerosols emitted during embalming, these simulations required the ventilation rates at the various air intakes and outlets as parameters. For purposes of comparison of the various simulated ventilation scenarios with reality, it was also necessary to experimentally obtain the ACH rate in the various premises.

4.6.1 Measurement of airflow at air intakes and outlets

Airflows at the intakes were measured using a balometer (Model 8710, TSI Inc., Shoreview, MN, USA) with a measurement range of from 42 to 4,250 m^3/h and accuracy of 3% of reading. Because of the different shapes and sizes of the outlets, their airflows were calculated on the basis of air speed measurements at different points in their zone. These measurements were done with a hot wire anemometer (Model 8355, TSI Inc.) with a measurement range of from 0.15 to 50 m/s and accuracy of 2.5% of reading.

4.6.2 Measurement of the rate of air changes per hour

The ACH rate was determined using the American Society for Testing and Materials' tracer gas technique (ASTM, 2017). A uniform concentration of a tracer gas, SF_6, is first established in the room being studied. Concentrations of SF_6 are then measured as a function of time and at different measurement points (volume fractions in parts per billion – ppb). The speed of the decrease in SF_6 concentrations enables the age of air at different measurement sites and its renewal rate to be assessed. The SF_6 concentration rates were measured at a height of 1.7 m, as recommended in the ASHRAE-55 standard (ASHRAE, 2004), with an Autotrac portable electron capture detector (Autotrac model 101, Lagus Applied Technology Inc., Escondido, CA, USA). The accuracy of this device is ± 5%.

The data on the decrease over time in the concentration of tracer gas (SF_6) in the rooms were also used to validate the calculation code chosen for the numerical simulations.

Finally, it should be mentioned that, if the volume of the room being studied is known, it is also possible to obtain ACH values from the balometer measurements. A good match between the ACH rates obtained with the two methods (SF_6 and balometer) strengthens the validity of the results.

4.6.3 Numerical simulation

The numerical simulations of the aerodynamic behaviour of bioaerosols for different emission scenarios and different ventilation strategies were done in the three embalming labs. These labs, identified with the letters A, B and C, differ in their surface area and the number of embalmments that can be carried out simultaneously. The characteristics of each lab are presented in Table 5. Schematic diagrams are also presented (Figure 2, Figure 3, Figure 4).

Table 5. Simulated characteristics of laboratories

Embalming lab	Volume (m^3)	Surface area (m^2)	Ventilation	
			Air delivery	Extraction
A	712.4	261.9	6 square diffusers on the ceiling	8 grilles on the ceiling and 8 grilles at the counter
B	66.8	27.8	None	1 grille on the ceiling
C	112.7	46.7	4 wall grilles and 1 square diffuser on the ceiling	4 wall grilles

As Figure 2 shows, Laboratory A is ventilated by six square air diffusers, located on the ceiling and labelled S1 to S6. This lab also has eight extraction grilles 20 cm × 20 cm, located above each bed, and eight 8 cm × 12 cm wall grilles, located at counter height.

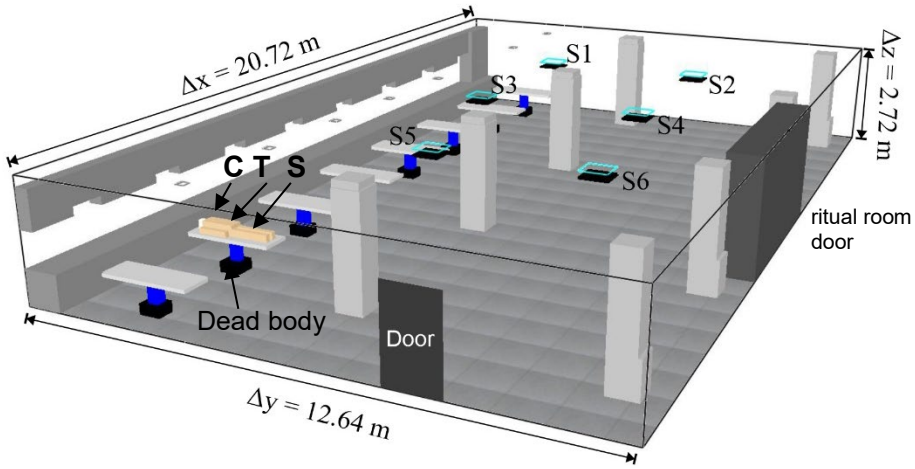

Figure 2. Schematic diagram of Laboratory A and sources for three aerosol-generating tasks (C = cannula, T = trocar, S = suturing).

In Laboratory B, which is smaller (Figure 3), a return air grille (44 cm × 80 cm), located on the ceiling, extracts the stale air from the room. The room does not have any diffusers or fresh air intake grilles. The extracted air is replaced by an infiltration flow under and over the entrance door to the laboratory.

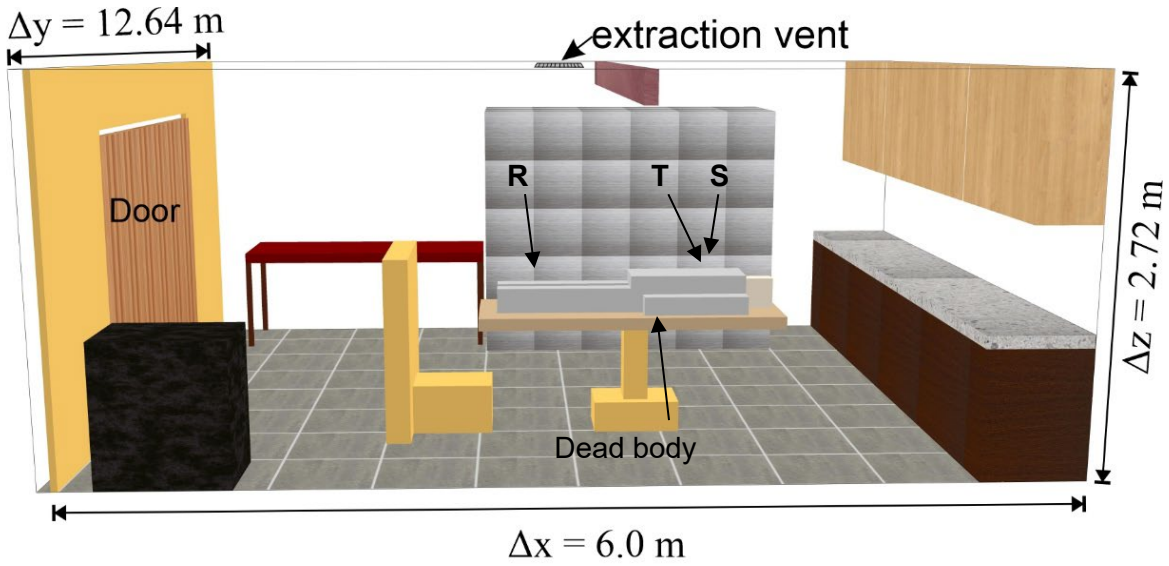

Figure 3. Schematic diagram of Laboratory B and sources for three aerosol-generating tasks (R = retractor, T = trocar, S = suturing).

Air enters Laboratory C (Figure 4) through four wall grilles labelled S1 to S4. In addition, this lab has an entrance area adjacent to the main room with a floor area of 9.6 m^2. This area is supplied with fresh air by a square diffuser on the ceiling labelled S5. The air is extracted by two grilles at floor level and two wall grilles at a height of 1.12 m above the floor. Laboratories A and C are ventilated by the dilution principle.

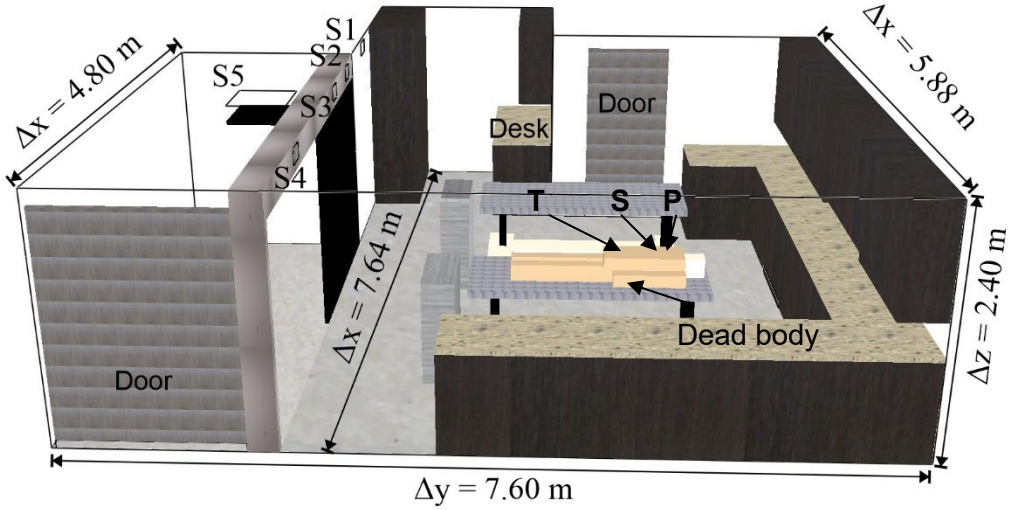

Figure 4. Schematic diagram of Laboratory C and sources for three aerosol-generating tasks (P = sealing powder, T = trocar, S = suturing).

To model the aerodynamic behaviour of bioaerosols and determine the effect of certain influencing factors, it is necessary to define realistic particle emission scenarios that are in phase with the experimental observations. These scenarios were chosen based on the time sequence of events reported and described in section 4.2. For each bioaerosol-generating activity, the modelling was done by hypothesizing that the aerodynamic diameter of the particles was identical to the median optical diameter measured by the WIBS-NEO during the activity in question. Table 6 presents the simulated scenarios for the three labs.

Table 6. Emission scenarios modelled

Laboratory	Activity	Aerodynamic diameter of particles emitted (µm)	Emission massflow rate (mg/s)	Emission duration (min)	Total mass of emitted particles (mg)	Location of emission source
A	cannula	1.18	4.00×10^{-5}	3	7.20×10^{-3}	plastron
	suturing	1.25	4.56×10^{-5}	2	5.47×10^{-3}	right leg
	trocar	0.99	2.34×10^{-5}	4	5.62×10^{-3}	stomach
B	retractor	1.58	0.76×10^{-5}	4	1.83×10^{-3}	right leg
	suturing	1.67	0.71×10^{-5}	3	1.28×10^{-3}	neck
	trocar	1.74	0.55×10^{-5}	5	1.64×10^{-3}	epigastric region
C	sealing powder	3.47	1.60×10^{-5}	3	2.88×10^{-3}	neck
	suturing	3.01	0.69×10^{-5}	5	2.07×10^{-3}	epigastric region
	trocar	3.68	0.14×10^{-5}	6	0.50×10^{-3}	navel

The location of the emission sources (tasks) for each activity is indicated in Figure 2, Figure 3 and Figure 4. The emission scenarios presented in Table 6 were modelled with four different ventilation rates and according to several ventilation strategies (Laboratories A and C). These ventilation conditions are summarized in Table 7. The ACH numbers in the grey table cells correspond to the number of ACH in the embalming rooms, determined experimentally based on tracer gas measurements. The values of 1 and 4 ACH were retained in accordance with recommendations from Quebec (Lajoie et al., 2011) and France (Guez-Chailloux et al., 2005). The American Society of Heating, Refrigerating and Air-Conditioning Engineers (ASHRAE), a professional association, has not issued any specific recommendations for embalming labs. However, a ventilation rate of 12 ACH was chosen based on ASHRAE's recommendations for autopsy departments (ASHRAE, 2017).

Seven air delivery strategies were simulated for Laboratory C. These strategies consisted in setting the total ventilation rate (Q_T) at 7.51 m^3/min, or 4 ACH, and varying the airflow suppled by diffuser S5 (Q_{S5}) in relation to the flow from the four wall grilles (S1 to S4). Similarly, three strategies were studied for Laboratory A. In that case, the ACH was set at 2.1 (Q_T = 24.93 m^3/min)

and the airflow supplied by diffusers S2, S4 and S6 varied in relation to the air supplied by diffusers S1, S3 and S5 (Figure 2).

Table 7. Number of air changes per hour (ACH) and air delivery strategies

Laboratory	Number of ACH (h^{-1})	Air delivery strategies
A	1	-
	2.1	$\frac{(Q_{s2}+Q_{s4}+Q_{s6})}{Q_T}=[44, 54, 64]\%$
	4	-
	12	-
B	1	-
	4	-
	10.3	-
	12	-
C	1	-
	4	$\frac{Q_{s5}}{Q_T}=[0, 6, 30, 48, 70, 86, 94]\%$
	7.9	-
	12	-

The numerical simulations were done with Fire Dynamics Simulator software (FDS version 6.7.1), which has been the subject of verification (McGrattan et al., 2019a) and validation studies (McGrattan et al., 2019b). The methodology applied for modelling the ventilation and aerodynamic behaviour of bioaerosols is identical to that described in report R-879 published by the IRSST in 2015 (Lavoie et al., 2015). Nevertheless, only the Eulerian model was retained in this study. This model is based on the solution of a passive scalar transport equation, modified to take into account particle sedimentation and turbulent deposition on the walls of the modelled rooms. This model does not consider particle inertia, which limits its use to diameters on the order of 10 μm at most (Parker et al., 2010). A grid independence study was done for each lab modelled, which led to the selection of grids with 4.03×10^6, 1.06×10^6 and 1.75×10^6 nodes for Laboratories A, B and C, respectively.

Each air delivery strategy underwent preliminary initialization of the velocity field. For example, modelling at 4 ACH of the “suturing” scenario in Laboratory A was done twice. The first modelling, without bioaerosol generation, was done for sufficient time (typically 900 s) to obtain an established velocity field. Then, the velocity field served as an initial condition for modelling with bioaerosol generation. This approach was applied to the 20 air delivery scenarios presented in Table 6. The final time for simulating the exposure scenarios was set at 30 minutes.

5. RESULTS AND DISCUSSION

5.1 Aerosols and bioaerosols

5.1.1 Emission profiles per laboratory during embalmments

For each of the three labs visited, the daily changes over time in the emission factor for fluorescent (biological) and non-fluorescent (non-biological) particles are presented (Figure 5, Figure 6, Figure 7). This factor corresponds to the ratio of the particle concentration measured at time *t* (C) over the baseline level (C_0). Each of the graphs also shows the tasks (keywords) that were done, matched with the main emission peaks. The peaks without such notes are either unidentified or attributable to tasks that generated more marked increases at another point in the embalming process. The identification of tasks in these figures shows that a majority of the tasks defined by a keyword generated marked increases in the concentration of fluorescent and/or non-fluorescent particles.

A. Laboratory A

The baseline level, C_0, for Laboratory A is 0.45 particles/cm^3 for non-fluorescent particles and 0.13 particles/cm^3 for fluorescent particles. For Laboratory A, it is noteworthy that the concentrations of fluorescent particles increase more than those of non-fluorescent particles in relation to their respective baselines. Thus, the fluorescent particle emission factor is mainly between 3 (0.39 particles/cm^3) and 7 (0.91 particles/cm^3), whereas the emission factor for non-biological particles is usually close to 2 (0.90 particles/cm^3), with maximums of approximately 3 (1.35 particles/cm^3).

In general, we observe greater variability in concentrations of the fluorescent fraction. Indeed, Figure 5 shows that the appearance of peaks of biological particle concentration is not necessarily correlated with an increase in the number of non-fluorescent particles. There is a very visible example during a “suturing, powdering” operation. Emissions of fluorescent particles during operations corresponding to the keywords “suturing, powdering,” “plastic wrapping,” “trocar,” “cannula, incision, injection,” “washing, drying,” “table cleaning” and “manipulation” are clearly identifiable for Laboratory A. Although substantial emission factors may be reached while a task is being performed, it is important to remember that levels achieved at a particular point may not be due only to that task but may be attributable to an accumulation of particles related to actions in the recent past.

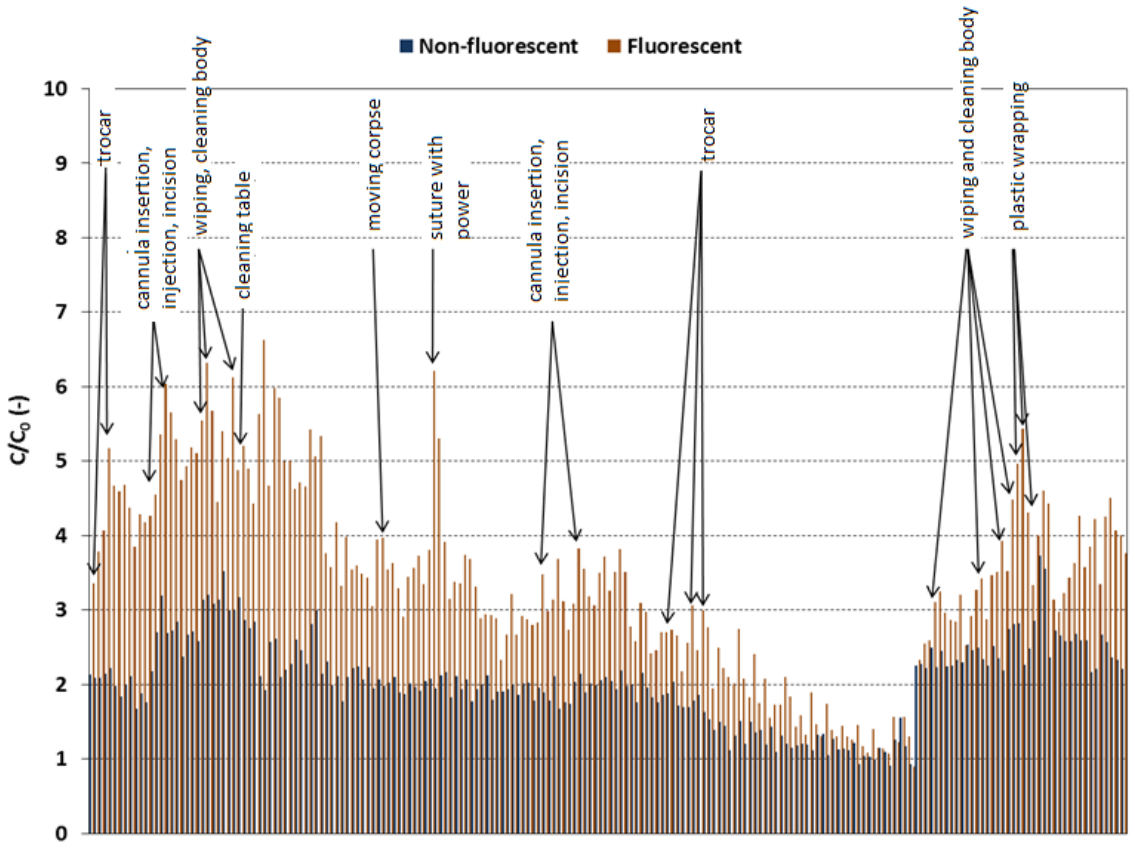

Figure 5. Chronology of emission factors (C/C_0) for fluorescent and non-fluorescent particles for Laboratory A (total duration: 207 min).

B. Laboratory B

The baseline level, C_0, for Laboratory B is 1.41 particles/cm^3 for non-fluorescent particles and 0.24 particles/cm^3 for fluorescent particles. Unlike Laboratory A, concentrations of fluorescent particles increase in similar proportions to those of non-fluorescent particles. The fluorescent and non-fluorescent emission factors fall between 1 (0.24 particles/cm^3 for fluorescent particles and 1.41 particles/cm^3 for non-fluorescent particles) and 2 (0.48 particles/cm^3 for fluorescent particles and 2.82 particles/cm^3 for non-fluorescent particles). Maximums of approximately 4 (0.96 particles/cm^3) and 2.5 (3.53 particles/cm^3), respectively, were observed for the fluorescent (bioaerosols) and non-fluorescent fractions (non-biological particles).

Figure 6 shows an overall synchronization of the main fluctuations in emission factors for the two kinds of particles in Laboratory B. Emissions of fluorescent particles during the “preparation, equipment cleaning,” “suturing, powdering,” “plastic wrapping,” “trocar,” “cannula, incision, injection,” “washing, drying,” and “retractor” operations are clearly identifiable in this lab.

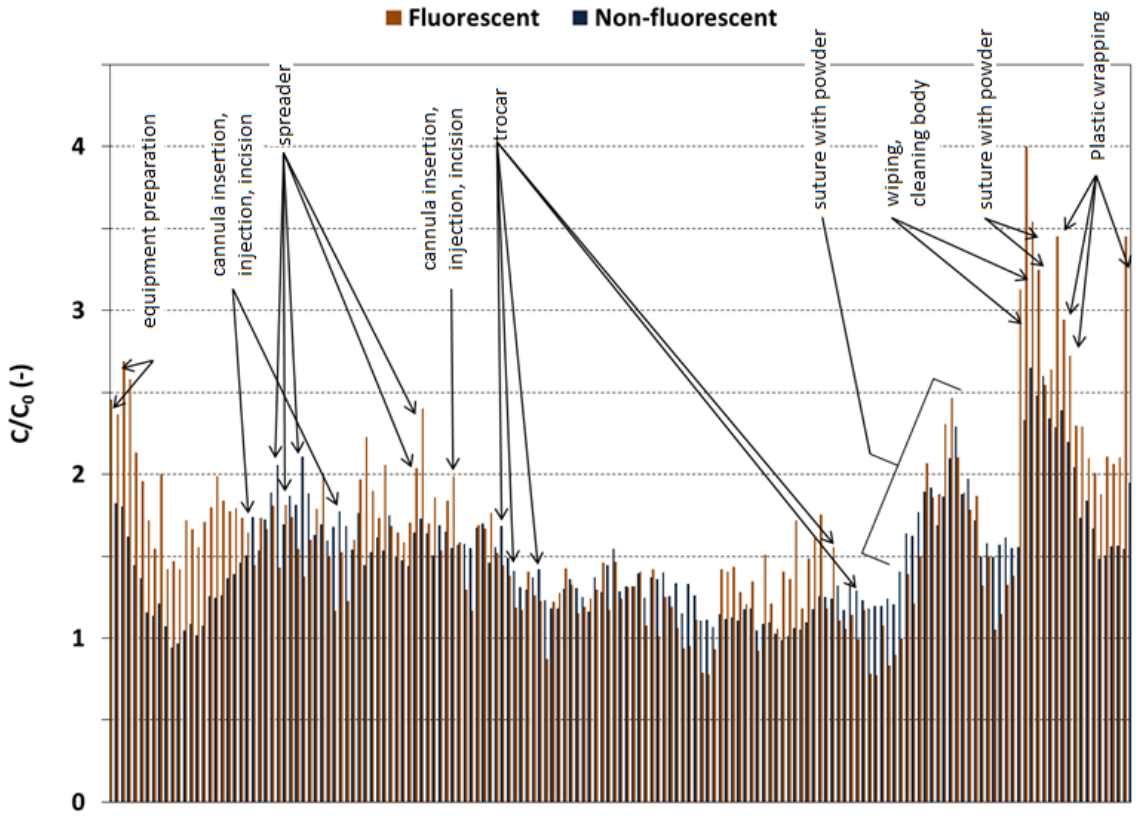

Figure 6. Chronology of emission factors (C/C_0) for fluorescent and non-fluorescent particles for Laboratory B (total duration: 210 min).

C. Laboratory C

In this laboratory, two separate baseline levels (C_0) had to be established (AM and PM) for non-fluorescent particles. These baseline levels are 1.44 particles/cm^3 (AM) and 0.31 particles/cm^3 (PM). As for fluorescent particles, the baseline level is 0.17 particles/cm^3 – the same for both periods. As in Laboratory A, concentrations of fluorescent particles increase more sharply than concentrations of non-fluorescent particles over their respective baseline levels. The emission factors for non-fluorescent particles fall between 1 and 2 (0.31 particles/cm^3 (PM) and 2.88 particles/cm^3 (AM)), whereas those for fluorescent particles range between 1 and 5.5 (0.17 particles/cm^3 and 0.93 particles/cm^3). Laboratory C stands out mainly due to its very high and simultaneous emission peaks for fluorescent particles (between 2.04 particles/cm^3 and 7.65 particles/cm^3, emission factors ranging from 12 to 45) and non-fluorescent particles (between 0.93 particles/cm^3 and 26.35 particles/cm^3, emission factors ranging from 3 to 85).

In this lab, emissions of fluorescent particles during the “orifice occlusion,” “suturing, powdering,” “trocar,” “cannula, incision, injection,” “washing, drying,” “manipulation,” “preparation, equipment cleaning,” and “table cleaning” operations are clearly identifiable in Figure 7.

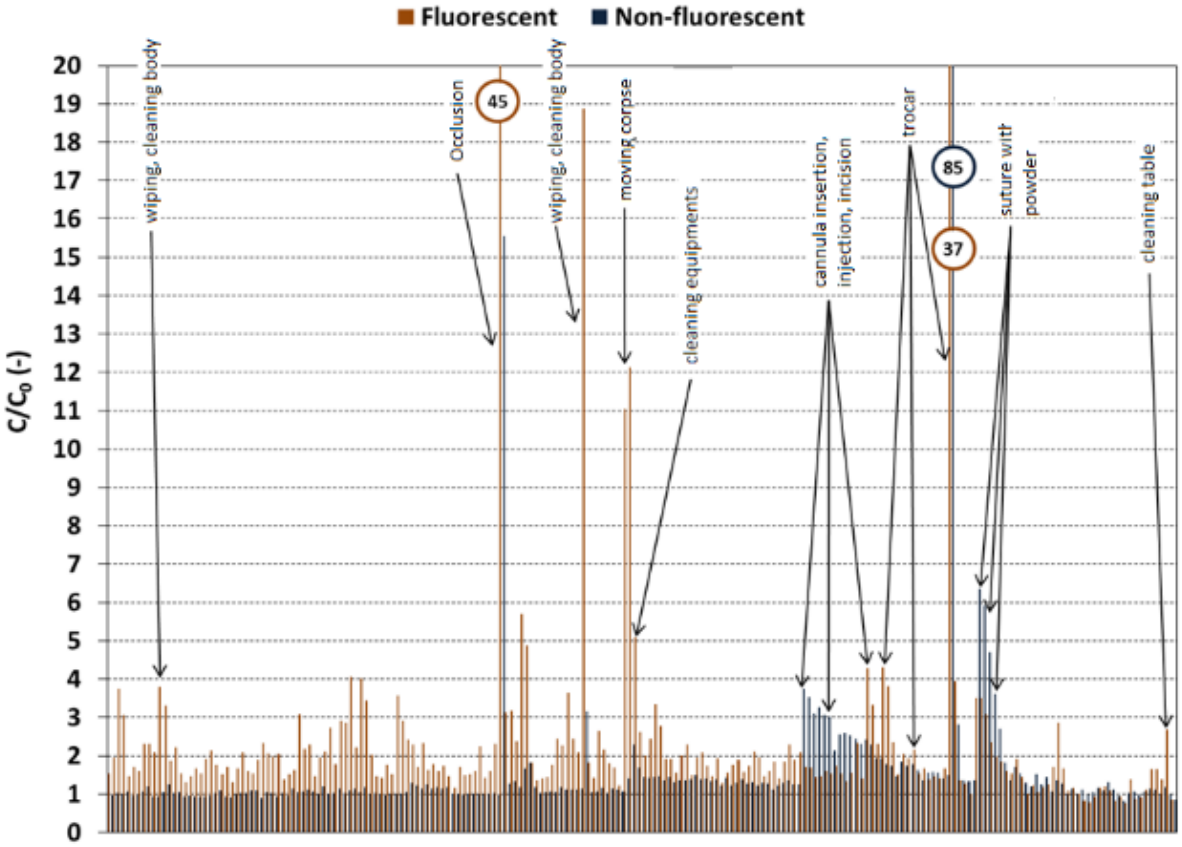

Figure 7. Chronology of emission factors (C/C_0) for fluorescent and non-fluorescent particles for Laboratory C (total durations: AM – 211 min, PM – 147 min).

D. Comparison of concentrations and emission factors between laboratories

Figure 8 presents the concentrations and emission factors for fluorescent and non-fluorescent particles measured in each lab.

For fluorescent particles, in addition to showing relatively similar concentrations among labs, the results present a fairly low dispersion rate compared to the non-fluorescent fraction. For Laboratory C, there were some notably extreme values; for example, five points exceeded 1.9 particles/cm^3 and reached as much as 7.65 particles/cm^3.

For non-fluorescent particles, the concentrations are higher than for fluorescent particles. In addition, the concentrations in Laboratory B are higher than in Laboratories A and C. For Laboratory C, we observe, as with fluorescent particles, extreme values of as much as 26.35 particles/cm^3.

Concerning emission factors, the graph shows the dispersion of values for each parameter and each lab. We can see that the emission factors in Laboratory A are more dispersed than in Laboratories B and C. We can also note that Laboratory C has the highest emission factors, reaching as much as 45 times the baseline level, compared to less than 7 times for Laboratories

A and B. In addition, the emission factors for the fluorescent fractions are higher than those for non-fluorescent particles in all three laboratories.

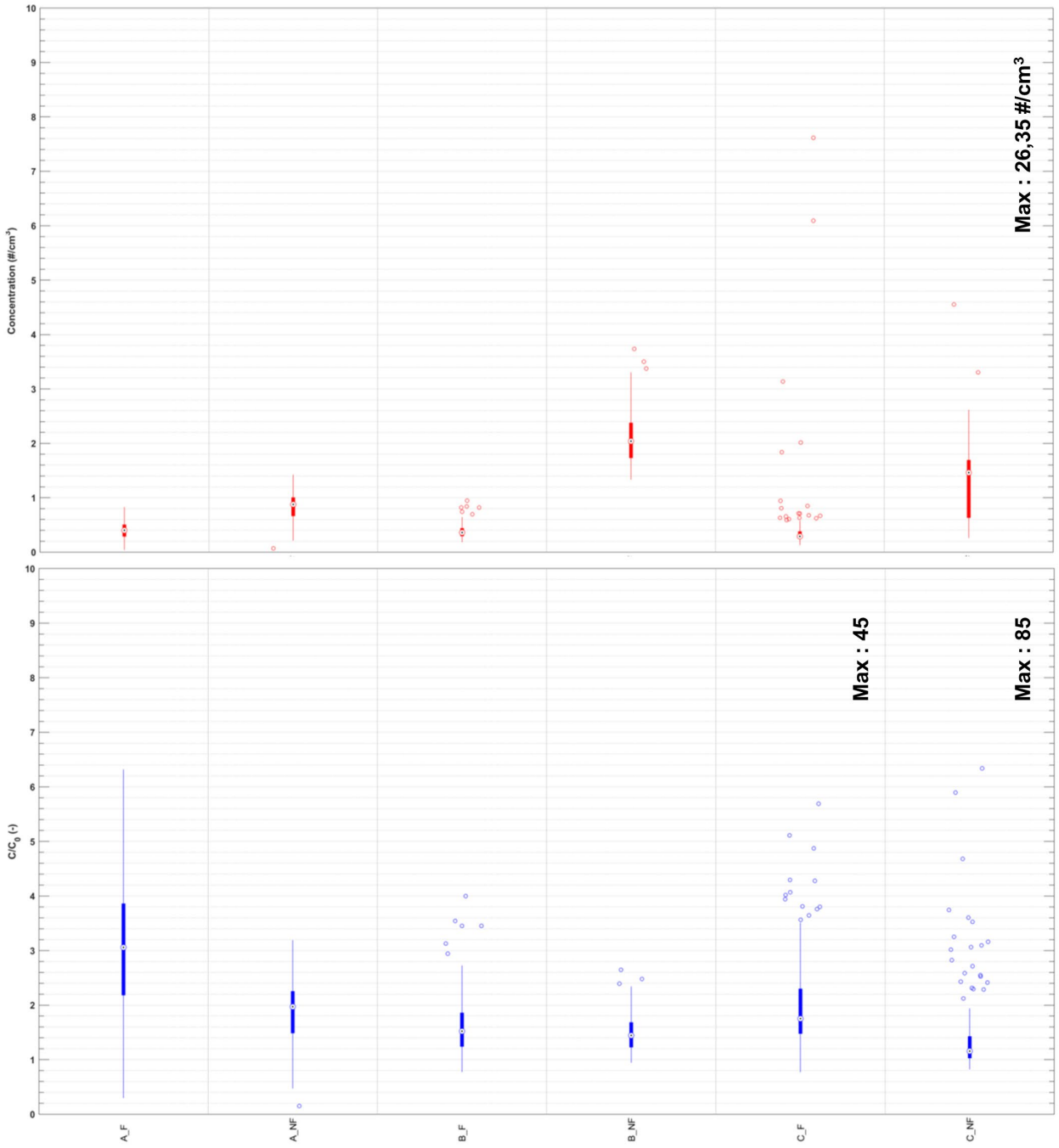

Figure 8. Concentration (top) and emission factor (bottom), by laboratory (A, B and C), of fluorescent (F) and non-fluorescent (NF) particles.

The results show that Laboratory C differs from Laboratories A and B given its occasionally very high emission factors, reaching as much as 85 x C_0. The field observations suggest that the embalmer's practices might explain these extreme data.

5.1.2 Comparison of the various tasks' emission characteristics for each laboratory

The results presented above have revealed that, for all three laboratories visited, there were emission peaks that were attributed to the tasks defined by keywords. Several of these tasks recurrently appeared to generated biological or non-biological particles. In this section, the concentrations and emission factors are compared for each keyword. Beyond comparisons of the tasks with each other, the graphs presented below allow us to compare the concentrations and emission factors of fluorescent and non-fluorescent particles for each task.

A. Laboratory A

Concentrations

The concentrations of non-fluorescent particles vary from one task to another, ranging from 0.62 particles/cm^3 for "suturing, powdering" and 1.11 particles/cm^3 for "plastic wrapping" (Figure 9), excluding "shaving/depilation" (1.37 particles/cm^3) and "table cleaning" (1.35 particles/cm^3), which only occurred once each. The low frequency of these two tasks in the lab means there is a high level of uncertainty as to the levels measured. All the other tasks were performed between 4 and 32 times. Four tasks ("orifice occlusion," "suturing, powdering," "washing, drying" and "plastic wrapping") present greater variability in concentrations of non-fluorescent particles. Conversely, "massage" is exceptional in having very low variability.

Unlike non-fluorescent particles, the concentrations of bioaerosols vary little from one task to another. Concentrations fall between 0.25 particles/cm^3 ("suturing, powdering") and 0.56 particles/cm^3 for "plastic wrapping," considering only the tasks that were performed more than once. From the point of view of variability of concentrations, Figure 9 shows that the same four tasks stand out for both fluorescent and non-fluorescent particles. It is important to remember that, despite the low variation in concentrations of bioaerosols, certain tasks can occasionally trigger marked increases ("cannula, incision, injection," "orifice occlusion," "suturing, powdering," "washing, drying," and "plastic wrapping").

Emission factors

Logically enough, the behaviour of emission factors is similar to that of concentrations. Considering only the tasks observed multiple times, the maximum emission factor for non-fluorescent particles is 2.48 for "plastic wrapping."

As for fluorescent particles, the emission factors for tasks observed multiple times range between 1.95 and 4.3; these are "suturing, powdering" and "plastic wrapping."

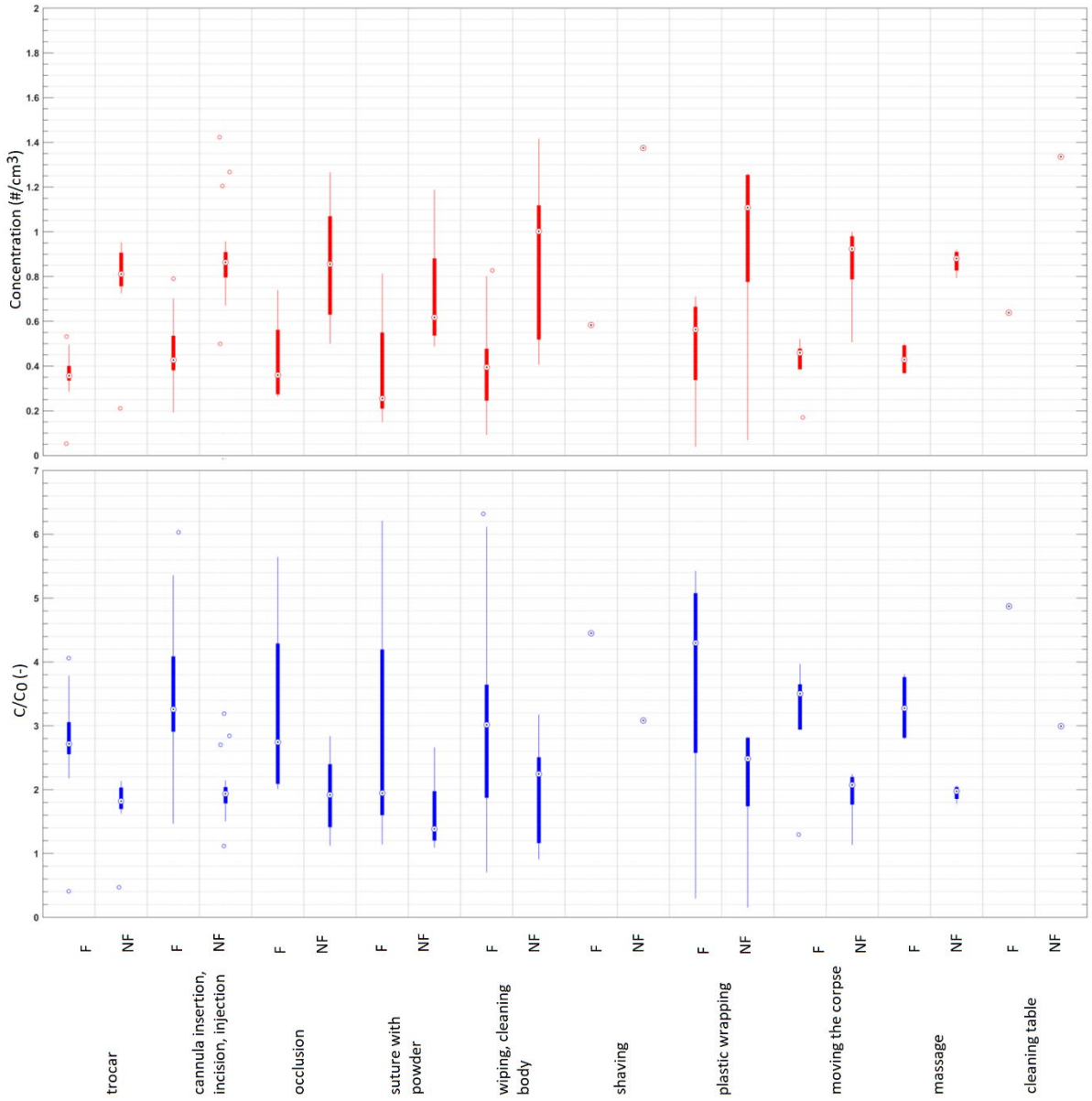

Figure 9. Concentration (top) and emission factor (bottom), of fluorescent (F) and non-fluorescent (NF) particles, per task, for Laboratory A.

Beyond the values for concentrations and emission factors of fluorescent and non-fluorescent particles, Figure 9 highlights, above all, the preferential aerosolization of bioaerosols during embalming. Indeed, even though the concentrations of bioaerosols (fluorescent fraction) are lower than those of non-biological particles, there is a clear opposite tendency for emission factors since the fluorescent fractions are higher than the non-fluorescent fractions for a given task.

Granulometry

The particle size distributions of fluorescent particles and their fraction per size are depicted in Figure 10 for four of the most aerosol-generating tasks: “plastic wrapping,” “manipulation,” “massage,” and “cannula, incision, injection.” This figure reveals the existence of an almost unique profile in terms of both particle size distribution and fluorescent fractions. Indeed, the concentration of fluorescent particles decreases monotonically at the same time as the diameter of the particles increases. Conversely, their proportion of the total aerosols tends to grow with the diameter of the particles, reaching 50% and 80%, respectively, for particles more than 1 and 2 µm in diameter. Although we cannot explain this, it is noteworthy that, for “massage” and “manipulation,” the fluorescent fraction decreases substantially and briefly for particles 3 µm in diameter before regaining the same general appearance as the other curves.

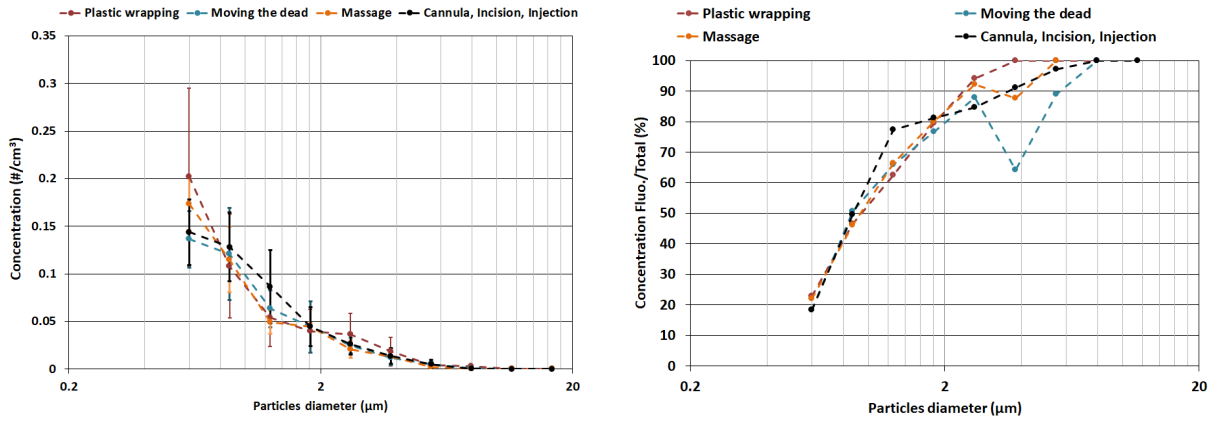

Figure 10. Concentration of fluorescent particles (left) and fluorescent fraction (right), for the four most aerosol-generating tasks in Laboratory A, according to particle size.

B. Laboratory B

Concentrations

As in Laboratory A, the concentrations of non-fluorescent particles differed little from one task to another: between 1.62 particles/cm^3 (“shaving, depilation”) and 2.82 particles/cm^3 (“plastic wrapping”) (Figure 11), excluding “manipulation,” a task that was only observed twice in this lab. All the other tasks occurred between 5 and 29 times each. However, the variability of concentrations of non-biological particles for the different tasks was lower than in Laboratory A; two tasks stood out for their fairly low value dispersion: “shaving, depilation” and “trocar.”

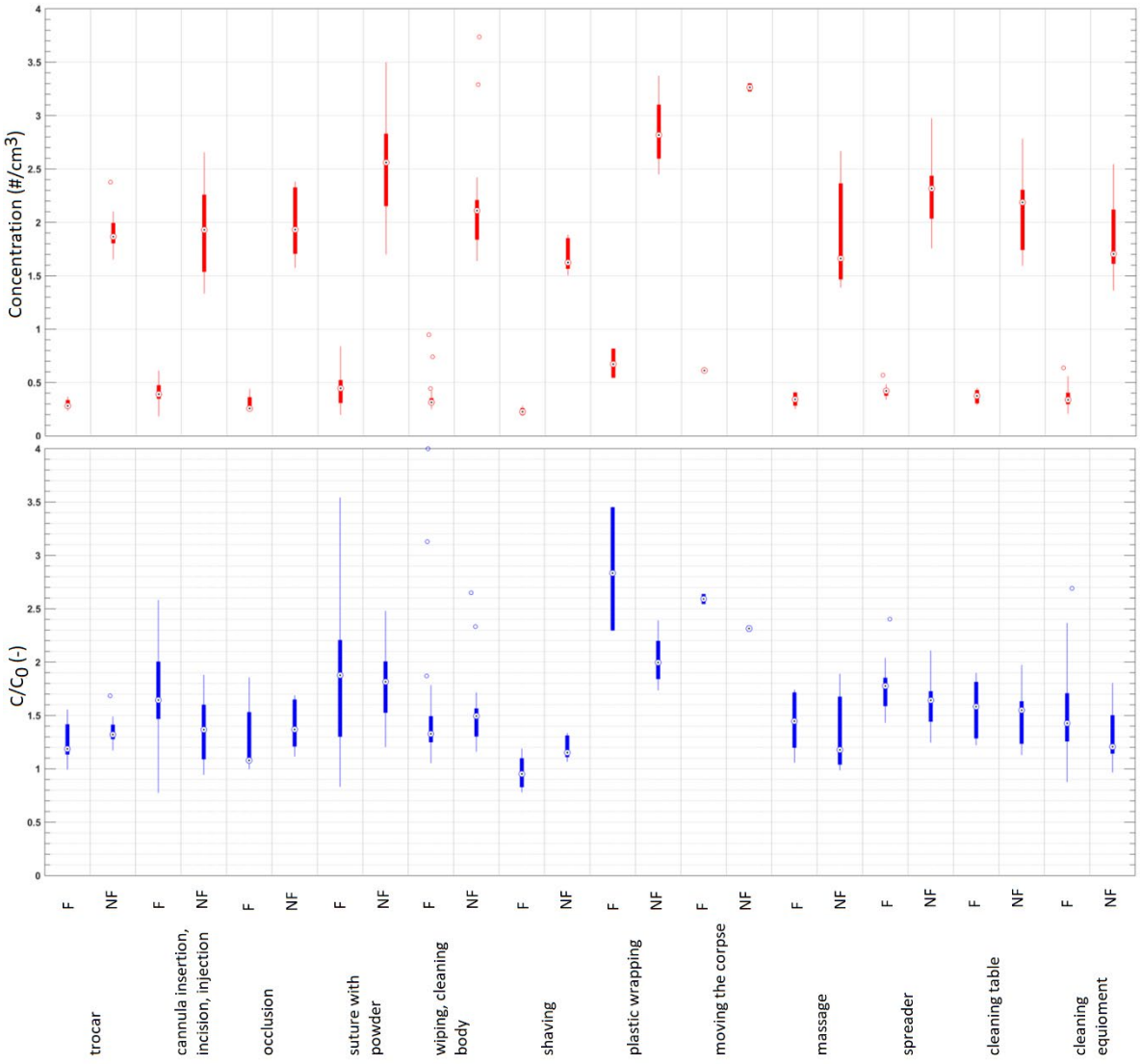

Figure 11. Concentration (top) and emission factor (bottom), of fluorescent (F) and non-fluorescent (NF) particles, per task, for Laboratory B.

Like non-fluorescent particles, the concentration of bioaerosols varied little from one task to another and was comparable to that measured in Laboratory A. The median value for concentration fell between 0.23 particles/cm^3 (“shaving, depilation”) and 0.67 particles/cm^3 (“plastic wrapping”). Similarly to Laboratory A, “plastic wrapping” appeared to be the task that generated the most fluorescent particles. Unlike non-fluorescent particles, Figure 11 shows that four tasks stand out due to their greater variability: “plastic wrapping,” “washing, drying,” “preparation, equipment cleaning” and “suturing, powdering.”

Granulometry

Regarding the particle size distributions of fluorescent aerosols, the higher concentrations observed for particles larger than 1 µm, measured for the various tasks in Laboratory B, but also for the baseline levels, seem to be related to the fact that its ventilation system included only one air extraction outlet and no intake of filtered air.

Figure 12 presents the same types of data for three tasks as Figure 10. It shows that two profiles tend to emerge regarding the particle size distribution of biological particles. Emissions from the "plastic wrapping" and "suturing, powdering" tasks are comparable, even though the absolute values of the concentrations are different. The profiles present a plateau for particles with a diameter between 0.9 and 4 µm. The distribution of bioaerosols during "manipulation" of bodies is very similar, except that there is a peak for particles approximately 0.9 µm in diameter.

However, regarding the fluorescent fraction, there is no difference in the profiles presented in Figure 12. In fact, apart from a decline in particles more than 8 µm in diameter during "plastic wrapping," the fluorescent fraction of aerosols increases with particle diameter in the same way for the three tasks selected. Thus, 50% of the 2.5 µm particles and 80% of the 6 µm particles are fluorescent. Finally, it is interesting to note that the results for Laboratory A and Laboratory B differ mainly in respect of the greater emission of particles more than 1 µm in diameter in Laboratory B, which explains the shift in the diameters corresponding to the 50% and 80% fluorescent fractions.

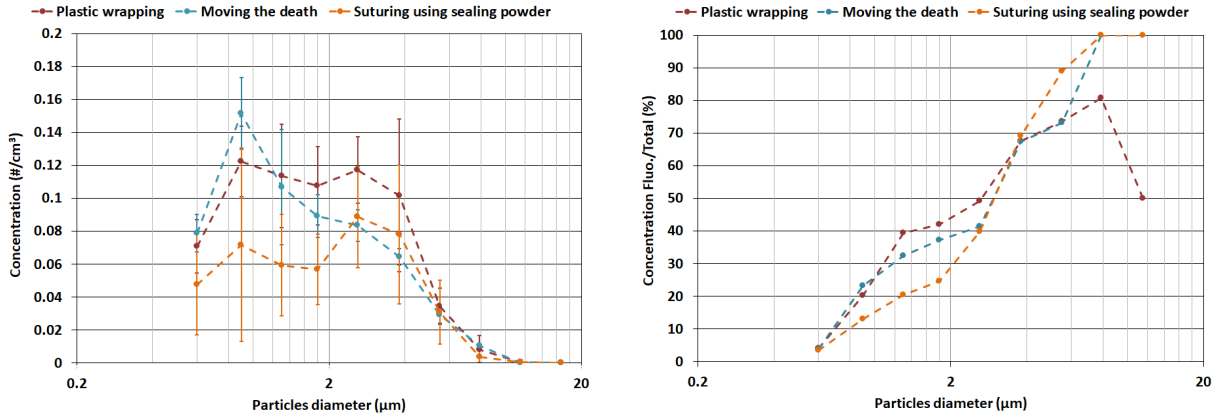

Figure 12. Concentration of fluorescent particles (left) and fluorescent fraction (right), for the three most aerosol-generating tasks in Laboratory B, according to particle size.

C. Laboratory C

Concentrations

As in the other two labs, the concentrations of non-fluorescent particles varied moderately from one task to another: between 0.58 particles/cm^3 ("trocar") and 1.78 particles/cm^3 ("retractor") (Figure 13). Six tasks showed particularly variable concentrations of non-biological particles: "preparation, equipment cleaning," "trocar," "orifice occlusion," "suturing, powdering," "washing,

drying" and "manipulation." In particular in this lab, the reported minimum and maximum concentrations of non-biological particles should not obscure the presence of the extreme values mentioned above ("trocar": 26.35 particles/cm^3 and "orifice occlusion": 22.32 particles/cm^3).

The concentration of bioaerosols varies less from one task to another but remains on the same order of magnitude as measured in Laboratories A and B. This concentration falls between 0.26 particles/cm^3 ("washing, drying") and 0.38 particles/cm^3 ("table cleaning"). The tasks already identified as having particularly variable concentrations of non-fluorescent particles stand out in the case of bioaerosols as well. Finally, extreme values are also found here for the same tasks that produced the very high concentrations of non-fluorescent particles, with levels of 6.30 particles/cm^3 ("trocar") and 7.65 particles/cm^3 ("orifice occlusion").

Emission factors

The emission factors for non-fluorescent particles vary moderately among tasks, from 1.09 ("cannula, incision, injection") to 1.51 ("massage"). Exceptionally for non-fluorescent particles, there is a difference between the least emitting and most emitting tasks in terms of concentration and emission factor. This is related to the consideration of two different baseline levels during the sampling day (AM/PM) for these particles.

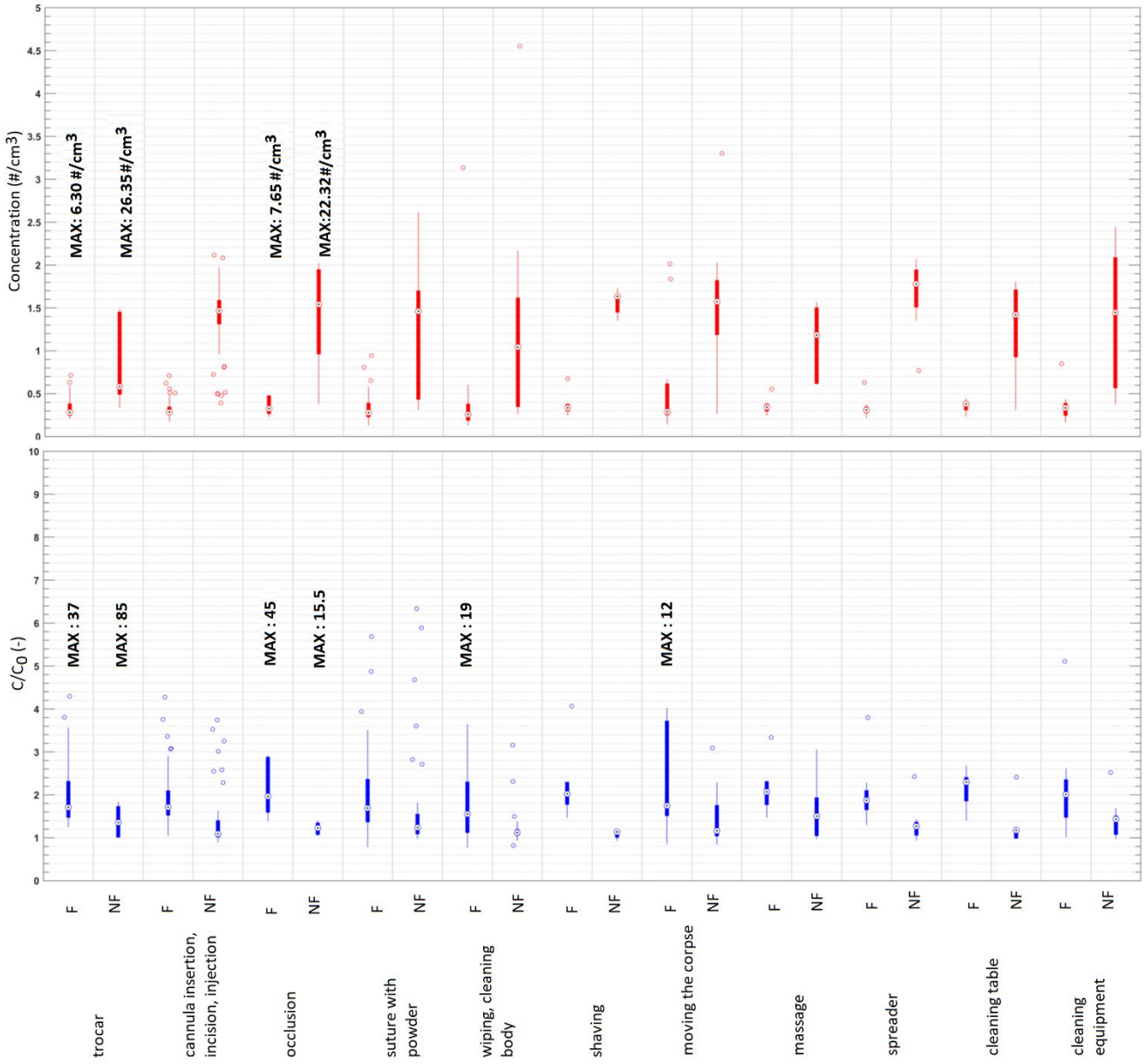

Figure 13. Concentration (top) and emission factor (bottom), of fluorescent (F) and non-fluorescent (NF) particles, per task, for Laboratory C.

For fluorescent particles, the emission factor for the various tasks ranged between 1.56 and 2.29; these values correspond to the “washing, drying” and “table cleaning” tasks, respectively.

The representation of emission factors better illustrates the extreme aerosolizations detected during embalmments in Laboratory C. Thus, the extreme concentrations of biological and non-biological particles described above correspond, respectively, to emission factors of 37 and 85 (“trocar”) and of 45 and 15.5 (“orifice occlusion”). Figure 13 presents more details on the other noteworthy extreme emission values that were already shown in part in Figure 7, such as those

reached during “washing, drying” and “manipulation” of the bodies, with maximum emission factors of 19 and 12, respectively. Finally, short-term peaks in bioaerosol emission are also observable for the “suturing, powdering” and “preparation, equipment cleaning” tasks.

As at Laboratory A, Figure 13 clearly shows the preferential aerosolization of bioaerosols during embalming.

Granulometry

Four tasks for Laboratory C were selected to best present the actions that generated the most particles or had some kind of singular feature in their particle size distribution (Figure 14, left). This figure reveals the existence of two separate profiles. Thus, the emission profile as a function of particle size for the “manipulation” and “table cleaning” tasks is very comparable to the profiles illustrated for Laboratory A, with a regular decrease in the concentration of fluorescent particles as the particles become larger. The second kind of profile concerns “trocar” use and the “orifice occlusion” task and takes the form of a peak centred at a diameter of 4 µm, for a size ranging from 2 to 8 µm. For this profile, the concentration of fluorescent particles with diameters less than 2 µm appears to be almost constant and shows similar levels for all four selected tasks. Finally, it is interesting to note that the 4 µm diameter, for which a peak in concentration is observable, also corresponds in the case of the “trocar” task to a marked 30% to 60% increase in the fluorescent fraction (Figure 14, right). The peak in emission of particles with a 4 µm diameter during “orifice occlusion” operations also involves the generation of primarily fluorescent particles (80%).

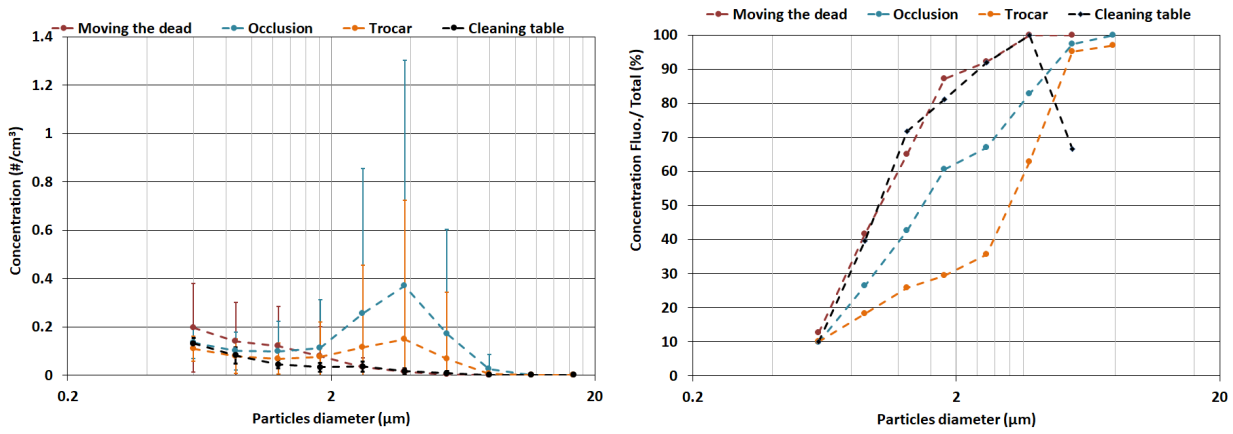

Figure 14. Concentration of fluorescent particles (left) and fluorescent fraction (right), for the four most aerosol-generating tasks in Laboratory C, according to particle size.

5.1.3 Real-time data analysis

In this section, we will recapitulate the highlights, some of which are common to all three labs. Although the median levels achieved appear low, at approximately 0.2 to 0.5 biological particles per cm^3 of air, this still represents between 200,000 and 500,000 particles per m^3. Ultimately,

these concentrations do not appear negligible when one considers that a worker inhales 10 to 20 litres of air per minute during low-intensity work. Thus, this represents between 2,000 and 10,000 particles inhaled each minute.

Another major point concerning embalmers' exposure is undoubtedly the preferential aerosolization of fluorescent particles, whether we consider the temporal evolution of fluorescent and non-fluorescent emission factors or their median values for each task. Thus, on the basis of measurements done with the WIBS-NEO, there is a strong presumption that bioaerosols are generated during embalming. Nevertheless, it appears that the various tasks are not equivalent with regard to increases in concentration or the frequency of such increases. Although the median concentration does not differ much from one task to another, certain actions are easily distinguishable for their ability to generate short-term peaks in bioaerosol emissions. The main tasks in question are "suturing, powdering," "trocar," "washing, drying," "plastic wrapping" and "orifice occlusion." To assess whether a certain logic is discernible in the appearance of short-term peaks in bioaerosols during different tasks, the tasks were grouped according to the following different mechanisms or processes, which are potentially responsible for aerosolization:

Emission due to bellows effect: ejection of air by means of compression ("suturing, powdering," "orifice occlusion," "plastic wrapping");

Emission due to splashing: projection related to the use of water ("washing, drying," "table cleaning," "preparation, equipment cleaning");

Inertial emission: during an aspiration process, particles that escape the suction element and become suspended ("trocar");

Emission due to venous insertion: emission triggered by the incision or insertion of an object into a vein or artery ("cannula, incision, injection," "retractor");

Emission due to friction: emission or resuspension due to friction ("manipulation," "shaving, depilation," "massage").

Since the baseline concentrations of bioaerosols varied from one lab to another, the maximum bioaerosol emission factors were considered in order to compare tasks. For each laboratory, the emission factors for each of the 12 tasks were ranked in decreasing order and the mean rank for the various emission mechanisms presented above was calculated. Figure 15 presents the results of this classification based on the mechanism responsible for aerosolization. The bellows effect and splashing account for the tasks that generated the most bioaerosols. Bioaerosol emission due to the bellows effect is intensified by the addition of sealing powder and formaldehyde during the "suturing, powdering" and "plastic wrapping" operations, respectively. These powders, which are initially non-fluorescent, become fluorescent upon contact with the human body before being resuspended due to the bellows effect. Finally, the case of inertial emissions generated by the use of the "trocar" should be modulated. Although the aspiration generated by the trocar logically limits the quantity of particles emitted and explains its relatively low rank in Figure 15, it should be remembered that trocar use can also result in significant emission peaks, particularly if the trocar is removed roughly, in an uncontrolled way, from the dead body (e.g., Laboratory C: fluorescent and non-fluorescent emission factors of 37 and 85, respectively).

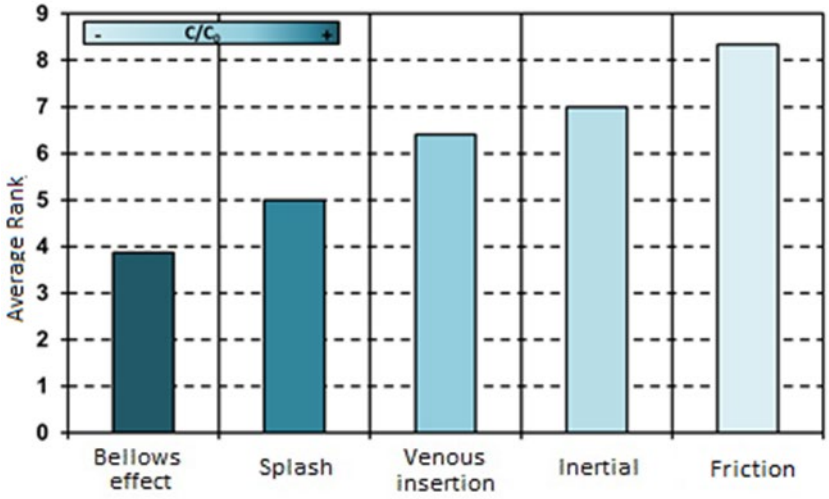

Figure 15. Mean rank of maximum bioaerosol emission factors (in decreasing order), according to aerosolization mechanism.

As mentioned in the description of the various labs, air is supplied to Laboratory B by infiltration from the neighbouring garage. In general, this kind of heated room with a high humidity level is propitious for the development of mould, which may potentially explain the larger diameter of the particles present in the baseline level for fluorescent emissions. However, it is interesting to note that this coarser mode does not mask certain increases in concentration (Figure 16). Particularly in this laboratory, trocar use generates an increase in the number of 3 to 4 µm particles coherent with what is measured in Laboratory C.

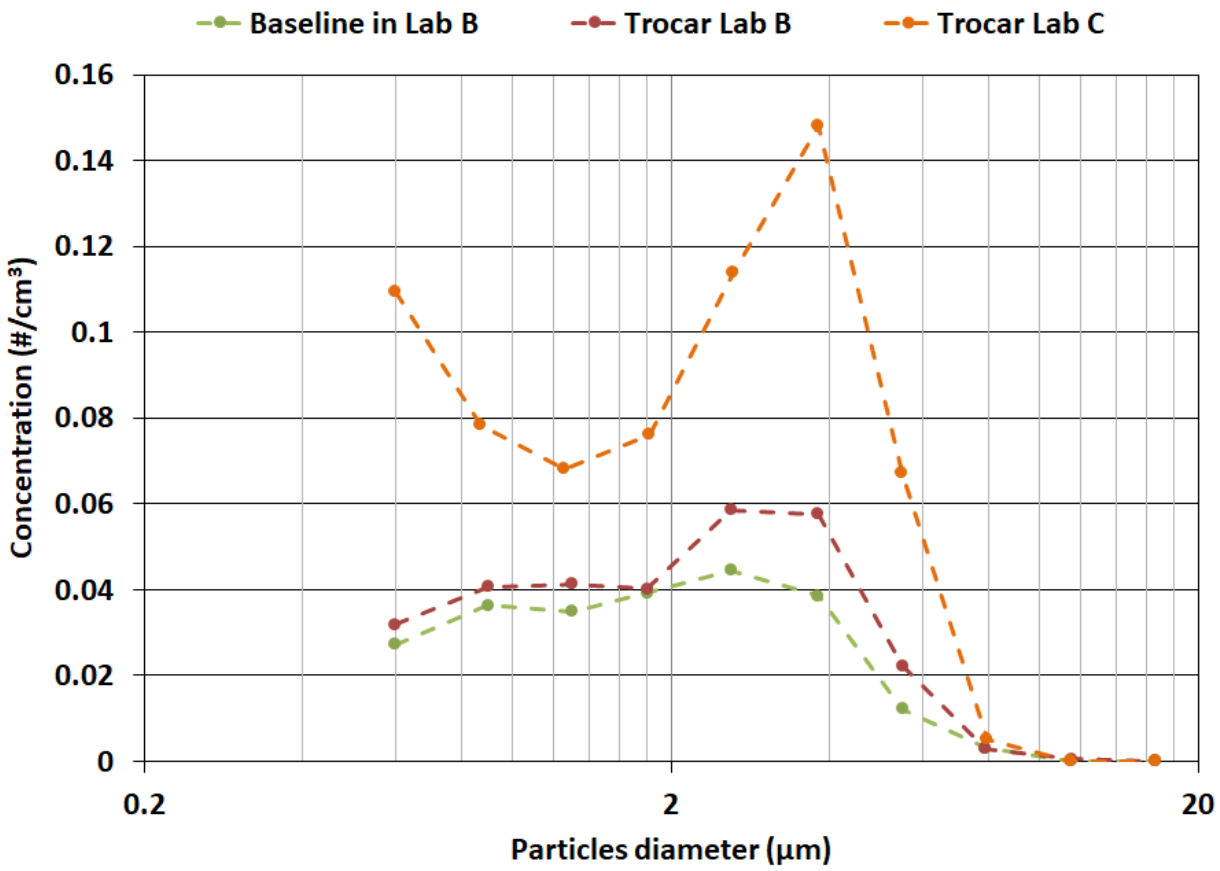

Figure 16. Comparison of mean particle size distributions of bioaerosols, for Laboratories B and C.

5.2 Cultural bacterial microbiota

5.2.1 Ambient air

A. Concentrations

The concentrations of culturable bacteria sampled in the ambient air with the Andersen are presented for each laboratory in Figure 17, Figure 18 and Figure 19. The samples were taken successively and represent time variations at 15-minute intervals. Although the concentrations of culturable microbiota remain generally low (< 100 colony-forming units [CFU]/m^3 of air), it is still possible to distinguish at least one period for each laboratory during which concentrations increased considerably compared to others. It should be pointed out that these results represent mean concentrations over 15 minutes, which makes it difficult to detect short-term increases and to associate them with a particular task. In addition, the relation between concentrations of culturable bacteria and the temporal profiles of fluorescent particles obtained with the WIBS-NEO could only be determined for Laboratory B, since the samples of culturable bacteria were not taken on the same day in the other two labs.

For Laboratory A, Figure 17 reveals that some samples had higher concentrations than the others. A link between the increase in bacteria concentrations and the use of water to clean the table or the body was possible three times in this lab. Concentrations three times higher than baseline are observable for two of these three occurrences. Cleaning the floor with a mop also created an increase in the concentrations measured. In this lab, a third association is possible in an episode when the trocar was accidentally inverted. This sometimes happens when the evacuation tube is obstructed, which causes its contents to back up and, in this case, produced splashing.

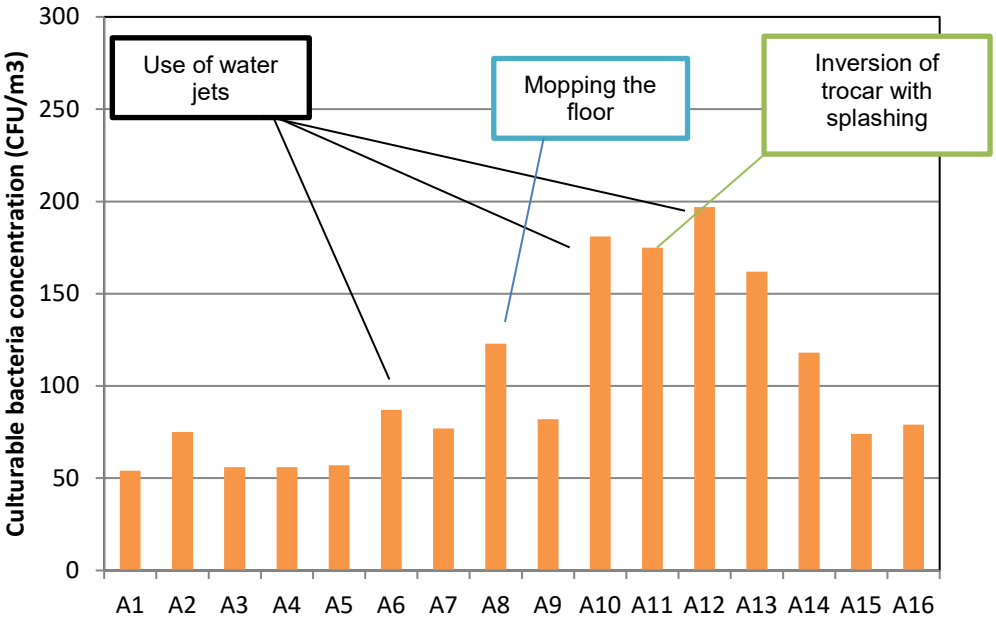

Figure 17. Concentration of culturable bacteria in the air (Laboratory A).

In Laboratory B, higher concentrations are discernible for samples B7 and B10 (Figure 18). The two tasks mainly observed while sample B7 was being taken were the use of water jets and the cannula. Since these two tasks were also identified as generating bioaerosols in the real-time measurement of fluorescent particles, the association between these tasks and an increase in bioaerosol exposure appears credible. Sample B10 was taken while the body was being wrapped at the end of the embalmment. Once again, the marked increase in the concentration of fluorescent particles during the same period supports the recognition of plastic wrapping as being a bioaerosol-generating activity. During this task, the embalmer must move and handle the body considerably, and these actions probable result in the aerosolization of the numerous microorganisms present on the dead body's skin.

Figure 19 shows that only the concentration of sample C15 differs considerably from the concentrations measured for the other samples obtained at Laboratory C. This sample was taken during use of the trocar, during cleaning of the table or the body and during suturing at the plastron level. For this sample, it is difficult to identify a more specific task, since all these tasks were previously targeted as potentially generating culturable bioaerosols. It may be accurate to consider that this represents the accumulation of bacteria generated by all the tasks executed during this period.

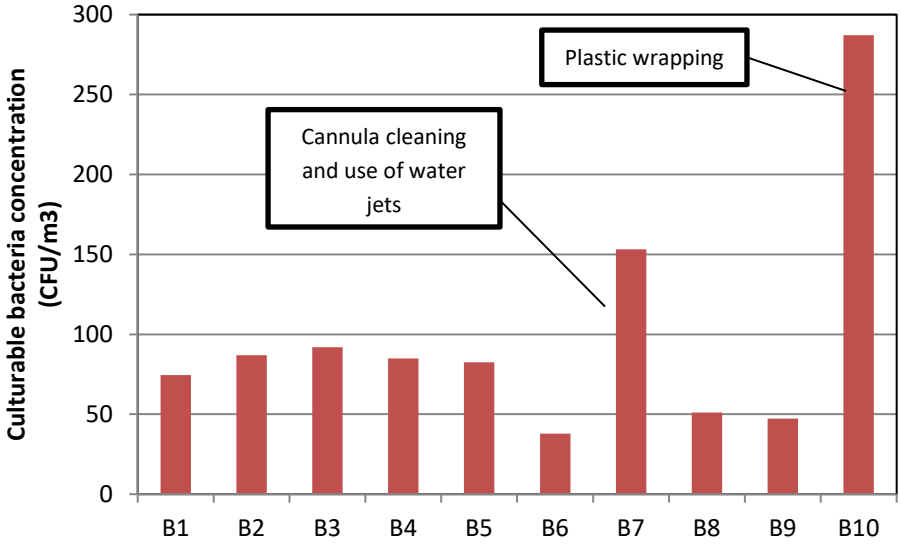

Figure 18. Concentration of culturable bacteria in the air (Laboratory B).

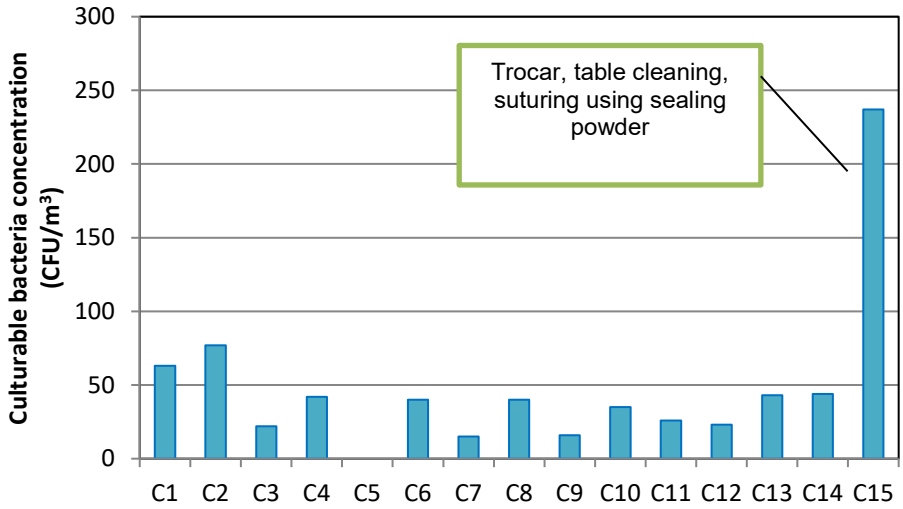

Figure 19. Concentration of culturable bacteria in the air (Laboratory C).

Although, in general, concentrations remain low, some activities carried out during embalming were identified as generating culturable bioaerosols. The most bioaerosol-generating tasks are trocar use, suturing, incisions, washing the body and the table with water jets, and plastic wrapping, sometimes done at the end of the embalming process. The ongoing handling of the body during plastic wrapping and washing seems to result in substantial aerosolization of bacteria. In embalming rooms, the risks associated with bioaerosols have to do with infection, and the recommended levels for industrial environments cannot be used (Goyer et al., 2001). Nevertheless, there is no recommendation concerning the exposure limit for infectious agents.

Several factors remain unknown to this day and the recognition of risk varies according to specialist.

B. Identification

From the 55 air samples (Andersen impactor) and surface samples from the three labs, approximately 950 colonies were isolated and then identified. Of these strains, 49 different genera were characterized, mostly from the *Actinobacteria, Firmicutes* and *Proteobacteria* phyla. The genera *Bacillus, Staphylococcus* and *Micrococcus* were found most abundantly during this project. These results agree with what several researchers had previously reported for interior environments (Górny & Dutkiewicz, 2002; Kim & Kim, 2007; Nevalainen, 1989; Pastuszka et al., 2000).

Most *Actinobacteria* are recognized as being telluric (living in soil), saprophytic bacteria. This does not prevent several of them from colonizing many parts of the human body. It should be remembered that some *Corynebacteriaceae* and *Mycobacteriaceae* are known to be opportunistic, even pathogenic, for humans (Goodfellow et al., 2012). In this project, strains of non-tuberculous mycobacteria (Risk Group 2) were cultured from two of the three labs, although without speciation. Since the culture media used in this project do not support the growth of *Mycobacterium tuberculosis* (Risk Group 3), it was not possible to culture that bacterium and, consequently, it is not possible to guarantee that it is totally absent from the embalming labs.

In addition to *Corynebacterium* and *Mycobacterium* species, several bacteria from the *Dietziaceae*, *Gordoniaceae*, *Nocardiaceae* and *Streptomycetaceae* families were recovered in the three labs. We were able to relate the presence of *Streptomyces sp.* to the use of a mop in Laboratory A. Indeed, as soon as an employee started mopping, analyses done with the direct reading device identified a substantial increase in concentrations of fluorescent particles in the air. This increase observed in real time was also reflected in the samples taken by means of culturing during the same period. The presence of *Streptomyces* persisted throughout the rest of the samples taken the same day, proving that the small spores (0.5 µm) (Goodfellow et al., 2012) these bacteria produce can remain airborne for a long time (up to 1.5 hours after the second time the mop was used). Almost all the *Streptomyces* colonies collected were impacted on stage 6 of the Andersen impactors, confirming their small aerodynamic diameter (Reponen et al., 1998). The genus *Micrococcus*, whose main habitat is the skin (Goodfellow et al., 2012), is undoubtedly the one that was most frequently found. It represents slightly more than 20% of all the isolates characterized in this project. This frequency is somewhat below the 36% reported by Pastuszka et al. (2000) in homes and office buildings. This difference may be attributable to the different sources of bacteria present in an embalming lab, which increases their diversity.

Bacteria in the phylum *Firmicutes* are widespread Gram-positive bacteria, which include the genera *Bacillus*, *Staphylococcus* and *Streptococcus* (De Vos et al., 2009). Although most of them are saprophytic, these genera also include bacteria that are opportunistic or pathogenic to humans. In this project, *Streptococcus pneumoniae,* a human pathogen in Risk Group 2*,* was cultured in several samples from Laboratories A and C. Although this bacterium may be asymptomatically present in the human upper respiratory tract, where it colonizes the surface of the mucous membranes of the nasal pharynx (Weiser, 2010), its culturing shows that bacteria that probably come from the respiratory tract are found in culturable condition in the air of embalming labs. In addition, three of the four samples in which *Streptococcus pneumoniae* was

isolated were taken during the embalming of a person who died of pneumonia. Although *Streptococcus pneumoniae* is not the only etiological agent responsible for pneumonia, it is interesting to have demonstrated its presence in the air. *Streptococcus agalactiae, mitis, oralis* and *parasanguis* were also cultured in some samples taken from the three labs. The different species of *Staphylococcus* identified come almost exclusively from the surface of the human skin, nasal membranes and scalp. We should mention the presence in several samples from Laboratory B of the opportunistic bacterium *Staphylococcus aureus*. The presence of numerous bacteria from the order *Bacilliales* is not at all surprising since these bacteria produce endospores that make them very resistant. The vast majority *Bacillus* bacteria come from the soil (De Vos et al., 2009). Their resistance means that they frequently cause contamination problems in various locations (operating rooms, food, pharmaceuticals) (De Vos et al., 2009) and they are found in most air samples (Goyer et al., 2001).

Gram-negative bacteria are mainly included in the phylum *Proteobacteria* (Brenner et al., 2005). Over half of the Gram-negative bacteria characterized in the three labs belong to the *Gammaproteobacteria*, a group that has a relatively wide-ranging ecological niche. Several of these bacterial genera naturally colonize the skin, mucous membranes, respiratory tract and intestines (Brenner et al., 2005). *Pseudomonas* species are known to be commensal in the nasal cavities and intestines. However, since they are abundantly distributed in all environments (soil and water), their presence in these air samples cannot be related only to aerosolization attributable to embalming activities. Although few studies have reported their presence in air samples, Górny and Dutkiewicz (2002) report that they isolated them in 80% of their samples. *Moraxella* species are naturally present in the oropharynx, mucous membranes, skin and genital tract, while *Enterobacter, Serratia, Leclercia* and *Hafnia* come mainly from the intestines. Their presence in the air samples establishes the aerosolization of intestinal bacteria during embalming.

Biodiversity of the culturable bacterial microbiota

The identifications and abundances reported in Figure 20 represent the genera of bacteria characterized for each stage of the Andersen impactor. In addition to the identifications reported in the previous section, this representation of results makes it possible to determine which kinds of bacteria were collected as a function of their aerodynamic diameter. The abundance reported here is the sum of the colonies obtained on a given stage for all the laboratory's samples. It is reported in CFU and does not constitute a concentration per m^3 of air. These analyses did not have the objective of making identifications one by one but rather of assessing the overall picture of the diversity of the culturable microbiota collected on the basis of size. A brief look at Figure 20 will allow readers to quickly see that the culturable bacteria collected in the air of Laboratory B were found mainly on stages 1 and 2 of the Andersen impactor (stages where the concentrations are highest), whereas for Laboratories A and C, they were mainly on stages 4 to 6. The culturable bacteria–bearing particles taken from the air of Laboratory B had larger diameters than those observed in the other labs. This finding is in accordance with the particle diameters measured in real time with the WIBS-NEO (section 5.1.2).

In addition to providing information about overall biodiversity, these graphs highlight the polydisperse nature of the culturable bacteria–bearing particles found in all three labs. Colonies of bacteria were recovered on all stages of the Andersen impactor, and thus for different sized particles, regardless of the lab. Bacterial cells are situated mainly between 0.5 and 3 µm in size (Goodfellow et al., 2012). Nevertheless, it is well known that bioaerosols may exist as single cells,

in aggregates of cells or in association with other particles (Górny et al., 2003; Pastuszka et al., 2000), which explains why they can impact all the stages. Bacteria that are found alone are probably impacted on the lower stages, whereas those that are in agglomerates or in association with other particles are collected on the upper stages. The degree of agglomeration of microbial cells is affected by many factors, including the type of bacteria, relative humidity, source, growth medium, emission mechanism and air velocity (Kim & Kim, 2007; Reponen et al., 1998). Studies have proven that, when there is more dust, there is more likely to be an association between microorganisms and dust (Górny et al., 2003). Notwithstanding the polydispersion, it is important to emphasize that, for all three labs, the fraction of particles smaller than 4.7 µm represents the majority fraction. These results prove that, regardless of laboratory, the majority of culturable bacteria collected may be single cells that are able to penetrate a worker's respiratory tract.

When assessing microbial risk, it is important to consider the microbial load that may be breathed in. In an outdoor environment, researchers have observed R/T ratios (respirable particles over total particles) ranging between 30% and 50% (Pastuszka et al., 2000), whereas in dwellings and hospitals R/T ratios between 30% and 60% were reported (DeKoster & Thorne, 1995; Kim & Kim, 2007). The higher the ratio, the larger the proportion of small particles in the aerosol and the better able the particles are to penetrate deep into a worker's respiratory tract. In this study, R/T ratios calculated in the three labs were 78% for A, 58% for B and 69% for C. These ratios are relatively high compared to what other researchers have reported.

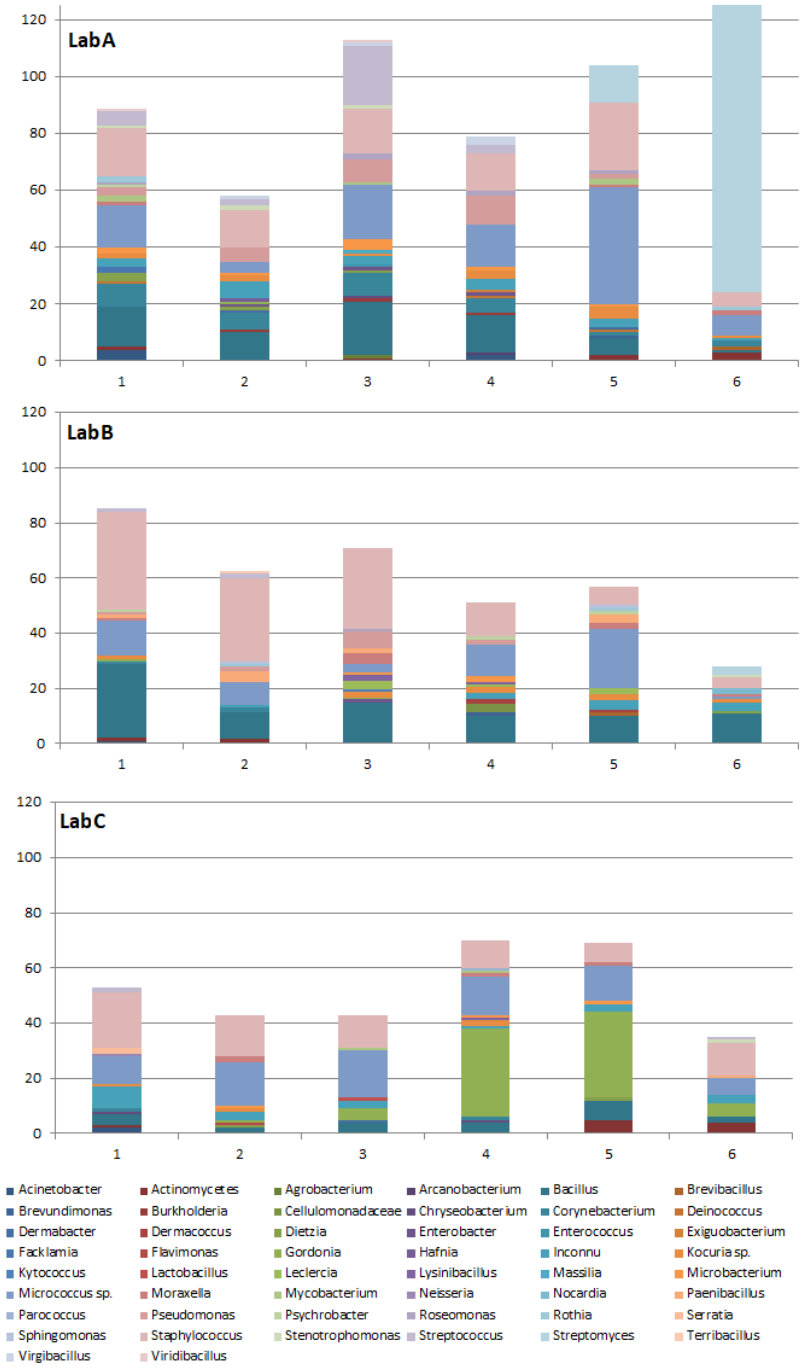

Figure 20. Identification and abundance (CFU) of culturable bacteria collected with the Andersen impactor for each laboratory and reported as a function of their granulometry.

5.2.2 Surfaces

Figure 21 presents the bacterial diversity and abundance measured in the samples taken on the horizontal surfaces surrounding embalming tables. The surfaces in Laboratory C have the highest bacterial load, whereas those in Laboratory A have the lowest load. These differences may be attributable to the many splashes of liquid observed in Laboratory C, combined with the lack of proactive cleaning in response to this splashing.

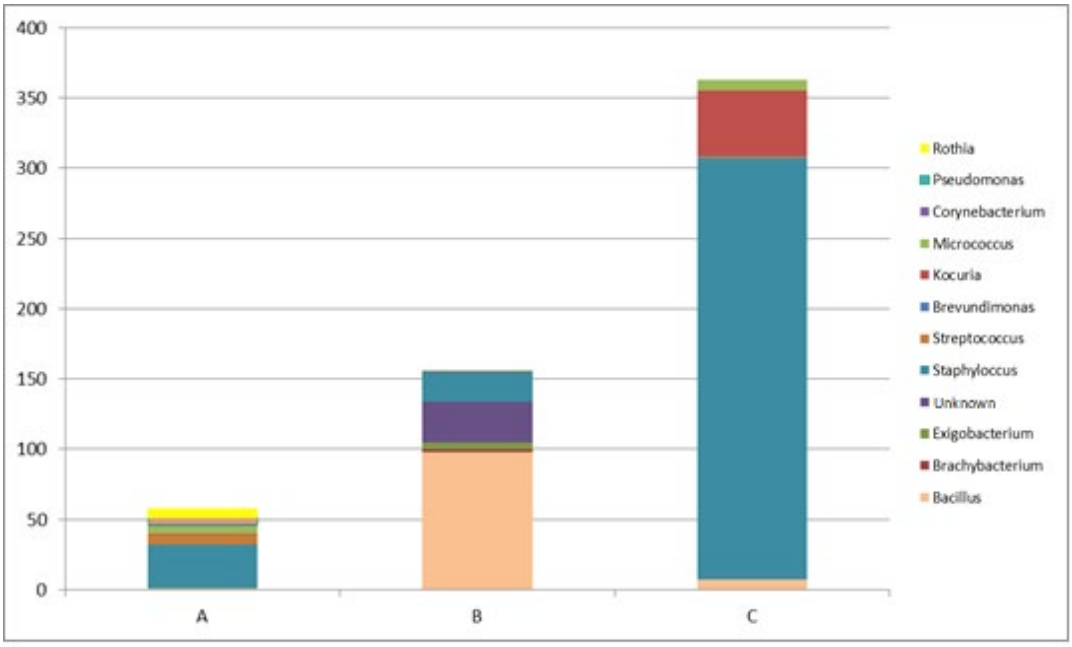

Figure 21. Identification and abundance (CFU) of culturable bacteria collected on horizontal surfaces surrounding embalming tables, for Laboratories A, B and C.

Compared to what was identified in the air of the labs, the biodiversity of their surfaces appears more limited. The use of cleaning products and disinfectants may partially explain this result. The absence of *Streptomyces* on Laboratory A's floor is particularly surprising and hard to explain, given that their presence when the floor was mopped provided proof that the air was substantially contaminated with this bacterium. The virtual absence of bacteria in the *Bacillus* genus on surfaces in Laboratories A and C is also astonishing. These endospore-producing bacteria are very resistant and should have constituted the majority of the microbiota present on surfaces, as they did in Laboratory B. Although preferential aerosolization is a recognized phenomenon, it seems quite unlikely that it explains the large difference observed between air and surfaces here (Liu et al., 2019; Veillette et al., 2018).

5.3 Microbial indicators and bacterial biodiversity

Due to the very low levels of DNA recovered from the samples taken with the CIP-10 and the SASS® 3100, it was not possible to produce results for the ddPCR analyses targeting microbial indicators. Despite this result, this project was still able to develop and validate 8 ddPCR detection

systems targeting indicator microorganisms. These systems will remain available for future studies.

For the biodiversity analyses, after the bioinformatic processing done with the “pipeline” prepared by the C³G and the DADA2 tool, the libraries of sequences for each sample were assessed. The mean number of unique sequences obtained per sample was less than 1,200, which is very low, although it is in accordance with the PCR quantification. Despite the very low bacterial DNA load, taxonomic attribution was still attempted, but given the overly small number of sequences, the results were not interpretable and this analysis was abandoned.

5.4 Numerical results

5.4.1 Comparison between tracer gas and CFD simulations

In each laboratory, the number of air changes per hour was determined with the tracer gas technique, using the decay method. The concentrations of tracer gas as a function of time, measured with the Autotrac portable chromatograph, made it possible to estimate the real ventilation rate. Expressed in number of ACH, the ventilation rates were 2.1, 10.3 and 7.9, respectively, for Laboratories A, B and C.

The first modelling processes done had the objective of verifying whether the CFD was able to adequately reproduce the ventilation conditions in the rooms we studied. For each lab, the tracer gas concentrations measured were compared to the model’s predictions (Figure 22). The ventilation rate was set numerically based on the number of ACH determined by the tracer gas technique. Since gas concentrations in Laboratory B were higher than concentrations in the other labs, they are related to the vertical axis on the right side of the graph.

As Figure 22 shows, the modelled concentrations of SF_6 as a function of time are comparable with the experimental data. The mean deviations between the measured and modelled concentrations are 0.5 ppb, 2.6 ppb and 0.6 ppb for Laboratories A, B and C, respectively. These results validate our numerical model’s capacity to represent the ventilation conditions that are found in real environments.

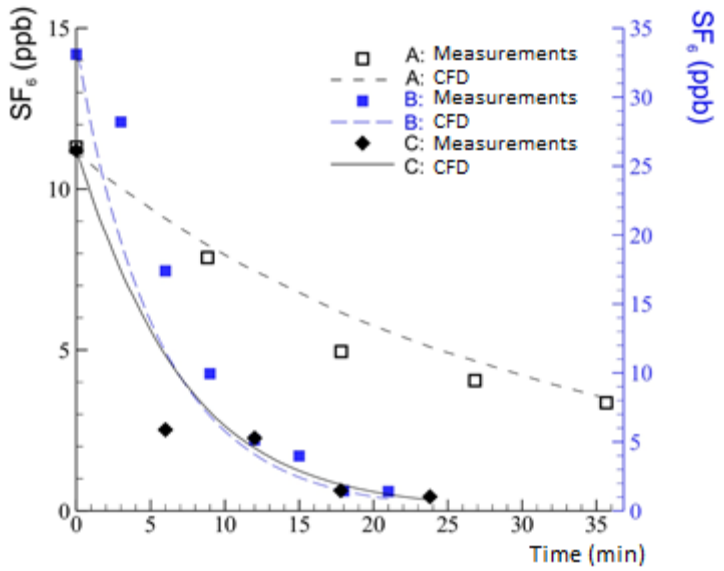

Figure 22. Comparison of concentrations of SF_6 measured and modelled for the three laboratories.

5.4.2 Fate of airborne particles

Regardless of the particle-generating activity and the location and source of the emission, bioaerosols may (i) be found in the ambient air, (ii) be deposited on surfaces, including the floor, or (iii) be extracted from the room by the ventilation system. These three fates are mutually exclusive and their respective proportions vary over time.

The temporal evolution of the fractions of airborne, extracted or deposited particles is illustrated in Figure 23 for Laboratory A with a ventilation rate set at 4 ACH. The dashed vertical line marks the end of the emission period for the task. Each fraction is traced as of the second minute, which corresponds to the end of the emission period for the “suturing” activity (see Table 6). The fraction deposited as a function of time is presented on an independent vertical scale ranging from 0% to 0.7% (scale on the right side of the graph). At the end of the emission period, the airborne and extracted fractions are 90% and 10%, respectively, and the deposited fraction is nil. Then the airborne fraction decreases quasi-exponentially as a function of time, reaching 1.6% after 30 min. The two elimination mechanisms – particle extraction by means of ventilation and deposition – present similar curves over time. We see an increase in the deposited fraction with time, but this fraction remains small and only reaches 0.66% at the end of the simulation (t = 30 minutes).

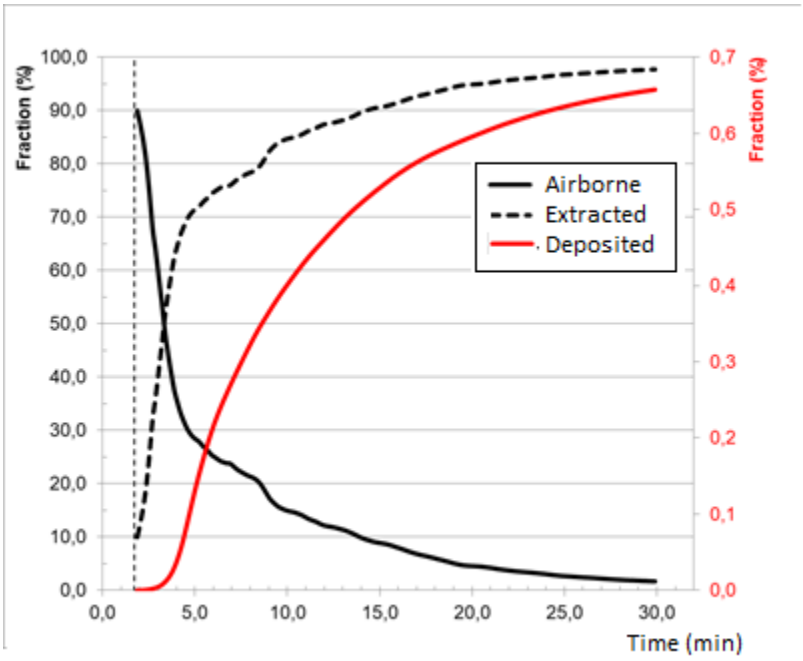

Figure 23. Evolution of airborne, extracted and deposited fractions for the "suturing" scenario.

5.4.3 Local age of air

Although the sedimentation mechanism is mainly influenced by the density and diameter of particles, the movements of air created by the air supply and extraction conditions are mainly responsible for the dispersion of bioaerosols in space and their elimination. Nevertheless, the configuration of spaces and the presence of furniture can present obstacles to natural air movements and lead to the existence of poorly ventilated zones, even if the total air delivery rate appears to be appropriate. The local age of air (τ) is one of the parameters that enables one to identify the efficiency of ventilation and the speed with which contaminants are extracted from a room. With the aim of identifying the efficiency of their ventilation, the local age of air was determined for each lab using the following equation:

$$\tau_{zone} = \int_0^{\infty} \left[\frac{\bar{Z}_{zone}(t)}{Z(t=0)} \right] dt \qquad \textbf{(Equation 1)}$$

where τ_{zone} and $\bar{Z}_{zone}(t)$ are, respectively, the age of the air and the mean mass fraction of a tracer gas (SF_6) in a given zone. Each zone has a surface area of 1.5 m x 1.5 m on the *x*–*y* plane and is delimited vertically by the coordinates *z* = 1.52 m and *z* = 1.72 m. Local age of air was calculated by setting the ventilation rate and initial concentration of SF_6 (i.e., $Z(t=0)$) at 4 ACH and 6.0×10^{-8} kg/kg_{air}, respectively. The integral of equation 1 was calculated by the trapezoidal rule based on the spatial mean of mass fractions in each zone and at each interval of time, set at 1 second. The minimum age of air in Laboratory A is 639 s. Laboratories B and C have minimum

ages of 731 s and 335 s, respectively. Figure 24 presents the relative local ages in relation to the minimum values calculated for each laboratory.

The results show that the airflow in Laboratories A and B is close to ideal mixing conditions. These two labs are architecturally simple and the presence of obstacles does not seem to disrupt the air movements induced by ventilation. In Figure 24(a), we can see that the relative age of air is higher above the beds. This is explained by the presence of extraction grilles above the beds and the left-hand counter, which leads to a slower decrease in the concentration of gas over time in this zone. Despite the lack of an air outlet in Laboratory B, the local age of air is similar in all four zones. Air infiltration around the folding door creates almost ideal mixing conditions in this lab, which has a floor area of less than 28 m^2. The local age of air in Laboratory C presents much greater deviations. The highest ventilation efficiency is found in the zone corresponding to the vestibule. This zone is ventilated by diffuser S5, whose air delivery rate is similar to the flow provided by the four wall grilles. The zone with a relative age of 427% is problematic. As illustrated in Figure 4, the closest air outlet to this zone is wall grille S1. Despite its proximity, the air jet created by this grille does not reach the zone and the flow speeds are approximately 10 times lower than in the other zones. Moreover, the presence of two cabinets and a counter hinders air circulation.

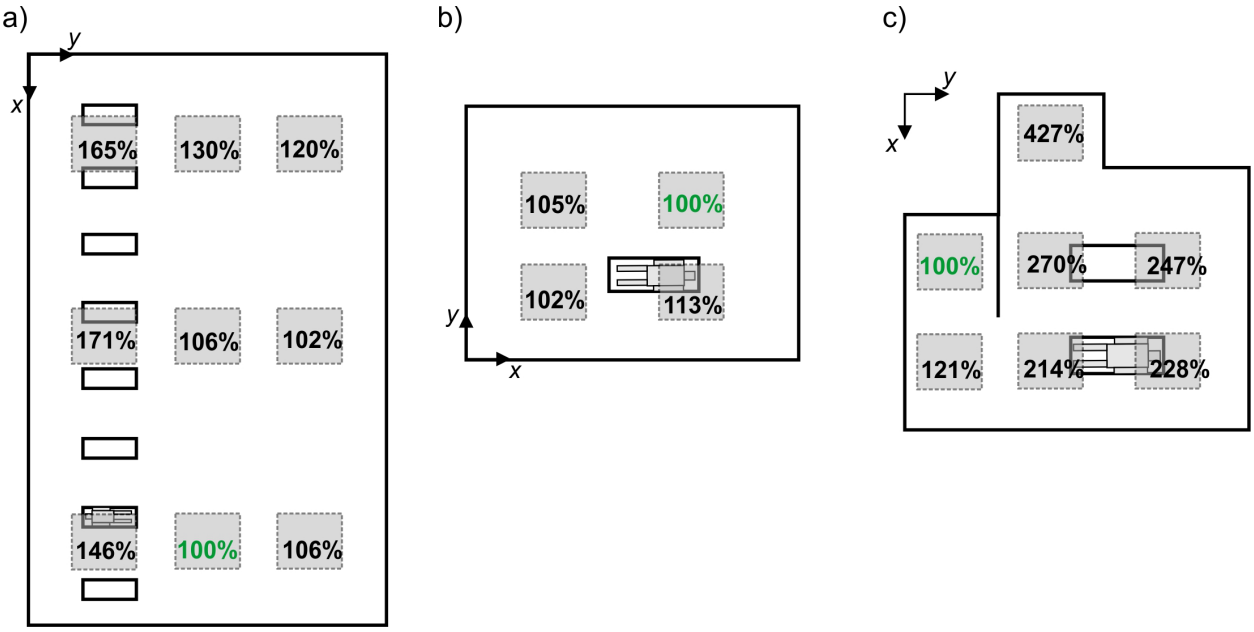

Figure 24. Local age of air in the breathing zone for (a) Laboratory A, (b) Laboratory B and (c) Laboratory C, expressed in relation to the minimum values calculated for each laboratory.

5.4.4 Impact of ventilation rate

General ventilation of spaces is the engineering-based control technique that is most commonly used to mitigate exposure to gaseous or particulate contaminants. The efficiency of general ventilation to reduce concentrations of bioaerosols was determined for four values for air changes per hour and for all the emission scenarios presented in Table 6. This section presents the

concentrations in terms of number of airborne particles as a function of time for the “trocar” (Laboratory A), “retractor” (Laboratory B) and “powdering” (Laboratory C) particle-generating activities. The mass fractions obtained from the CFD code were converted into number of particles per m^3 using the particles’ aerodynamic diameter (Table 6) and density, set at 1,050 kg/m^3.

Figure 25, Figure 26, Figure 27 and Figure 28 present the number concentration in the breathing zone, at 5-minute intervals, for the three labs. The breathing zone is defined as being a volume delimited vertically between 8 cm and 1.8 m and located 0.6 m from the walls (ASHRAE, 2016). Regardless of laboratory or of emission scenario, we observe that an increase in air delivery rate reduces the number concentration, and this reduction is faster at a high ventilation rate. All the temporal changes in concentrations (Figures 25, 26, and 27) follow a trend line of the following form:

$$C(t) = C_1 e^{-(C_2 \times t)} \quad \textbf{(Equation 2)}$$

with a coefficient of determination (R^2) falling between 0.97 and 0.99, depending on the number of ACH. The two constants C_1 and C_2 depend on the number of air changes and the starting concentration. Laboratories B and C show temporal variations in concentration that follow the same trend.

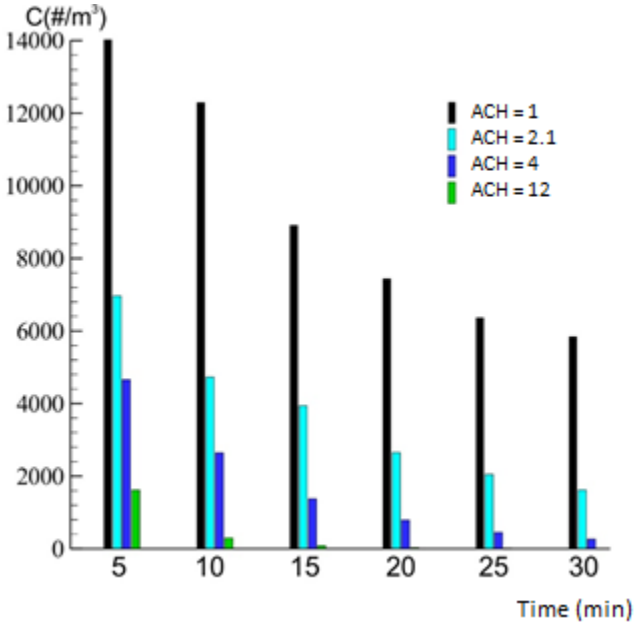

Figure 25. Laboratory A – “trocar.”

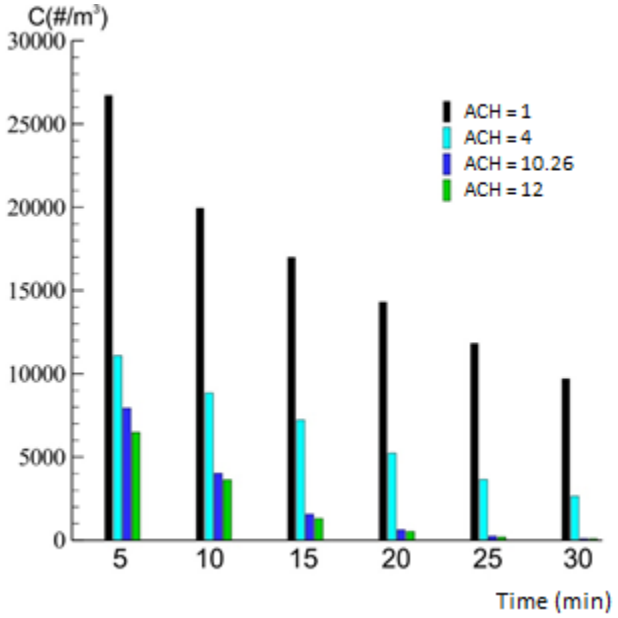

Figure 26. Laboratory B – "retractor."

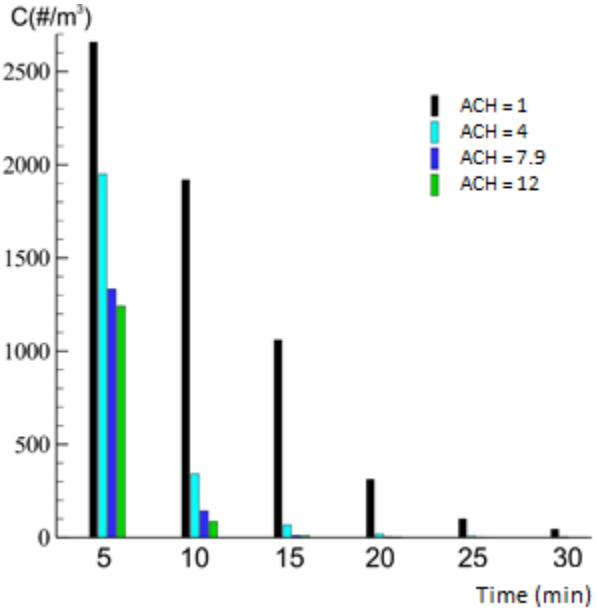

Figure 27. Laboratory C – "powdering."

In all three labs, the concentrations are highest at 1 ACH. An increase in air delivery rate from 1 to 4 ACH reduces concentrations by 28% to 67% depending on the lab modelled. In Laboratory B, concentrations in number of particles per m^3 for ventilation rates of 10.26 and 12 ACH are comparable. This result appears to indicate that an increase in ventilation above 12 ACH will not have a significant impact on concentrations.

5.4.5 Impact of task performed

The results of the previous section showed that the air delivery rate has a considerable effect on concentration in the breathing zone and the speed with which particles are eliminated from a workspace. However, ventilation is not the only factor that determines exposure level. The type of particle-generating activity also has an impact on number concentration in laboratories' breathing zone. These activities stand out because of (i) the aerodynamic diameter of emitted particles, (ii) the duration of emission, (iii) the location of the source, and (iv) the emission mass flow rate per unit of time.

Figure 28 shows the effect of task performed on number concentrations in the breathing zone in Laboratory C. The ventilation rate corresponds to that measured experimentally: 14.8 m^3/min (7.9 ACH). At t = 5 min, concentrations for the "powdering" task are higher than for the other two tasks. This first task presented the highest particulate mass flow rate. The number concentration per unit of volume for the "trocar" task is the lowest, at 754 particles per m^3. Note that, at this exact time in the simulation, emissions related to the "powdering" task had been terminated 2 minutes previously, the "suturing" task had just been completed, and the "trocar" task was still under way. This may explain why this task, which presented the lowest concentration at t = 5 min, became the task with the highest concentration at t = 10 min. The spatial location of the emission also plays a role in the aerosol elimination speed. The "powdering" task, located at neck level, and the "trocar" task, at the navel, are separated by 50 cm on the y axis (Figure 4). Since the "powdering" task took place closer to the extraction zone, the emitted particles were extracted faster. Particle diameter (d_p) has a limited impact on concentrations. The fractions deposited after 30 minutes were 1.8%, 1.0% and 2.0%, respectively, for the "powdering," "suturing" and "trocar" tasks.

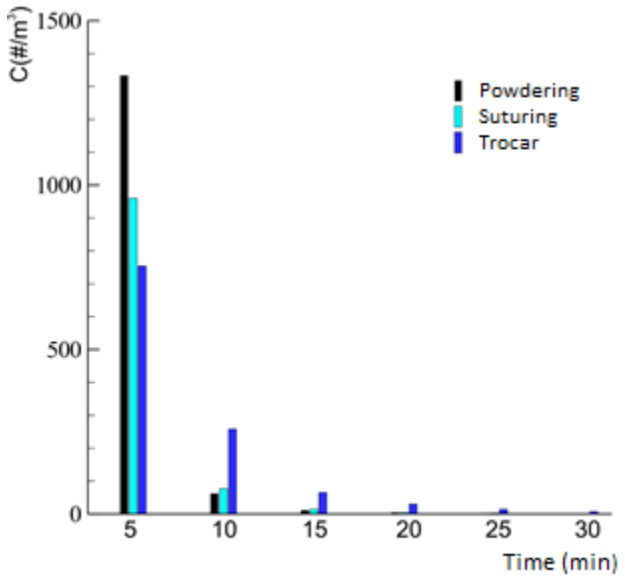

Figure 28. Impact of task performed on concentrations, in Laboratory C.

5.4.6 Impact of ventilation strategy

The results presented in section 5.2.3 showed that ventilation rate is an effective control method for reducing bioaerosol concentrations. According to Memarzadeh and Xu (2012), another factor that is even more important than number of ACH is the path between the source of contaminants and the extraction grilles. When this path is disrupted by airflows, obstacles, recirculation zones, etc., bioaerosols are more likely to migrate to other areas of the room, which increases concentrations in the air and elimination time. The impact of three ventilation strategies on bioaerosol concentrations was verified for Laboratory A. In Laboratory C, seven different strategies were simulated. For both laboratories, these strategies consisted in varying the airflows delivered by air outlets while keeping number of ACH at a set value.

Referring to Figure 2 and Table 7, the airflow rates for diffusers S2, S4 and S6 in Laboratory A were set at 44%, 54% and 64% of the total ventilation rate (Q_T=24.9 m^3/min). The middle value (54%) corresponds to the experimentally measured fraction. Figure 29(a) presents concentrations in the breathing zone as a function of different ventilation strategies, at t = 10 and t = 15 min. Since extraction grilles in this lab are located at counter level and above the beds, the increase in air delivery rates from diffusers S2, S4 and S6 from 10.96 to 15.94 m^3/min favours the creation of a flow from clean zones to contaminated zones. However, changes in ventilation strategies did not have a major impact on bioaerosol concentrations. In fact, a 20% increase in flow from diffusers S2, S4 and S6 reduced concentration in the breathing zone by 5% at t = 10 min and 13% at t = 15 min.

In Laboratory C, the airflow measured at the ceiling diffuser (Q_{S5}) represents 48% of the total ventilation rate. As indicated in Table 7, this proportion ranged from 0% to 94% depending on ventilation strategy. Bioaerosol concentrations in the breathing zone as a function of the ratio Q_{S5}/Q_T are presented in Figure 29(b). Unlike Laboratory A, strategies involving variations in air delivery rate had a considerable impact on bioaerosol concentration values. We see a 65% reduction in number concentration between Q_{S5}/Q_T = 0 and 48%. An increase in this ratio reduces concentrations more, with similar results for Q_{S5}/Q_T = 70%, 86% and 94%, with very low concentrations ranging between 12 and 34 particles/m^3.

The visualization of the trajectories taken by air exiting the wall grilles (not shown here) showed that air jets promote mixing conditions in Laboratory C. On the other hand, an increase in air delivery rate in the zone corresponding to the vestibule created a flow in the work zone that has the characteristics of a laminar airflow, whereby aerosols are not mixed with the room air but sent directly to the extraction grilles.

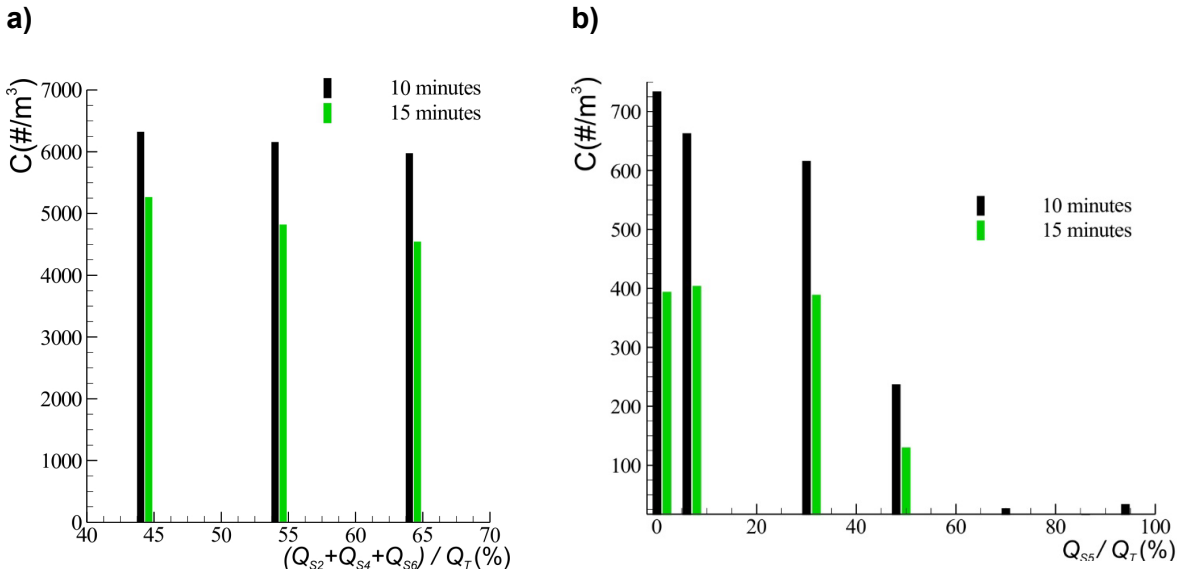

Figure 29. Impact of ventilation strategy on concentrations at (a) Laboratory A and (b) Laboratory C.

5.4.7 Particle movement

Gravitational sedimentation and molecular and turbulent diffusion have an impact on the trajectories followed by particles emitted from a given surface. However, advection (transport of a quantity by the air velocity) is the dominant transport mechanism. Thus, the consequence of an increase in the ventilation rate is that the mean air velocity is increased in the ventilated room, which has an impact on aerosol dispersion in space.

Figure 30(a) to (d) illustrates airborne particles in Laboratory C, for ACH rates of 1, 4, 7.9 and 12, respectively. The “powdering” task was retained, with an emission lasting 3 min at the level of the deceased’s neck. Each image shows the position of particles at the end of the emission period related to this task, namely t = 190 s. The diameter of the emitted particles is 3.47 µm. Given this diameter and the particles’ density, the deposition speed is approximately 2.4 cm/min, lower than the mean air speed in the emission zone, which ranges between 30 and 360 cm/min, depending on the ACH rate.

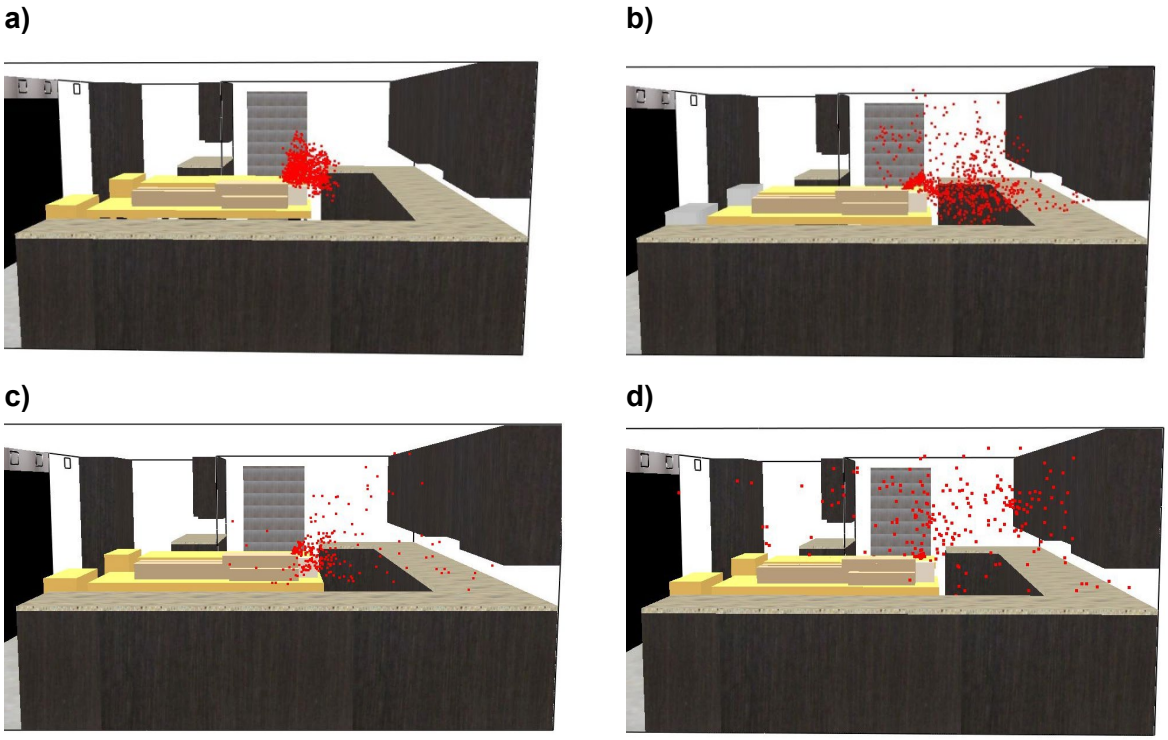

Figure 30. Particle dispersion at t = 190 s as a function of ventilation rate: (a) 1 ACH, (b) 4 ACH, (c) 7.9 ACH and (d) 12 ACH.

At a ventilation rate of 1 ACH, the particles are still clustered close to the emission source. The entire emitted mass is located less than 70 cm from the source. With an increase in ventilation rate, the aerosol is dispersed. At a ventilation rate of 4 ACH, some particles have already been extracted from the lab. At the maximum ventilation rate (12 ACH), dispersion is generalized throughout the entire volume except the entrance zone. The increased rate favours dispersion, resulting in lower mean values and concentration gradients in space.

5.4.8 Deposited fraction

The illustration of the fate of particles in Figure 23 and the data in section 5.4.2 showed that deposition is a less important elimination mechanism than ventilation. Nevertheless, in his monograph, Memarzadeh (2013) states that most transmission in health care institutions seems to be related to contact and inhalation of droplet nuclei in the air. In addition, infections are most often caused by a combination of aerial transmission and contact. For example, SARS-CoV can be transmitted by means of airborne mechanisms and contact. The SARS virus can survive on surfaces for up to 3 hours after droplets have dried (Memarzadeh, 2013). Consequently, physical contact with contaminated surfaces constitutes a risk that must not be neglected.

The minimum and maximum fractions of particles deposited on surfaces in each lab are presented in Table 8. These fractions, expressed as percentages, were calculated with the total mass of particles deposited at t = 30 min, divided by the mass of particles emitted (Table 6). We can see that the fractions are lowest for Laboratory A. This is due to the ventilation conditions but also to

the mean aerodynamic diameter of the particles, which is 1.14 μm compared with 1.66 and 3.39 μm, respectively, for Laboratories B and C. The deposited fractions for Laboratory C are comparable to the values for Laboratory B, even though the mean diameter of emitted particles is twice as large.

Table 8. Minimum and maximum fractions of particles deposited on the surfaces for the three laboratories

	Laboratory A	Laboratory B	Laboratory C
Minimum fraction (%)	0.02	0.12	0.08
Maximum fraction (%)	1.48	2.73	2.43

Figure 31(a) and (b) present the mass of deposited particles per unit area in Laboratory C, for ventilation rates of 4 and 12 ACH, respectively. The “trocar” task was retained and the simulation time is identical in both figures. For these two emission scenarios, the deposited fractions are 2.43% and 1.64%, respectively. We can see that the deposition maps are similar in both cases. Deposition is mainly concentrated on the floor and the counter near the extraction grilles. In addition, the entrance area (vestibule) has no significant deposit, with values of approximately 0.1×10^{-6} mg/m^2. At a ventilation rate of 12 ACH, bioaerosols are more dispersed and the deposition surface is larger. Consequently, the surface area where the deposited mass is equal to or greater than 5 mg/m^2 (shown in red) is more limited than the area observable for a ventilation rate of 4 ACH.

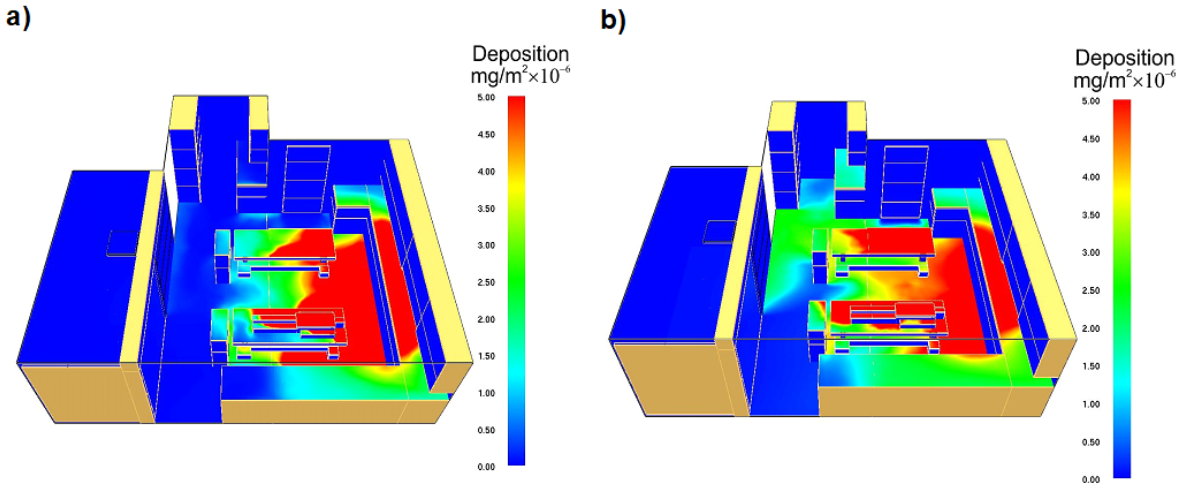

Figure 31. Deposited mass per unit area for Laboratory C at t = 1,200 s for a ventilation rate of (a) 4 ACH and (b) 12 ACH.

5.5 Limitations of the study

The recommendations made in this report are based exclusively on our observations, the measurements taken during our interventions and the modelling done thereafter. Given the many factors that can influence generation levels and residual concentrations, the data presented in this report are representative of the premises studied, the state of preservation of the bodies, and

the working methods of the embalmers we observed. Any other specific situations should be subject to an in-depth evaluation by a professional in the area of bioaerosols or risk of infection.

The use of the SASS® 3100 to sample volumes of ambient air may have resulted in a non-negligible underestimate in the quantification of low-diameter particles (50% efficiency regarding 0.5 µm particles at a rate of 300 litres/min). Nevertheless, this sampling device remains an appropriate choice (Mbareche et al., 2018), as it offers the possibility of using a high rate, and given that no sampling method underestimates any granulometric fraction.

Our interventions took place when embalming activities were planned. Thus, the sampling days were not necessarily representative of all working days for embalmers, but they specifically targeted common tasks related to thanatomorphosis. The research team did not request any changes in working methods, so the work tasks assessed were representative of reality.

The methods for counting bacteria involved culturing on nutrient media. Although these methods are widely used, they underestimate exposure, since only microorganisms that are culturable in the particular conditions are considered.

6. CONCLUSION

6.1 Bioaerosols

This study established that, on average, workers engaged in embalming activities were not much exposed to bioaerosols but that certain tasks were likely to generate an increase in concentrations of bioaerosols near the worker. Strains of non-tuberculous mycobacteria (Risk Group 2) were identified in two of the three laboratories studied. In addition to mycobacteria, several bacteria from the *Corynebacterium, Dietziaceae, Gordoniaceae, Nocardiaceae* and *Streptomycetaceae* families were found in the three labs. Finally, *Streptococcus pneumoniae,* a human pathogen in Risk Group 2, was cultured in samples from Laboratories A and C. The culturing of *Streptococcus pneumoniae* proves that bacteria from human respiratory tracts are found in culturable condition in the air of embalming labs.

The main finding from the measurements taken with the WIBS-NEO was the preferential aerosolization of biological (fluorescent) particles during embalming over non-biological (non-fluorescent) particles. The results showed that most tasks performed by an embalmer are likely to trigger aerosol emission peaks of as much as 7.65 particles/cm^3, or 45 times the baseline level. The actions likely to cause the greatest peaks in concentration are the ones that involve a bellows effect with the addition of sealing powder ("suturing, powdering", "orifice occlusion", "plastic wrapping"), those that cause splashing ("washing, drying", "table cleaning", "preparation, equipment cleaning"), and those related to "trocar" use. Particle generation is a key determinant of embalmers' exposure.

Furthermore, the particle size distributions measured indicate that bioaerosols emitted during embalming do not belong only to the inhalable fraction (< 10 µm); indeed, they most frequently belong to the respirable fraction (< 4 µm, emission during trocar use) or even to a still finer fraction (< 2.5 µm). These particles therefore have the ability to penetrate deep into the respiratory tract and be deposited there. In addition, since small particles remain airborne for long distances and periods of time, embalmers may be exposed to microbial bioaerosols produced by other embalmers' activities, unless they are working alone in the lab; they may also be exposed long after an embalmment has been carried out.

6.2 Numerical simulations (CFD)

The numerical simulations showed that deposition is a less important elimination mechanism than ventilation, as the maximum fractions of deposited particles were lower than 3%. The simulations also highlighted the efficiency of general ventilation as a method for controlling bioaerosols in embalming labs. Depending on the laboratory modelled, the increase in the ACH rate from 1 to 12 caused modelled concentrations in the worker's breathing zone to drop by 75% to 90% in the first 10 minutes in the scenarios studied. The calculation of the local age of air revealed a poorly ventilated zone in Laboratory C, with a relative local age of 427%. In Laboratories A and B, airflow was relatively uniform and no problem zones were detected. An important finding of the CFD component of this study was the importance of ventilation strategy. In Laboratory C, the increase in air delivery rate at diffuser S5 from 0 to 7 m^3/min allowed for a 95% reduction in the concentration of bioaerosols in the breathing zone.

In all three labs, the CFD modelling showed that particle concentrations were highest at ventilation rates of 1 ACH. An increase in the rate from 1 to 4 ACH reduced concentrations by 28% to 67%, depending on the laboratory modelled. In Laboratories A and C, changing mechanical ventilation by increasing the number of ACH may be a way of controlling bioaerosols, even though capture at source is always the preferred option. In Laboratory B, number concentrations of particles at 10.3 and 12 ACH are comparable. This result appears to indicate that an increase in ventilation rate above 12 ACH will not have a significant impact on concentrations; other emission control methods must then be envisaged.

6.3 Prevention

This metrological study identified bioaerosol generation during different embalming tasks. These bioaerosols have small diameters that give them a high probability of being deposited in respiratory tracts and a strong potential to move around in the air of embalming rooms. Various authors have shown that numerous pathogens have been recovered from the bodily fluids coming from cadavers whose cause of death was nonetheless certified not to be an infectious disease (Cattaneo et al., 1999; Creely, 2004; Rose & Hockett, 1971). Other studies remind us that a substantial percentage of dead bodies are identified as being infectious only during the autopsy or embalmment (Burton, 2003; Stephenson & Byard, 2019). Thus, Keane et al. (2013) state that it is impossible to guarantee that there is no infectious pathogen on a dead body. Embalmers' exposure to an infectious pathogen in Risk Group 2 or 3, by inhalation, therefore cannot be ignored. This factor is particularly important during a pandemic, such as the COVID-19 pandemic in 2020: with numerous asymptomatic or untested cases, embalmers may be exposed to respiratory tract viruses from a deceased individual (e.g., SARS-CoV-2), who was not diagnosed with the disease.

Consequently, the choice of wearing respiratory protection equipment should not be based on the identification of an infectious risk on the basis of the death certificate, particularly as this form definitely does not have the purpose of protecting funeral home workers' health and safety. For all work done after death – applying a risk management approach – all bodily fluids, tissues or aerosols should be considered to be potentially infectious. Practices to prevent exposure to infectious agents and chemicals should be applied at all times, for all dead bodies, regardless of the established or presumed cause of death, the time elapsed since death, or any other information contained in the death certificate. Embalmers must be aware of the presence of infectious aerosols, their source and their dispersion, and their working methods must be adapted to reduce exposure risks at all times.

Although currently no level of exposure to infectious agents is recommended, it is possible, by combining the results of this study and the tool developed jointly by researchers at the IRSST and Université de Montréal called *A support tool for choosing respiratory protection against bioaerosols,*[8] to choose an appropriate respiratory protection device. For example, by selecting health care and considering exposure to bioaerosols in Risk Group 2 or 3 with a low exposure level, RPE such as an air-purifying respirator with half-mask (N/R/P-95/99/100) or elastomer half-mask with P100 filtering cartridges is recommended. Exposure at higher levels will necessitate the use of RPE with higher characteristic protection factors.

[8] https://www.irsst.qc.ca/bioaerosol/Accueil.aspx?l=en

A respiratory protection program, including the identification of a program leader and training concerning the right way to don and doff RPE, and how to maintain it and conduct the adjustment test that should be done before every use, should be set up in the workplace.

Considering the difficulty of identifying pathogens in dead bodies, the embalmer's proximity to the body, the great diversity of working tasks and the uncertainty associated with the dilution of contaminants by general ventilation, the authors of this report recommend considering at least wearing air-purifying RPE during the embalming process.

REFERENCES

Act respecting medical laboratories and organ and tissue conservation, CQLR, c. L-0.2, r. 1-128. https://www.legisquebec.gouv.qc.ca/en/document/cs/l-0.2

Anctil, G., Beaudreau, L., Bégin, N., Bolduc, D., Dancause, V., Frenette, C., Galarneau, L.-A., Paré, R., Pigeon, N., Rodrigues, R., Savard, P., Titeica, G., Tremblay, C., & Tremblay, M. (2017). *La prévention et le contrôle des infections nosocomiales: cadre de référence à l'intention des établissements de santé et de services sociaux du Québec*. http://collections.banq.qc.ca/ark:/52327/3108840.

Andersen, A. A. (1958). New sampler for the collection, sizing, and enumeration of viable airborne particles. *Journal of Bacteriology*, *76*(5), 471–484. https://www.ncbi.nlm.nih.gov/pmc/articles/PMC290224/pdf/jbacter00507-0033.pdf

ASHRAE. (2004). *Thermal environmental conditions for human occupancy.* ANSI/ASHRAE Standard 55:2004. ASHRAE.

ASHRAE. (2013a). *HVAC design manual for hospitals and clinics*. ASHRAE.

ASHRAE. (2013b). *Ventilation of health care facilities*. ANSI/ASHRAE Standard 170:2013. ASHRAE.

ASHRAE. (2016). *Ventilation for acceptable indoor air quality*. ASHRAE.

ASHRAE. (2017). *Ventilation of health care facilities*. ANSI/ASHRAE Standard 170:2017. ASHRAE.

ASTM. (2017). *Standard test method for determining air change in a single zone by means of a tracer gas dilution*. ASTM Standard E741-11:2017. ASTM. https://webstore.ansi.org/standards/astm/astme741112017.

Azeredo, A. C., & Payeur, F. (2019). La mortalité et l'espérance de vie au Québec en 2018. *Institut de la statistique du Québec*, *23*(3), 9–14.

Barnett, R. L., & Brickman, D. B. (1986). Safety hierarchy. *Journal of Safety Research*, *17*(2), 49–55. https://doi.org/10.1016/0022-4375(86)90093-9

Beggs, C. B., Kerr, K. G., Noakes, C. J., Hathway, E. A., & Sleigh, P. A. (2008). The ventilation of multiple-bed hospital wards: Review and analysis. *American Journal of Infection Control*, *36*(4), 250–259. https://doi.org/10.1016/j.ajic.2007.07.012

Bekal, S., Gaudreau, C., Laurence, R. A., Simoneau, E., & Raynal, L. (2006). *Streptococcus pseudoporcinus sp. nov.*, a novel species isolated from the genitourinary tract of women. *Journal of Clinical Microbiology*, *44*(7), 2584–2586. https://doi.org/10.1128/JCM.02707-05

Bourque, G. (2016). *Outil d'identification des risques: prise en charge de la santé et de la sécurité du travail*. CNESST. http://collections.banq.qc.ca/ark:/52327/2932283

Brenner, D. J., Garrity, G. M., & Bergey, D. H. (Eds.). (2005). *The Gammaproteobacteria* (2nd ed.). Springer.

Burton, J. L. (2003). Health and safety at necropsy. *Journal of Clinical Pathology*, *56*(4), 254–260.

Callahan, B. J., McMurdie, P. J., Rosen, M. J., Han, A. W., Johnson, A. J. A., & Holmes, S. P. (2016). DADA2: High-resolution sample inference from Illumina amplicon data. *Nature Methods*, *13*(7), 581–583. https://doi.org/10.1038/nmeth.3869

Can, I., Javan, G. T., Pozhitkov, A. E., & Noble, P. A. (2014). Distinctive thanatomicrobiome signatures found in the blood and internal organs of humans. *Journal of Microbiological Methods*, *106*, 1–7. https://doi.org/10.1016/j.mimet.2014.07.026

Canadian Centre for Occupational Health and Safety. (2018). *Hazard control: OSH answers fact sheets.* Government of Canada. https://www.ccohs.ca/oshanswers/hsprograms/hazard_control.html.

Cattaneo, C., Nuttall, P. A., Molendini, L. O., Pellegrinelli, M., Grandi, M., & Sokol, R. J. (1999). Prevalence of HIV and hepatitis C markers among a cadaver population in Milan. *Journal of Clinical Pathology*, *52*(4), 267–270.

Chakravorty, S., Helb, D., Burday, M., Connell, N., & Alland, D. (2007). A detailed analysis of 16S ribosomal RNA gene segments for the diagnosis of pathogenic bacteria. *Journal of Microbiological Methods, 69*(2), 330–339. https://doi.org/10.1016/j.mimet.2007.02.005

Cheong, C., & Lee, S. (2018). Case study of airborne pathogen dispersion patterns in emergency departments with different ventilation and partition conditions. *International Journal of Environmental Research and Public Health*, *15*(3), Article 510. https://doi.org/10.3390/ijerph15030510

Cooper, M. J. (1995). Training as a risk control measure. *Industrial and Commercial Training*, *27*(11), 26–29. https://doi.org/10.1108/00197859510100266

Correia, J. C., Steyl, J. L., & Villiers, H. C. D. (2014). Assessing the survival of *Mycobacterium tuberculosis* in unembalmed and embalmed human remains. *Clinical Anatomy*, *27*(3), 304–307. https://doi.org/10.1002/ca.22355

Creely, K. (2004). *Infection risks and embalming* (Report no. TM/04-/01). Institute of Occupational Medicine. http://www.ifsa.us/images/Article.IOM.InfectionRisksAndEmbalming.pdf

Davidson, S. S., & Benjamin, W. H. (2006). Risk of infection and tracking of work-related infectious diseases in the funeral industry. *American Journal of Infection Control*, *34*(10), 655–660. https://doi.org/10.1016/j.ajic.2006.05.290

De Vos, P., Whitman, W. B., & Bergey, D. H. (Eds.). (2009). *The Firmicutes* (2nd ed.). Springer.

DeKoster, J. A., & Thorne, P. S. (1995). Bioaerosol concentrations in noncomplaint, complaint, and intervention homes in the Midwest. *American Industrial Hygiene Association Journal*, *56*(6), 573–580.

Demiryürek, D., Bayramoğlu, A., & Ustaçelebi, Ş. (2002). Infective agents in fixed human cadavers: A brief review and suggested guidelines. *The Anatomical Record*, *269*(4), 194–197. https://doi.org/10.1002/ar.10143

Dhariwal, A., Chong, J., Habib, S., King, I. L., Agellon, L. B., & Xia, J. (2017). MicrobiomeAnalyst: A web-based tool for comprehensive statistical, visual and meta-analysis of microbiome data. *Nucleic Acids Research*, *45*(W1), W180–W188. https://doi.org/10.1093/nar/gkx295

Douceron, H., Deforges, L., Gherardi, R., Sobel, A., & Chariot, P. (1993). Long-lasting postmortem viability of human immunodeficiency virus: A potential risk in forensic medicine practice. *Forensic Science International*, *60*(1–2), 61–66. https://doi.org/10.1016/0379-0738(93)90093-P

Éditeur officiel du Québec. (2019). *Regulation respecting the application of the Act respecting medical laboratories and organ and tissue conservation.* https://www.legisquebec.gouv.qc.ca/en/document/cr/l-0.2,%20r.%201

Farcas, G. A., Poutanen, S. M., Mazzulli, T., Willey, B. M., Butany, J., Asa, S. L., Faure, P., Akhavan, P., Low, D. E., & Kain, K. C. (2005). Fatal severe acute respiratory syndrome is associated with multiorgan involvement by coronavirus. *The Journal of Infectious Diseases*, *191*(2), 193–197. https://doi.org/10.1086/426870

Gajdusek, D. C., Gibbs, C. J., Traub, R. D., & Collins, G. (1976). Survival of Creutzfeldt-Jakob-disease virus in formol-fixed brain tissue. *New England Journal of Medicine*, *294*(10), 553–553. https://doi.org/10.1056/NEJM197603042941015

Gershon, R. R. M., Vlahov, D., Escamilla-Cejudo, J. A., Badawi, M., McDiarmid, M., Karkashian, C., Grimes, M., & Comstock, G. W. (1998). Tuberculosis risk in funeral home employees. *Journal of Occupational and Environmental Medicine*, *40*(5), 497–503.

Goodfellow, M., Kämpfer, P., Busse, H.-J., Trujillo, M. E., Suzuki, K., Ludwig, W., & Whitman, W. B. (Eds.). (2012). *Bergey's manual® of systematic bacteriology: Volume five: The Actinobacteria: Part A and B*. https://doi.org/10.1007/978-0-387-68233-4

Górny, R. L., & Dutkiewicz, J. (2002). Bacterial and fungal aerosols in indoor environment in Central and Eastern European countries. *Annals of Agriculture and Environmental Medicine*, *9*(2), 17–23. https://www.researchgate.net/profile/Jacek_Dutkiewicz2/publication/11287910_Bacterial_and_Fungal_Aerosols_in_Indoor_Environment_in_Central_and_Eastern_European_Countries/links/5447fbd60cf2f14fb8141c6a/Bacterial-and-Fungal-Aerosols-in-Indoor-Environment-in-Central-and-Eastern-European-Countries.pdf

Górny, R., Dutkiewicz, J., & Krysińska-Traczyk, E. (2003). Size distribution of bacterial and fungal bioaerosols in indoor air. *Annals of Agricultural and Environmental Medicine*, *6*(2), 105–113.

Goyer, N., Lavoie, J., Lazure L., & Marchand, G. (2001). *Les bioaérosols en milieu de travail: guide d'évaluation, de contrôle et de prévention*. IRSST. https://www.irsst.qc.ca/media/documents/PubIRSST/T-23.pdf

Guez-Chailloux, M., Le Bâcle, C., & Puymerail, P. (2005). *Dossier médico-technique: la thanatopraxie: état des pratiques et risques professionnels*. INRS.

Gupta, D. J., Chaturvedi, D. M., & Patil, D. M. (2013). Embalmed cadavers: Are they safe to handle, a study to see the microbial flora present in the embalmed cadavers. *International Journal of Pharma and Bio Sciences,* *4*(1), 382–386. http://citeseerx.ist.psu.edu/viewdoc/download?doi=10.1.1.450.7964&rep=rep1&type=pdf

Harf-Monteil, C. (2004). *Aeromonas simiae* sp. nov., isolated from monkey faeces. *International Journal of Systematic and Evolutionary Microbiology*, *54*(2), 481–485. https://doi.org/10.1099/ijs.0.02786-0

Healing, T. D., Hoffman, P. N., & Young, S. E. J. (1995). The infection hazards of human cadavers. *Communicable Disease Report,* *5*(5), 61–68. https://europepmc.org/article/med/7749455

Henry, W. K., Dexter, D., Sannerud, K., Jackson, B., & Balfour, H. H. (1989). Recovery of HIV at autopsy. *New England Journal of Medicine*, *321*(26), 1833–1834. https://doi.org/10.1056/NEJM198912283212614

HSE. (2005). *Controlling the risks of infection at work from human remains: A guide for those involved in funeral services (including embalmers) and those involved in exhumation*. HSE. http://www.hse.gov.uk/pUbns/web01.pdf

HSE. (2018). *Managing infection risks when handling the deceased: Guidance for the mortuary, post-mortem room and funeral premises, and during exhumation*. HSE. https://pdf4pro.com/view/managing-infection-risks-when-handling-the-deceased-5a3897.html

Janvier, M., & Grimont, P. A. (1995). The genus Methylophaga, a new line of descent within phylogenetic branch γ of proteobacteria. *Research in Microbiology*, *146*(7), 543–550. https://doi.org/10.1016/0923-2508(96)80560-2

Javan, G. T., Finley, S. J., Can, I., Wilkinson, J. E., Hanson, J. D., & Tarone, A. M. (2016). Human thanatomicrobiome succession and time since death. *Scientific Reports*, *6*(1), Article 29598. https://doi.org/10.1038/srep29598

Keane, E., Dee, A., Crotty, T., Cunney, R., Daly, E., Griffin, S., Horgan, M., Keane, S., Kenny, E., Lyon, C., McKeown, P., Natin, D., Reid, A., & MacKenzie, K. (2013). *Guidelines for the management of deceased Individuals harbouring infectious disease*. Health Protection Surveillance Centre. https://www.hpsc.ie/a-z/lifestages/modi/File,14302,en.pdf

Kelly, N., & Reid, A. (2011). A health and safety survey of Irish funeral industry workers. *Occupational Medicine*, *61*(8), 570–575. https://doi.org/10.1093/occmed/kqr131

Kim, K. Y., & Kim, C. N. (2007). Airborne microbiological characteristics in public buildings of Korea. *Building and Environment*, *42*(5), 2188–2196. https://doi.org/10.1016/j.buildenv.2006.04.013

Lajoie, É., Dupont, M., Pelletier, P., Portier, M., & Tremblay, M. (2011). *Guide de prévention des risques chimiques et infectieux chez les travailleurs du domaine funéraire*. Groupe de travail thanatopraxie Montérégie–Montréal. http://www.santeautravail.qc.ca/documents/13347/375318/378923_doc-5gJJo.pdf

Lavoie, J., Marchand, G., Cloutier, Y., Hallé, S., Nadeau, S., Duchaine, C., & Pichette, G. (2015). Evaluation of bioaerosol exposures during hospital bronchoscopy examinations. *Environmental Science: Processes and Impacts*, *17*(2), 288–299. https://doi.org/10.1039/C4EM00359D

Li, Y., Leung, G. M., Tang, J. W., Yang, X., Chao, C. Y. H., Lin, J. Z., Lu, J. W., Nielsen, P. V., Niu, J., Qian, H., Sleigh, A. C., Su, H.-J. J., Sundell, J., Wong, T. W., & Yuen, P. L. (2007). Role of ventilation in airborne transmission of infectious agents in the built environment – A multidisciplinary systematic review. *Indoor Air*, *17*(1), 2–18. https://doi.org/10.1111/j.1600-0668.2006.00445.x

Liu, M., Nobu, M. K., Ren, J., Jin, X., Hong, G., & Yao, H. (2019). Bacterial compositions in inhalable particulate matters from indoor and outdoor wastewater treatment processes. *Journal of Hazardous Materials, 385,* Article 121515. https://doi.org/10.1016/j.jhazmat.2019.121515

Mbareche, H., Veillette, M., Bilodeau, G. J., & Duchaine, C. (2018). Bioaerosol sampler choice should consider efficiency and ability of samplers to cover microbial diversity. *Applied and Environmental Microbiology, 84*(23), Article e01589. https://doi.org/10.1128/AEM.01589-18

McGrattan, K. B., Hostikka, S., McDermott, R., Floyd, J., & Vanella, M. (2019a). *Fire dynamics simulator technical reference guide: Volume 2: Verification* (6th ed.). NIST.

McGrattan, K. B., Hostikka, S., McDermott, R., Floyd, J., & Vanella, M. (2019b). *Fire dynamics simulator technical reference guide: Volume 3: Validation* (6th ed.). NIST.

Memarzadeh, F. (2013). *Literature review: Room ventilation and airborne disease transmission*. American Hospital Association. https://ams.aha.org/eweb/DynamicPage.aspx?WebCode=ProdDetailAdd&ivd_prc_prd_key=4b1eae24-aed1-4376-b70e-a2cb469f67c9.

Memarzadeh, F., & Xu, W. (2012). Role of air changes per hour (ACH) in possible transmission of airborne infections. *Building Simulation*, *5*(1), 15–28. https://doi.org/10.1007/s12273-011-0053-4

Michaud, J. (2003). *Thanatopraxie: les risques biologiques et chimiques: manuel du participant*. Régie régionale de la santé et des services sociaux Côte-Nord.

Morris, J. A., Harrison, L. M., & Partridge, S. M. (2007). Practical and theoretical aspects of postmortem bacteriology. *Current Diagnostic Pathology*, *13*(1), 65–74. https://doi.org/10.1016/j.cdip.2006.07.005

Nevalainen, A. (1989). *Bacterial aerosols in indoor air*. Kansanterveyslaitos KTL. http://www.julkari.fi/bitstream/handle/10024/134619/Bacterial%20Aerosols%20in%20indoor%20air.pdf?sequence=1&isAllowed=y

Nyberg, M., Suni, J., & Haltia, M. (1990). Isolation of human immunodeficiency virus (HIV) at autopsy one to six days postmortem. *American Journal of Clinical Pathology*, *94*(4), 422–425. https://doi.org/10.1093/ajcp/94.4.422

Paczkowski, S., & Schütz, S. (2011). Post-mortem volatiles of vertebrate tissue. *Applied Microbiology and Biotechnology*, *91*(4), 917–935. https://doi.org/10.1007/s00253-011-3417-x

Parent, D., & Bouchard, F. (2017). *Guide de prévention: notions de base en prévention et contrôle des infections santé et sécurité du travail*. ASSTSAS. http://asstsas.qc.ca/sites/default/files/publications/documents/Guides_Broch_Depl/GP74%20-%20Notions%20de%20base%20en%20PCI%20Final%20Web.pdf.

Parker, S., Nally, J., Foat, T., & Preston, S. (2010). Refinement and testing of the drift-flux model for indoor aerosol dispersion and deposition modelling. *Journal of Aerosol Science*, *41*(10), 921–934. https://doi.org/10.1016/j.jaerosci.2010.07.002

Pastuszka, J. S., Paw, U. K. T., Lis, D. O., Wlazło, A., & Ulfig, K. (2000). Bacterial and fungal aerosol in indoor environment in Upper Silesia, Poland. *Atmospheric Environment*, *34*(22), 3833–3842.

Plog, B. A., & Quinlan, P. (Eds.). (2002). *Fundamentals of industrial hygiene* (5th ed.). National Safety Council Press.

Priola, S. A., Ward, A. E., McCall, S. A., Trifilo, M., Choi, Y. P., Solforosi, L., Williamson, R. A., Cruite, J. T., & Oldstone, M. B. A. (2013). Lack of prion infectivity in fixed heart tissue from patients with Creutzfeldt-Jakob disease or amyloid heart disease. *Journal of Virology*, *87*(17), 9501–9510. https://doi.org/10.1128/JVI.00692-13

Pruesse, E., Peplies, J., & Glöckner, F. O. (2012). SINA: Accurate high-throughput multiple sequence alignment of ribosomal RNA genes. *Bioinformatics*, *28*(14), 1823–1829. https://doi.org/10.1093/bioinformatics/bts252

Public Health Agency of Canada. (2019). *Pathogen safety data sheets*. https://www.canada.ca/en/public-health/services/laboratory-biosafety-biosecurity/pathogen-safety-data-sheets-risk-assessment.html

Reponen, T. A., Gazenko, S. V., Grinshpun, S. A., Willeke, K., & Cole, E. C. (1998). Characteristics of airborne Actinomycete spores. *Applied and Environmental Microbiology*, *64*(10), 3807–3812.

Rose, G. W., & Hockett, R. N. (1971). The microbiologic evaluation and enumeration of postmortem specimens from human remains. *Health Laboratory Science*, *8*(2), 75–78.

Rup, L. (2012). The human microbiome project. *Indian Journal of Microbiology*, *52*(3), Article 315. https://doi.org/10.1007/s12088-012-0304-9

Stephenson, L., & Byard, R. W. (2019). Issues in the handling of cases of tuberculosis in the mortuary. *Journal of Forensic and Legal Medicine*, *64*, 42–44. https://doi.org/10.1016/j.jflm.2019.04.002

Stockwell, R. E., Ballard, E. L., O'Rourke, P., Knibbs, L. D., Morawska, L., & Bell, S. C. (2019). Indoor hospital air and the impact of ventilation on bioaerosols: A systematic review. *Journal of Hospital Infection*, *103*(2), 175–184. https://doi.org/10.1016/j.jhin.2019.06.016

Su, C., de Perio, M. A., Cummings, K. J., McCague, A.-B., Luckhaupt, S. E., & Sweeney, M. H. (2019). Case investigations of infectious diseases occurring in workplaces, United States, 2006–2015. *Emerging Infectious Diseases*, *25*(3), 397–405. https://doi.org/10.3201/eid2503.180708

Tang, J. W., Noakes, C. J., Nielsen, P. V., Eames, I., Nicolle, A., Li, Y., & Settles, G. S. (2011). Observing and quantifying airflows in the infection control of aerosol- and airborne-transmitted diseases: An overview of approaches. *Journal of Hospital Infection*, *77*(3), 213–222. https://doi.org/10.1016/j.jhin.2010.09.037

Tang, J. W., To, K.-F., Lo, A. W. I., Sung, J. J. Y., Ng, H. K., & Chan, P. K. S. (2007). Quantitative temporal-spatial distribution of severe acute respiratory syndrome-associated coronavirus

(SARS-CoV) in post-mortem tissues. *Journal of Medical Virology*, *79*(9), 1245–1253. https://doi.org/10.1002/jmv.20873

Thatiparti, D. S., Ghia, U., & Mead, K. R. (2017). Computational fluid dynamics study on the influence of an alternate ventilation configuration on the possible flow path of infectious cough aerosols in a mock airborne infection isolation room. *Science and Technology for the Built Environment*, *23*(2), 355–366. https://doi.org/10.1080/23744731.2016.1222212.

Tuomisto, S., Karhunen, P. J., Vuento, R., Aittoniemi, J., & Pessi, T. (2013). Evaluation of postmortem bacterial migration using culturing and real-time quantitative PCR. *Journal of Forensic Sciences*, *58*(4), 910–916. https://doi.org/10.1111/1556-4029.12124

Van de Peer, Y., Chapelle, S., & De Wachter, R. (1996). A quantitative map of nucleotide substitution rates in bacterial rRNA. *Nucleic Acids Research, 24*(17), 3381–3391.

Veillette, M., Bonifait, L., Mbareche, H., Marchand, G., & Duchaine, C. (2018). Preferential aerosolization of Actinobacteria during handling of composting organic matter. *Journal of Aerosol Science*, *116*, 83–91. https://doi.org/10.1016/j.jaerosci.2017.11.004

Weed, L. A., & Baggenstoss, A. H. (1951). The isolation of pathogens from tissues of embalmed human bodies. *American Journal of Clinical Pathology*, *21*(12), 1114–1120. https://doi.org/10.1093/ajcp/21.12.1114

Weiser, J. N. (2010). The pneumococcus: Why a commensal misbehaves. *Journal of Molecular Medicine*, *88*(2), 97–102. https://doi.org/10.1007/s00109-009-0557-x

Yu, H., Mui, K., & Wong, L. (2018). Numerical simulation of bioaerosol particle exposure assessment in office environment from MVAC systems. *The Journal of Computational Multiphase Flows*, *10*(2), 59–71. https://doi.org/10.1177/1757482X17746919

Zhou, Q., Qian, H., & Liu, L. (2018). Numerical investigation of airborne infection in naturally ventilated hospital wards with central-corridor type. *Indoor and Built Environment*, *27*(1), 59–69. https://doi.org/10.1177/1420326X16667177

APPENDIX A

1) Reaction mixture and thermocycling protocol used to amplify 16S rRNA for characterization sequencing (PCR amplification)

Composition of reaction mixture

Master mix	Concentration	Final concentration	1X volume
Water			31.5 µl
HF 5x buffer*	5x	1x	10 µl
dNTPs	10 mM	200 µM	1 µl
Ai primer	25 µM	0.5 µM	1 µl
rJ primer	25 µM	0.5 µM	1 µl
Phusion polymerase	2 U/µl	0.02 U/µl	0.5 µl
			45 µl
		Volume of DNA added	5 µl
		Final volume	50 µl

** Phusion High-Fidelity DNA Polymerase Kit (Thermo Fisher Scientific)*

Thermocycling protocol

98 °C	30 s	
98 °C	10 s	35x
54 °C	30 s	
72 °C	45 s	
72 °C	10 min	
4 °C	∞	

Verification of amplicon bands on 1% agarose gel, 130 V, 45 min

2) *Reaction mixture and thermocycling protocol used for gene marking of 16S rRNA for characterization sequencing (Sequencing reaction)*

Composition of reaction mixture

Master mix	Concentration	Final concentration	1X volume
Water			11 µl
5x sequencing buffer	5x	Not provided	3 µl
Primer (D or rE)	10 µM	0.5 µM	1 µl
Big Dye v3.1	2.5x	Not provided	2 µl
			17 µl
		Volume of purified amplicon added	3 µl
		Final volume	20 µl

Thermocycling protocol

96 °C	1 min	
98 °C 50 °C 60 °C	10 s 5 s 4 min	25x
4 °C	∞	

3) Determination of the optimum annealing temperature for microbial exposure indicator detection systems (gradient qPCR)

and

Determination of the specificity of microbial exposure indicator detection systems (qPCR)

Composition of reaction mixture

Master mix	Concentration	Final concentration	1X volume
Water			5.4 µl
GoTaq qPCR Master Mix*	2x	0.8x	6 µl
Primer A	25 µM	0.5 µM	0.3 µl
Primer B	25 µM	0.5 µM	0.3 µl
			12 µl
		Volume of DNA added	3 µl
		Final volume	15 µl

* *GoTaq qPCR Master Mix (Promega, Madison, WI, USA)*

Thermocycling protocol (gradient qPCR)

95 °C	2 min	
95 °C	15 s	
Gradient		40x
49 °C to 62 °C	30 s	
↳reading		

Dissociation curve

65 °C to 95 °C	⇨reading
0.5 °C increase every 5 s	

N.B.: The dissociation curve is used to get a general idea of the specificity of the reaction and to detect potential primer dimers.

Thermocycling protocol (qPCR)

95 °C	2 min	
95 °C	15 s	40x
60 °C	1 min	
↳reading		

Dissociation curve

65 °C to 95 °C	⇨reading
0.5 °C increase every 5 s	

N.B.: All systems were optimized with the aim of achieving an optimum annealing temperature of 60 °C in qPCR.

4) *Microbial exposure indicator detection tests – total bacterial load per 16S rRNA gene detection (qPCR)*

Composition of reaction mixture

Master mix	Concentration	Final concentration	1X volume
Water			5.4 µl
GoTaq qPCR Master Mix	2x	0.8x	6 µl
E517F primer	25 µM	0.5 µM	0.3 µl
1387r-IRSST primer	25 µM	0.5 µM	0.3 µl
			12 µl
		Volume of DNA added	3 µl
		Final volume	15 µl

Thermocycling protocol

95 °C	10 min		
94 °C	15 s		
62.5 °C	30 s		40x
↳reading			
72 °C	30 s		

Dissociation curve

65 °C to 95 °C	⇨reading
0.5 °C increase every 5 s	

5) *Microbial exposure indicator detection tests (ddPCR)*

Composition of reaction mixture

Master mix	Concentration	Final concentration	1X volume
Water	–	–	5.56 µl
Super Mix[1]	2x	1x	10 µl
20X Mix[2]	20x	0.72x	0.72 µl
Mmu Assay[3]	20x	0.72x	0.72 µl
Mmu DNA Assay[3]	1/200	–	0.2 µl
$MgCl_2$	25 mmol	1 mmol	0.8 µl
		Volume of DNA added	2 µl
		Final volume	20 µl

[1] ddPCR Supermix for Probes (no dUTP), (Bio-Rad)
[2] The 20x mix is a mix of primers and probes specific to each system and defined in Table 3. 20x, this mix contains 10 µM of each primer and 7.5 µM of the probe. At 0.72x, each reaction contains 0.36 µM of each primer and 0.27 µM of probe.
[3] PrimePCR Assay/Template Tbp, Mmu, qMmuCIP0042759 (Bio-Rad)

Thermocycling protocol

95 °C	10 min	
94 °C	30 s	40x
55.5 °C	1 min	
72 °C	30 s	
98 °C	10 min	

N.B.: All systems were optimized with the aim of achieving an optimum annealing temperature of 55.5° C in ddPCR.